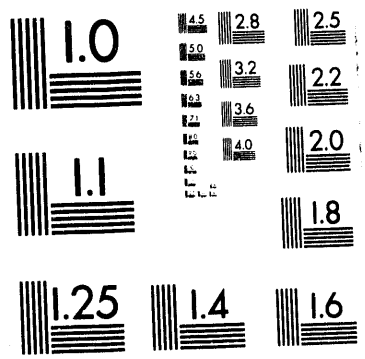
1.0
1.1
1.25
1.4
1.6
1.8
2.0
2.2
2.5
2.8
3.2
3.6
4.0
4.5
5.0
5.6
6.3
7.1
8.0
9.0

1 of 2

THE DEVELOPMENT OF COAL-BASED TECHNOLOGIES FOR DEPARTMENT OF DEFENSE FACILITIES

Semiannual Technical Progress Report
for the Period 03/28/1993 to 09/27/1993

by

Bruce G. Miller, Joel L. Morrison, Reza Sharifi, Joseph F. Shepard, and Alan W. Scaroni
Energy and Fuels Research Center
The Pennsylvania State University;
Richard Hogg, Subhash Chander, Heechau Cho, M.Thaddeus Ityokumbul, Mark S. Klima, and Peter T. Luckie
Mineral Processing Section
The Pennsylvania State University;
Adam Rose, Sam Addy, Timothy J. Considine, Richard L. Gordon, Katherine McClain, and A. Michael Schaal
Department of Mineral Economics
The Pennsylvania State University;
Peter M. Walsh and Jiang Xie
Fuel Science Program
The Pennsylvania State University;
Paul C. Painter and Boris Veytsman
Polymer Science Program
The Pennsylvania State University;
Michael J. Rini
ABB Combustion Engineering Systems;
Mahesh Jha
AMAX Research and Development; and
Don Morrison, Todd Melick, and Todd M. Sommer
Energy and Environmental Research Corporation

December 17, 1993

Work Performed Under Cooperative Agreement No. DE-FC22-92PC92162

for
U.S. Department of Energy
Pittsburgh Energy Technology Center
Pittsburgh, Pennsylvania

by
The Consortium for Coal-Water Slurry Fuel Technology
The Pennsylvania State University
University Park, Pennsylvania

DISCLAIMER

TABLE OF CONTENTS

TABLE OF CONTENTS (cont.)

LIST OF FIGURES

LIST OF TABLES

EXECUTIVE SUMMARY

The U.S. Department of Defense (DOD), through an Interagency Agreement with the U.S. Department of Energy (DOE), has initiated a three-phase program with the Consortium for Coal-Water Slurry Fuel Technology, with the aim of decreasing DOD's reliance on imported oil by increasing its use of coal. The program is being conducted as a cooperative agreement between the Consortium and DOE and the first phase of the program is underway.

To achieve the objectives of the program, a team of researchers has been assembled from Penn State (Energy and Fuels Research Center (EFRC), Mineral Processing Section, Fuel Science Program, Department of Mineral Economics, and Polymer Science Program), ABB Combustion Engineering Systems (CE), AMAX Research and Development Center (AMAX), and Energy and Environmental Research Corporation (EER). These four organizations are the current members of the Consortium.

Phase I activities are focused on developing clean, coal-based combustion technologies for the utilization of both micronized coal-water slurry fuels (MCWSFs) and dry, micronized coal (DMC) in fuel oil-designed industrial boilers. Phase II research and development activities will continue to focus on industrial boiler retrofit technologies by addressing emissions control and pre-combustion (*i.e.*, slagging combustion and/or gasification) strategies for the utilization of high ash, high sulfur coals. Phase III activities will examine coal-based fuel combustion systems that cofire wastes. Each phase includes an engineering cost analysis and technology assessment. The activities and status of Phase I are described below.

The objective in Phase I is to deliver fully engineered retrofit options for a fuel oil-designed watertube boiler located on a DOD installation to fire either MCWSF or DMC. This will be achieved through a program consisting of the following five tasks: 1) Coal Beneficiation and Preparation; 2) Combustion Performance Evaluation; 3) Engineering Design; 4) Engineering and Economic Analysis; and 5) Final Report/Submission of Design Package.

TASK 1: COAL BENEFICIATION/PREPARATION

This task includes the selection and procurement of suitable coal samples and the development of appropriate cleaning procedures to ensure that specifications (<5% ash and <1% sulfur) are met.

Subtask 1.1 Identify/Procure Coals

A set of five candidate coals has been selected. Samples of each have been procured and analyzed.

Subtask 1.2 Determine Liberation Potential

Standard float-sink testing is being performed on the coal samples ground to progressively finer sizes. Sufficient data have been obtained for three of the coals to establish cleaning strategies by which specifications can be met at yields of over 80%. Data on the fourth coal

suggest that finer grinding will be needed to meet the sulfur specification. Liberation testing on the fifth coal is in progress.

Research into the development of improved liberation models is also in progress. The use of such models should permit optimization of the grinding/beneficiation processes. The basic model has been developed; testing is in progress for determination of the various model parameters and functionalities.

Subtask 1.3 Produce Laboratory-Scale Quantities of Micronized Coal-Water Slurry Fuels

Various beneficiation procedures, generally involving combinations of fine-gravity and surface-based separations, are being investigated. These are complex processes with numerous interacting variables. Research is being conducted into the development of process models which can describe the specific role of these variables and can be used to predict performance and provide an improved basis for process simulation. The modeling effort is paralleled by laboratory studies of fine-gravity separations using dense-medium cyclones and centrifuges, and surface-based separations by advanced froth flotation and selective agglomeration.

Establishment of optimum particle size distribution to satisfy the conflicting requirements for high solids concentration and low viscosity is an important aspect of the research effort. Packing geometry and particle interaction forces are being investigated in regard to their influence on MCWSF stability and rheological behavior. The specific functions of chemical reagents for particle dispersion and MCWSF stabilization are being studied in detail.

Subtask 1.4 Develop a Dry Coal Cleaning Technique

Techniques for the preparation and beneficiation of dry, micronized coal for the production of MCWSF or for direct burning in industrial boilers are being evaluated. Current research in this area includes studies of fine-grinding in closed-circuit fluid-energy mills and the use of triboelectrostatic separation for sulfur and ash removal from aerosolized, micronized coal.

Subtask 1.5 Produce MCWSFs and DMC from Dry, Clean Coal

Work in this subtask will begin upon successful completion of Subtask 1.4.

Subtask 1.6 Produce MCWSFs and DMC for the Demonstration Boiler

The fuel preparation facility (MCWSF and DMC) associated with the demonstration boiler is approximately 75% complete. The DMC circuit is complete and work is underway setting up the MCWSF circuit.

TASK 2: COAL COMBUSTION PERFORMANCE

This task includes evaluating the combustion performance of the coals identified in Task 1. In addition, the technical aspects of converting a fuel oil-designed boiler at a DOD facility will be identified.

Subtask 2.1 Boiler Retrofit

Penn State is evaluating options for procuring and installing a MCWSF/DMC-fired burner on the demonstration boiler

Subtask 2.2 Fuel Evaluation Fuels in the Research (1,000 lb steam/h) Boiler

Combustion tests were conducted to evaluate a coal-based fuel called mulled coal. The mulled coal was fired as a CWSF and on an as-received basis. The mulled coal that was produced into a CWSF was stored, pumped, atomized, and burned in a similar manner to other CWSFs tested at Penn State. The combustion performance of the slurried mulled coal was similar to that of the other CWSFs. The mulled coal that was fired as received was more difficult to handle (feed from the hopper to the burner via the screw feeder and eductor) than other pulverized coals tested at Penn State.

Subtask 2.3 Performance Evaluation of MCWSF and DMC in the Demonstration Boiler

Evaluate Erosion/Deposition Characteristics

Recent work has focused on two areas: Improvement of the metal oxidation component of the erosion-corrosion model, and interpretation of the ash deposition measurements from the demonstration boiler.

Determine Erosion Characteristics of Materials Subjected to Atomized CWSF

In order to obtain more information on atomizer operation and materials of construction, a study has been started to evaluate the erosive behavior of different materials when subjected to an atomized CWSF spray. The test facility, atomizer, CWSF transport and containment systems, mist eliminator, material sample mounting, and sample orientation mounting have been designed.

Theoretical and Experimental Studies of Particle Behavior in the Demonstration Boiler

In order to increase understanding of pulverized coal and CWSF turbulent jet flames in an industrial boiler, theoretical and experimental work has been initiated. Initial work includes computational modeling of natural gas firing in the demonstration boiler. The next stage of the modeling work entails the injection of pulverized coal particles and CWSF droplets into the furnace and following their combustion histories. An in-situ particle counter, sizer, and velocimeter will be used to obtain data to verify the model.

TASK 3: ENGINEERING DESIGN

In this task, an engineering study will be performed for a complete retrofit of a DOD boiler facility to fire either MCWSF or DMC. EER started the conversion designs of the Crane facility (see Subtask 4.1) from natural gas/heavy oil to MCWSF and DMC. EER conducted a site visit and is performing the preliminary site layout, isometric, and piping and instrumentation diagrams.

TASK 4: ENGINEERING AND COST ANALYSIS

In this task, an engineering cost analysis and technology assessment of MCWSF and DMC combustion will be performed.

Subtask 4.1 Survey Boiler Population/Identify Boilers for Conversion

Penn State visited several military installations and has had discussions with both civilian and military personnel regarding the use of coal in the military. As a consequence of this activity, Penn State recommended to DOE the Naval Surface Warfare Center at Crane, Indiana as the site for the retrofit designs in Phase I of the program. DOE and DOD approved the selection.

Subtask 4.2 Identify Appropriate Cost-Estimating Methodologies

Subtask 4.2 was completed. The major conclusion was that no one cost-estimation method dominates all others, but that some methods, such as process analysis/linear programming, have very distinct advantages in the context of this project.

Subtask 4.3 Estimate Basic Costs of New Technologies

A baseline linear programming model was developed to evaluate costs of supplying fuels of acceptable quality to an oil-designed industrial boiler which has been retrofitted to fire MCWSF. The model will be expanded to evaluate other fuel supply options and for other potential retrofit sites.

Subtask 4.4 Process Analysis of MCWSF and DMC

Two types of economic models were used to evaluate retrofitting an existing oil-fired boiler to fire CWSF. These are spreadsheet models and algebraic programming models using the general algebraic modeling system (GAMS). In addition, a stochastic analysis was performed using Crystal Ball, a forecasting and risk management program.

In summary, the GAMS models currently give net present values of retrofitting. They can be modified to yield payback periods as well. The GAMS models analyses are more general and should be used for centralized decision making, while the spreadsheet models are more suitable for specific site decision-making. A combination of net present value and payback period is often used to make commercial investment decisions. For retrofitting scenarios, when the output of the GAMS models is payback periods, as well as their current output, they will become invaluable as decision aids on retrofitting.

Subtask 4.5 Analyze/Identify Transportation Cost of Commercial Sources of MCWSF and Cleaned Coal for DMC Production

No work was conducted in Subtask 4.5 during this reporting period.

Subtask 4.6 Determine Community Spillovers

No work was conducted in Subtask 4.6 during this reporting period.

Subtask 4.7 Regional Market Considerations and Impacts

An input-output model for an 8-county region surrounding the Crane Naval Weapons Center has been constructed using the IMPLAN Modeling System. A regional I-O table for 1990 and a set of multipliers were generated and the data are being verified by checking with local sources of information. The regional I-O tables will be used to determine the economic impacts of using MCWSF and DMC at Crane and two or three other sites.

1.0 INTRODUCTION

The U.S. Department of Defense (DOD), through an Interagency Agreement with the U.S. Department of Energy (DOE), has initiated a three-phase program with the Consortium for Coal-Water Slurry Fuel Technology, with the aim of decreasing DOD's reliance on imported oil by increasing its use of coal. The program is being conducted as a cooperative agreement between the Consortium and DOE and the first phase of the program is underway.

To achieve the objectives of the program, a team of researchers has been assembled from Penn State (Energy and Fuels Research Center (EFRC), Mineral Processing Section, Fuel Science Program, Department of Mineral Economics, and Polymer Science Program), ABB Combustion Engineering Systems (CE), AMAX Research and Development Center (AMAX), and Energy and Environmental Research Corporation (EER). These four organizations are the current members of the Consortium.

Phase I activities are focused on developing clean, coal-based combustion technologies for the utilization of both micronized coal-water slurry fuels (MCWSFs) and dry, micronized coal (DMC) in fuel oil-designed industrial boilers. Phase II research and development activities will continue to focus on industrial boiler retrofit technologies by addressing emissions control and pre-combustion (*i.e.*, slagging combustion and/or gasification) strategies for the utilization of high ash, high sulfur coals. Phase III activities will examine coal-based fuel combustion systems that cofire wastes. Each phase includes an engineering cost analysis and technology assessment. The activities and status of Phase I are described below.

The objective in Phase I is to deliver fully engineered retrofit options for a fuel oil-designed watertube boiler located on a DOD installation to fire either MCWSF or DMC. This will be achieved through a program consisting of the following five tasks: 1) Coal Beneficiation and Preparation; 2) Combustion Performance Evaluation; 3) Engineering Design; 4) Engineering and Economic Analysis; and 5) Final Report/Submission of Design Package. Following is an outline of the project tasks that comprise Phase I:

Task 1: Coal Beneficiation/Preparation
- Subtask 1.1 Identify/Procure Coals
- Subtask 1.2 Determine Liberation Potential
- Subtask 1.3 Produce Laboratory-Scale Quantities of Micronized Coal-Water Mixtures (MCWSFs)
- Subtask 1.4 Develop Dry Coal Cleaning Technique
- Subtask 1.5 Produce MCWSFs and Dry, Micronized Coal (DMC) From Dry Clean Coal
- Subtask 1.6 Produce MCWSF and DMC for the Demonstration Boiler
- Subtask 1.7 Project Management and Support

Task 2: Combustion Performance Evaluation
- Subtask 2.1 Boiler Retrofit
- Subtask 2.2 Fuel Evaluation in the Research Boiler

Subtask 2.3 Performance Evaluation of the MCWSF and DMC in the Demonstration Boiler
Subtask 2.4 Evaluate Emissions Reductions Strategies
Subtask 2.5 Project Management and Support

Task 3: Engineering Design
Subtask 3.1 MCWSF/DMC Preparation Facilities
Subtask 3.2 Fuel Handling
Subtask 3.3 Burner System
Subtask 3.4 Ash Removal, Handling, and Disposal
Subtask 3.5 Air Pollution Control
Subtask 3.6 Integrate Engineering Design
Subtask 3.7 Project Management and Support

Task 4: Engineering and Economic Analysis
Subtask 4.1 Survey Boiler Population/Identify Boilers for Conversion
Subtask 4.2 Identify Appropriate Cost-Estimating Methodologies
Subtask 4.3 Estimate Basic Costs of New Technologies
Subtask 4.4 Process Analysis of MCWSF and DMC
Subtask 4.5 Analyze/Identify Transportation Cost of Commercial Sources of MCWSF and Cleaned Coal for DMC Production
Subtask 4.6 Determine Community Spillovers
Subtask 4.7 Regional Market Considerations and Impacts
Subtask 4.8 Integrate the Analysis
Subtask 4.9 Project Management and Support

Task 5: Final Report/Submission of Design Package

The activities planned for Phase I are summarized below:

Task 1: The coal beneficiation and preparation effort is being conducted by Penn State's Mineral Processing Section with assistance from AMAX and Penn State's Polymer Science Program. This task involves identifying and procuring six coals that can be cleaned to <1.0 wt.% sulfur and <5.0 wt.% ash which have been, or possess the characteristics to enable them to be, made into MCWSFs. The coals will be subjected to detailed characterization and used to produce laboratory-scale quantities of MCWSF. A fundamental study of MCWSF stabilization will be conducted. Additional activities include developing a dry coal cleaning technique and producing MCWSFs and DMC from the resulting cleaned coal.

Task 2: The EFRC is conducting the combustion performance evaluation with assistance from CE and Penn State's Fuel Science Program. The technical aspects of converting a fuel oil-designed boiler at a DOD facility will be identified in this task. All appropriate components will be evaluated, including the fuel, the fuel storage, handling and delivery equipment, the burner, the boiler, the ash handling and disposal equipment, the emissions control system, and the boiler control system. Combustion performance as indicated by flame stability, completeness of combustion, and related issues such as system derating, changes in system maintenance, the occurrence of slagging, fouling, corrosion and erosion, and air pollutant emissions will be determined. As part of this task, MCWSF and DMC will be evaluated in EFRC's 15,000 lb steam/h watertube

boiler. CE will provide a proven coal-designed burner for retrofitting Penn State's boiler. In addition, CE will design the burner for the DOD boiler identified for retrofitting.

Task 3: An engineering study will be performed for a complete retrofit of a DOD boiler facility to fire either MCWSF or DMC. The designs will be performed by EER with input from the other project participants. The designs will include the coal preparation, the fuel handling, the burner, the ash removal, handling, and disposal, and the air pollution control systems. The two designs will be for the DOD boiler identified in Task 4. The retrofits will be designed for community/societal acceptability. The deliverables for this task will be a detailed design that can be used for soliciting bids from engineering/construction firms to retrofit the candidate DOD boiler.

Task 4: An engineering cost analysis and technology assessment of MCWSF and DMC combustion will be performed by Penn State's Department of Mineral Economics and the EFRC with assistance from the industrial participants. The effort will involve surveying the DOD boiler population, identifying boilers for conversion, identifying appropriate cost-estimating methodologies, estimating basic costs for new technologies, developing a process model, analyzing and identifying transportation costs for commercial sources of MCWSF and cleaned coal, determining community spillovers, and determining regional market considerations and impacts.

Task 5: The results from each of the tasks will be summarized in a final report. In addition, the design packages for the boiler retrofits will be submitted. These will include the engineering design and economic analysis.

The accomplishments and status of Tasks 1, 2, 3, 4, and 5 are presented in Sections 2.0, 3.0, 4.0, 5.0, and 6.0, respectively. Section 7.0 discusses miscellaneous activities that were conducted. Activities planned for the next semiannual period are listed in Section 8.0. References and acknowledgments are contained in Sections 9.0 and 10.0, respectively. The project schedule is given in Figure 1-1, with a description of the milestones contained in Table 1-1.

2.0 TASK 1: COAL BENEFICIATION/PREPARATION

The initial objectives of this activity were to select appropriate coals which could meet the specific requirements of the project and to prescribe the necessary cleaning steps. Longer-term objectives are to develop improved cleaning procedures which can be used to increase the yield of usable coal and to expand the reserve base of candidate fuels for retrofitted boilers.

2.1 Subtask 1.1 Identify/Procure Coals

The Mineral Processing Section, with assistance from AMAX, selected a set of candidate coals. The criteria used for the selection have been described previously (Miller, et al. 1993a). The choice of the final coal (Indiana VII) was based on the boiler selection (Subtask 4.1). The characteristics of the five test coals are presented in Table 2-1.

Task 1 - Coal Beneficiation/Preparation

Subtask 1.1 Identify / Procure Coals

Subtask 1.2 Determine Liberation Potential

- Subtask 1.2.1 Conventional Washability Analysis on Type I and Type II Samples
- Subtask 1.2.2 Fine Washability Analysis on Type II and Type III Samples

Subtask 1.3 Production of Lab-Scale Quantities of MCWSF

- Subtask 1.3.1 Identify Cleaning Strategies
- Subtask 1.3.2 Evaluate Conventional Gravity Separations
- Subtask 1.3.3 Evaluate Fine Gravity Separations
- Subtask 1.3.4 Evaluate Advanced Froth Flotation
- Subtask 1.3.5 Evaluate Column Flotation
- Subtask 1.3.6 Evaluate Selective Agglomeration
- Subtask 1.3.7 Investigate Solid-Liquid Separations
- Subtask 1.3.8 Select Cleaning Flowsheet(s)
- Subtask 1.3.9 Establish Required Size Consist for Slurry Formulation
- Subtask 1.3.10 Investigate Conventional Ball Milling
- Subtask 1.3.11 Stirred Media Milling
- Subtask 1.3.12 Investigate Attrition Milling
- Subtask 1.3.13 Lab-Scale Slurry Production
- Subtask 1.3.14 Modify Models to Account for PSD
- Subtask 1.3.15 Modify Models to Account for Inter-Particle Attractive Forces
- Subtask 1.3.16 Modify Models

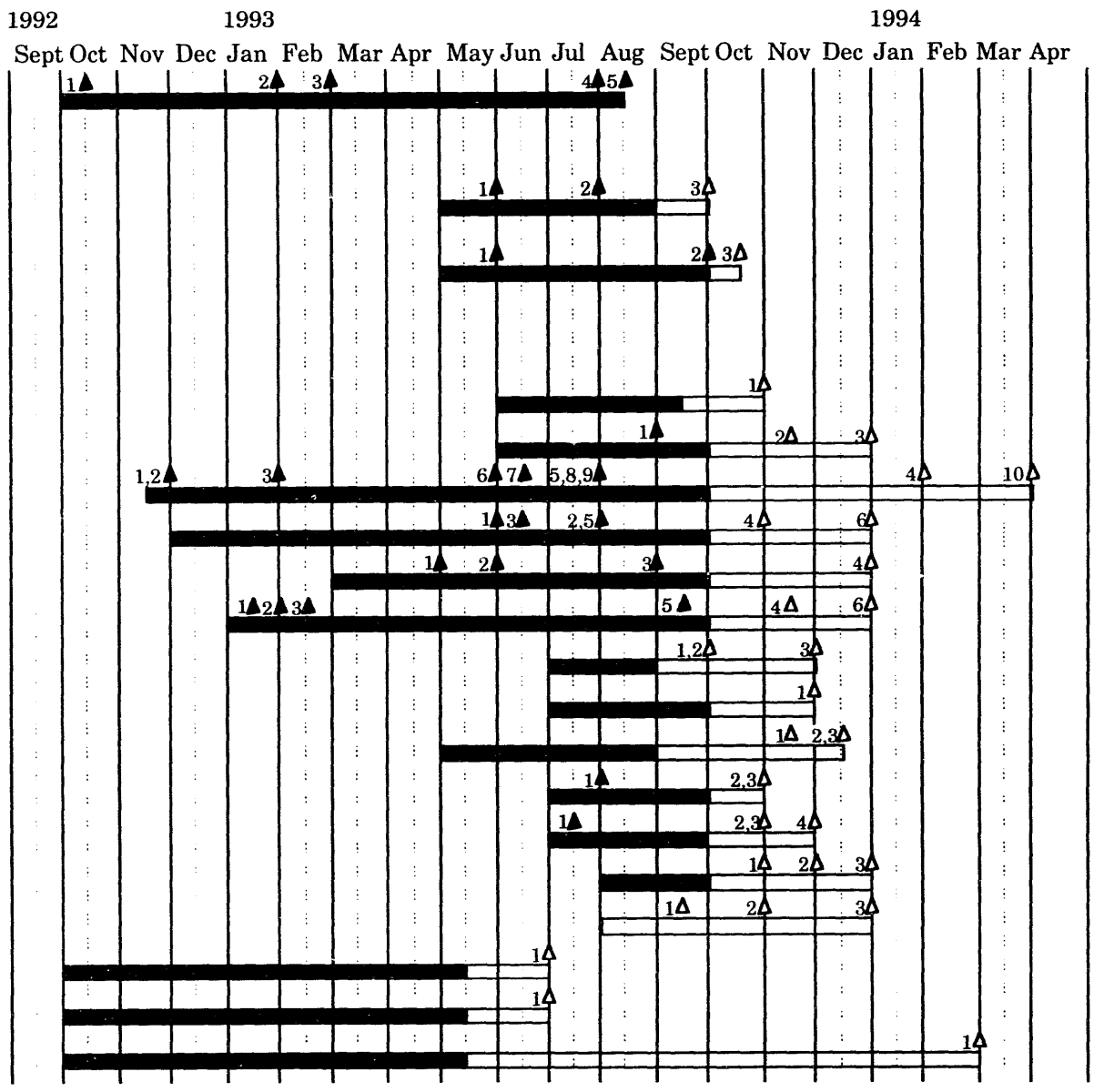

Figure 1-1. Milestone Schedule

Task 1 - Coal Beneficiation Preparation (cont.)

Subtask 1.4 Develop Dry Coal Cleaning Technique

Subtask 1.4.1 Dry Grinding Studies

Subtask 1.4.2 Deagglomeration Studies

Subtask 1.4.3 Dry Separations

Subtask 1.5 Produce MCWSFs and Micronized Coal from Dry, Clean Coal

Subtask 1.5.1 Produce Micronized Coal from Dry, Clean Coal

Subtask 1.5.2 Produce MCWM from Dry, Clean Coal

Subtask 1.6 Produce MCWSF and Dry, Micronized Coal for the Demonstration

Subtask 1.6.1 Shakedown Dry, Micronized Coal Circuit

Subtask 1.6.2 Install MCWSF Equipment

Subtask 1.6.3 Shakedown MCWSF Equipment

Subtask 1.6.4 Coal Cleaning

Subtask 1.6.5 Coal Micronizing

Subtask 1.6.6 MCWSF Preparation

Subtask 1.7 Project Management and Support

Subtask 1.7.1 Project Management and Technical Advisement

Subtask 1.7.2 Drafting / Technical Secretarial Support

Subtask 1.7.3 Budget Management / Project Administration

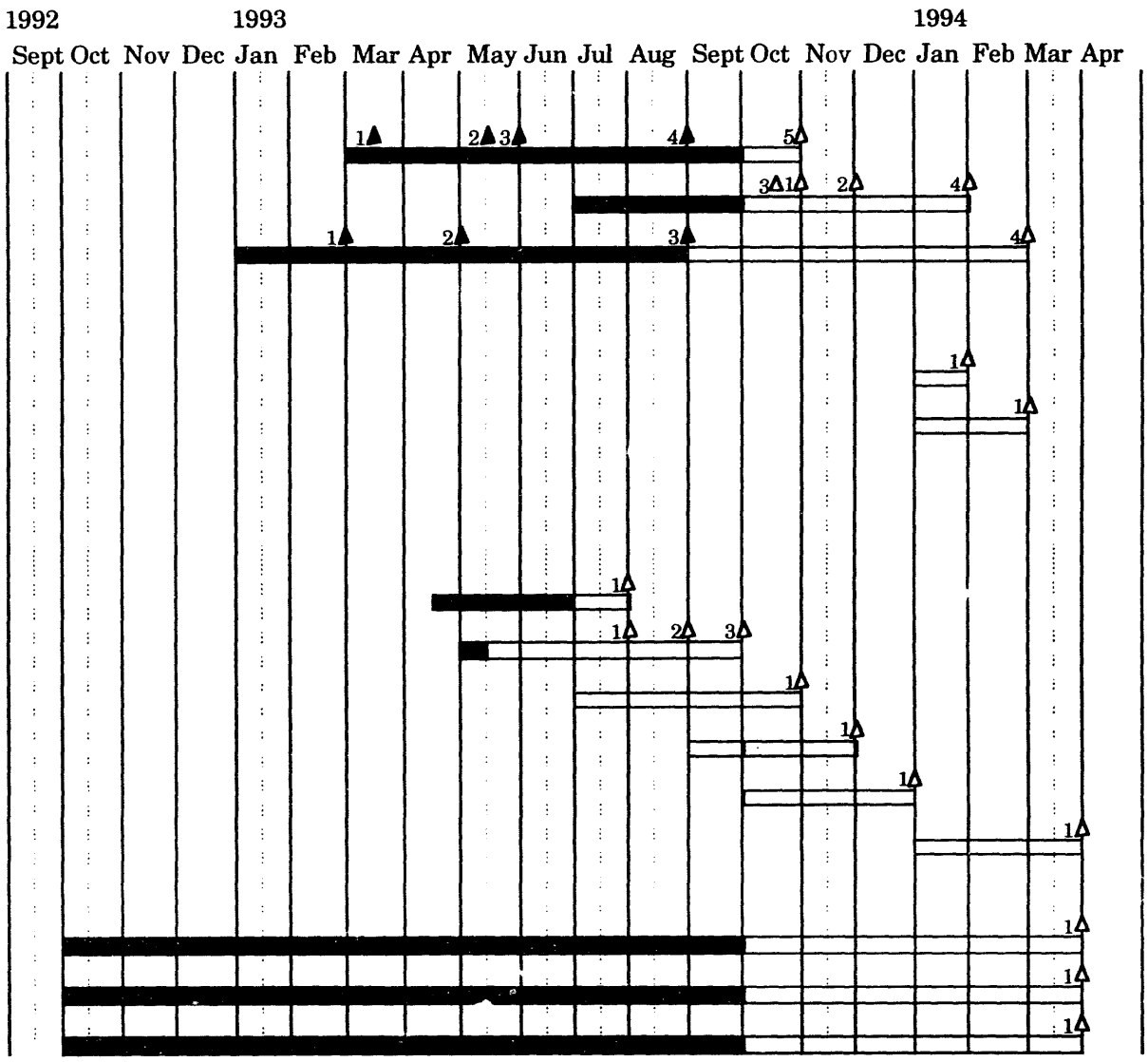

Task 2 - Combustion Performance Evaluation

Subtask 2.1 Boiler Retrofit

Subtask 2.1.1 Finalize Burner/Atomizer Design
Subtask 2.1.2 Procure and Install Burner
Subtask 2.1.3 Optimize Burner Firing Dry, Micronized Coal
Subtask 2.1.4 Optimize Burner Firing CWSF

Subtask 2.2 Fuel Evaluation in Research Boiler

Subtask 2.2.1 Test Sample of Type I CWSF
Subtask 2.2.2 Test Sample of Type II CWSF
Subtask 2.2.3 Test Sample of Type III CWSF

Subtask 2.3 Performance Evaluation of MCWSF and Dry, Micronized Coal in Demonstration Boiler

Dry, Micronized Coal Testing

Subtask 2.3.1 100-Hour Milestone
Subtask 2.3.2 200-Hour Milestone
Subtask 2.3.3 300-Hour Milestone
Subtask 2.3.4 400-Hour Milestone
Subtask 2.3.5 500-Hour Milestone
Subtask 2.3.6 600-Hour Milestone
Subtask 2.3.7 700-Hour Milestone
Subtask 2.3.8 800-Hour Milestone
Subtask 2.3.9 900-Hour Milestone
Subtask 2.3.10 1,000-Hour Milestone
Subtask 2.3.11 Technical Advisement by CE

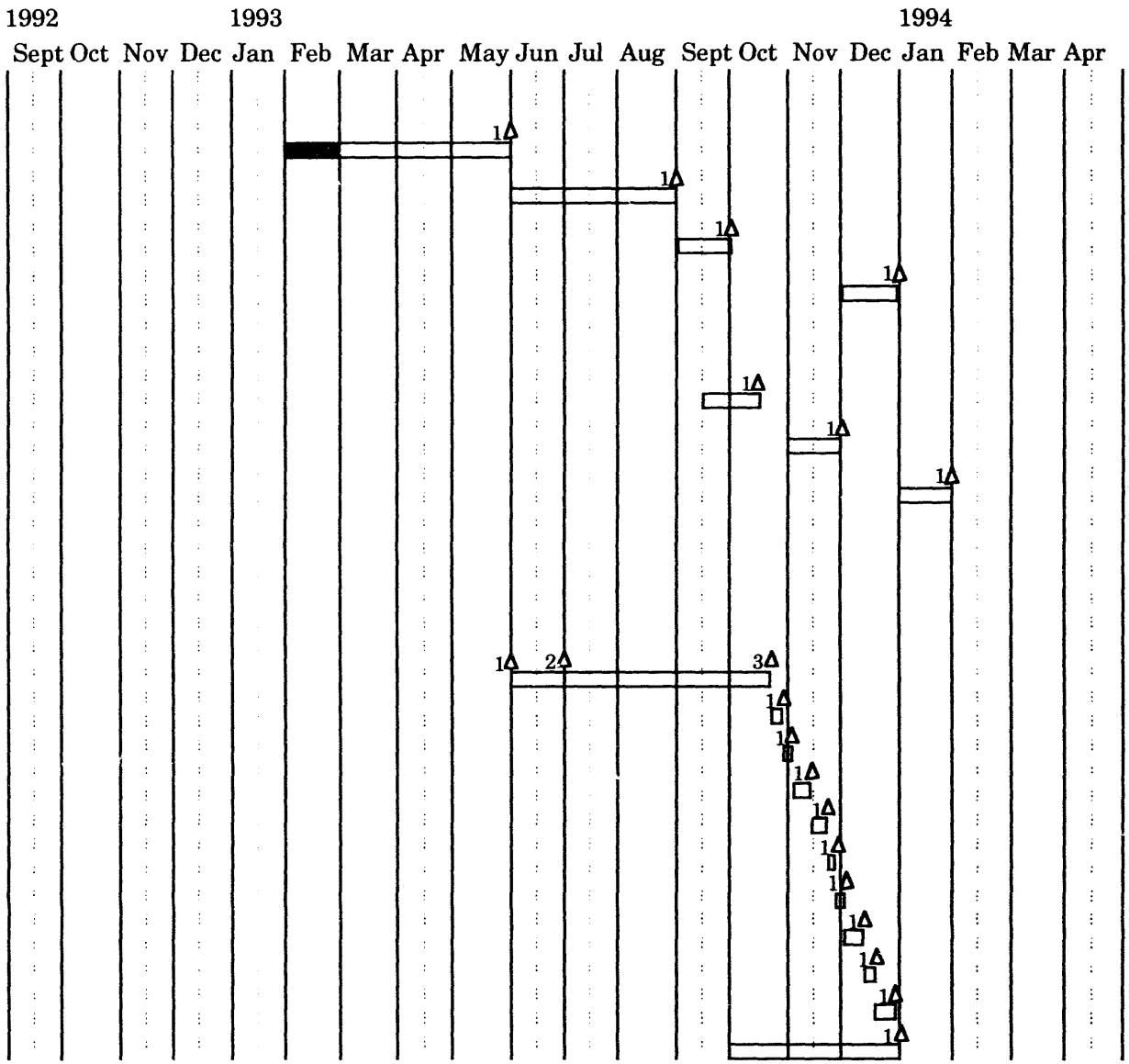

Task 2 - Combustion Performance Evaluation (cont.)

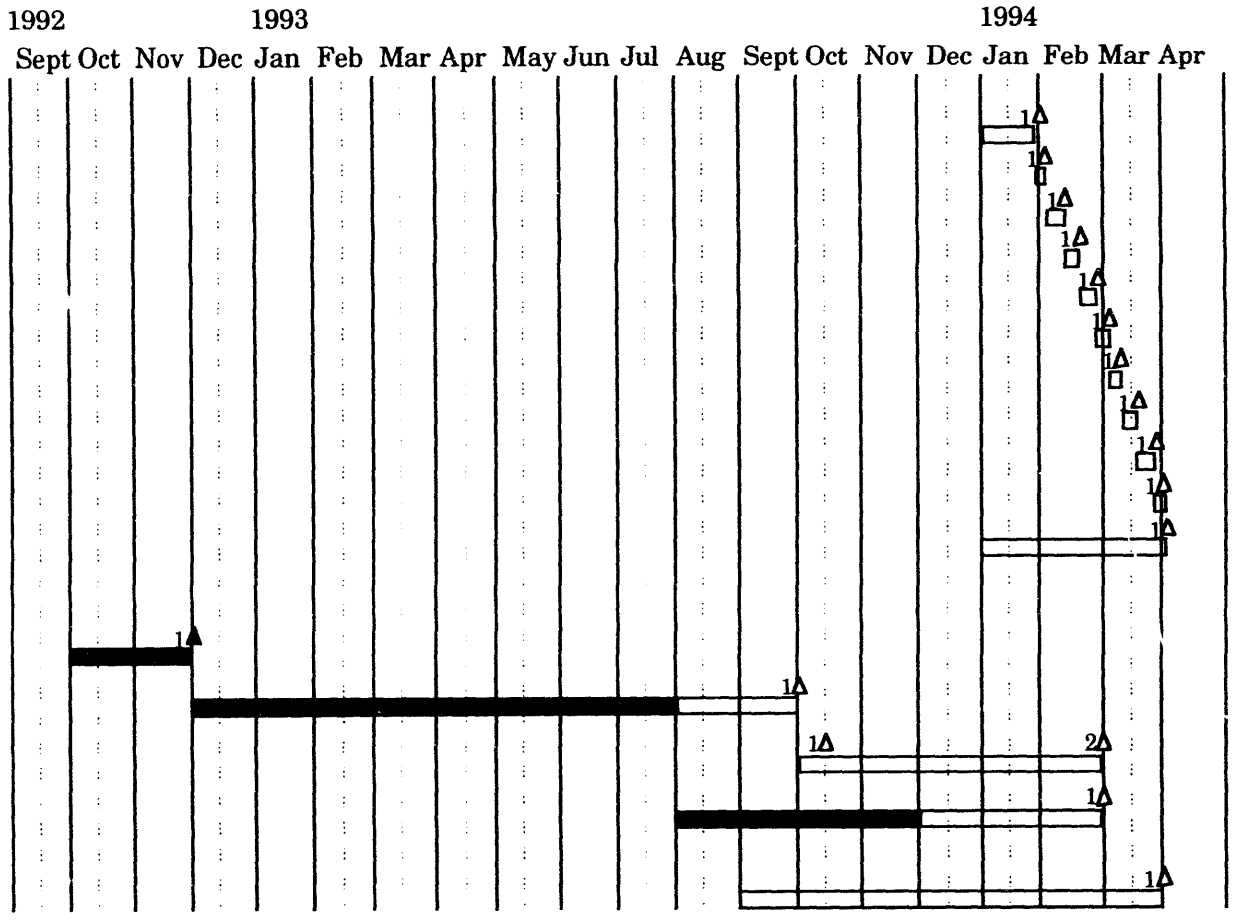

Task 2 - Combus tion Performance Evaluation (cont.)

Subtask 2.4 Evaluate Emissions Reduction Strategies

Subtask 2.4.1 Dry, Micronized Coal Testing

Subtask 2.4.2 CWSF Testing

Subtask 2.5 Project Management and Support

Subtask 2.5.1 Project Management and Advisement

Subtask 2.5.2 Staff Supervision Test Planning and Quality Control

Subtask 2.5.3 Data Reduction and Interpretation

Subtask 2.5.4 Drafting / Technical Secretarial Support

Subtask 2.5.5 Budget Management / Project Administration

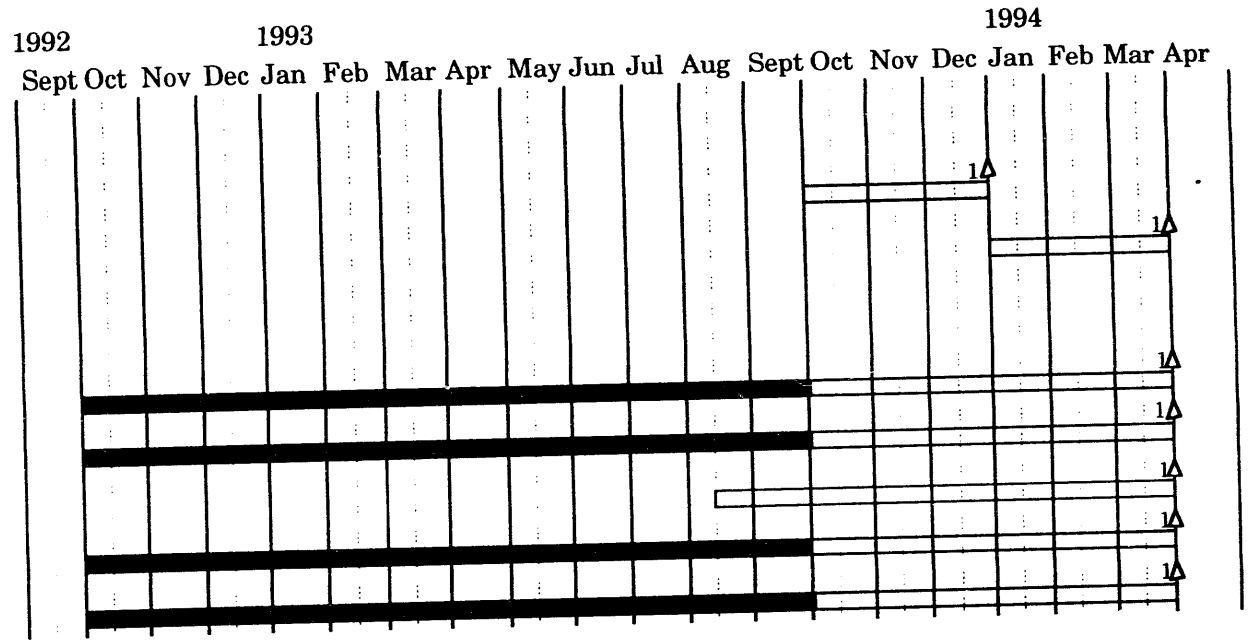

Task 3 - Engineering Design

Subtask 3.1 Micronized CWSF Dry, Micronized Coal Preparation Facilities

Subtask 3.1.1 Design of MCWSF Facility - AMAX

Subtask 3.1.2 Design of Dry, Micronized Coal Preparation System - EER / PSU

Subtask 3.2 Fuel Handling

Subtask 3.2.1 Design of Fuel System - EER

Subtask 3.2.2 Technical Support and Fuel System Design - PSU

Subtask 3.3 Burner System

Subtask 3.3.1 Burner Design - CE

Subtask 3.3.2 Auxiliary Component Design - EER

Subtask 3.4 Ash Removal, Handling and Disposal

Subtask 3.4.1 Design of Ash System - EER

Subtask 3.5 Air Polution Control

Subtask 3.5.1 Design of Emission Control - EER

Subtask 3.6 Integrate Engineering Design

Subtask 3.6.1 Integrate System Components

Subtask 3.7 Project Management and Support

Subtask 3.7.1 Project Management and Technical Advisement

Subtask 3.7.2 Penn State Technical Review

Subtask 3.7.3 Drafting / Technical Secretarial Support

Subtask 3.7.4 Budget Management / Project Administration

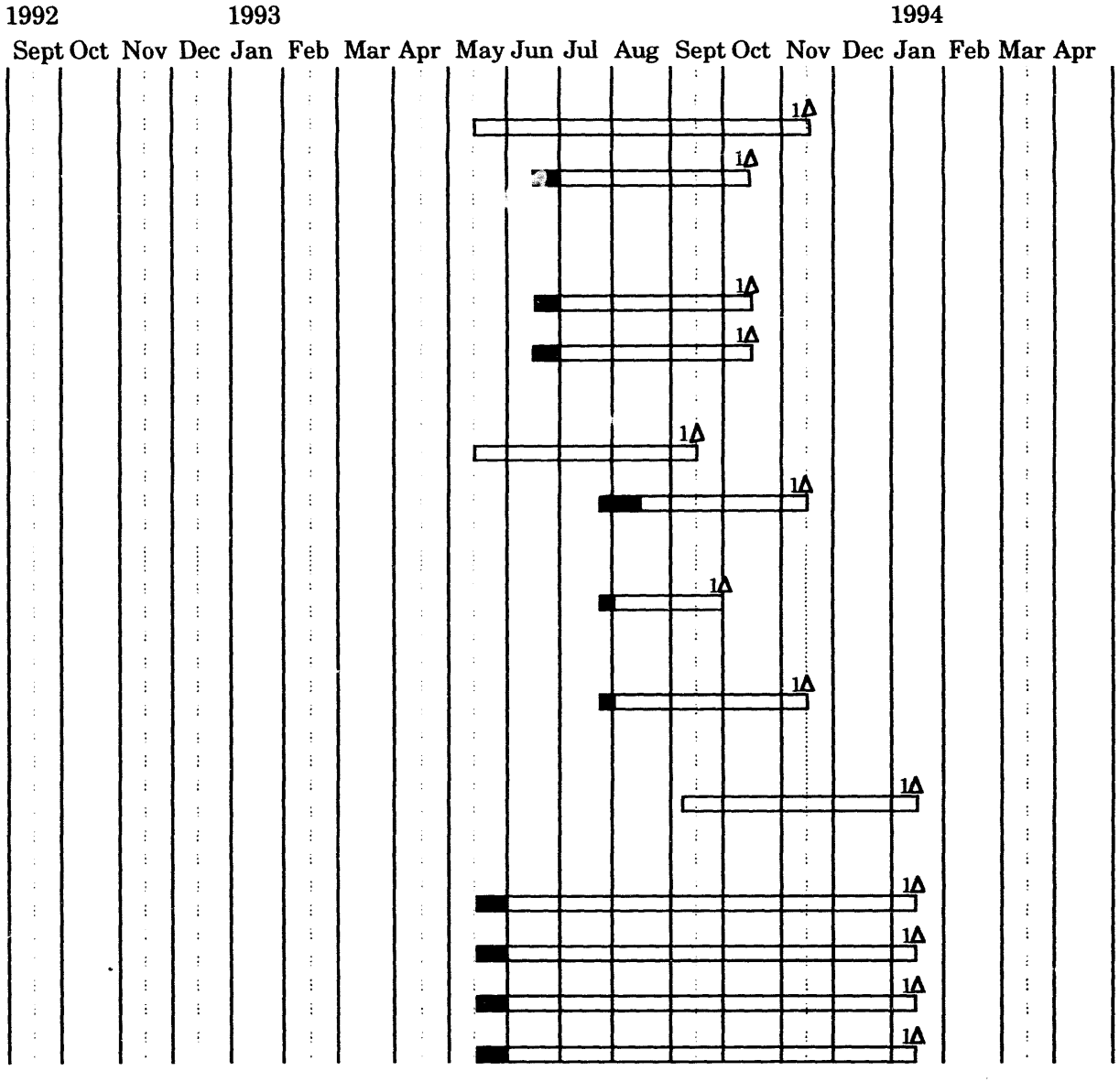

Task 4 - Engineering and Economic Analysis

Subtask 4.1 Survey Boiler Population / Identify Boilers for Conversion
Subtask 4.2 Identify Appropriate Cost - Estimating Methodologies
Subtask 4.3 Estimate Basic Costs of New Technologies
Subtask 4.4 Process Analysis of MCWSF and Dry, Micronized Coal
Subtask 4.4.1 Penn State Analysis
Subtask 4.4.2 Industrial Participants Assistance/Advisement
Subtask 4.5 Analyze / Identify Transportation Cost of Commercial Sources of MCWSF and Cleaned Coal for Dry, Micronized Coal Production
Subtask 4.6 Determine Community Spillovers
Subtask 4.7 Regional Market Considerations and Impacts
Subtask 4.8 Integrate the Analysis
Subtask 4.8.1 Penn State Review of Industrial Participants Contribution
Subtask 4.8.2 Penn State Integrate the Analysis
Subtask 4.8.3 Industrial Participants Assistance in Preparing, and Review of, the Integrated Analysis
Subtask 4.9 Project Management and Support
Subtask 4.9.1 Project Management and Advisement
Subtask 4.9.2 Drafting / Technical Secretarial Support
Subtask 4.9.3 Budget Management / Project Administration

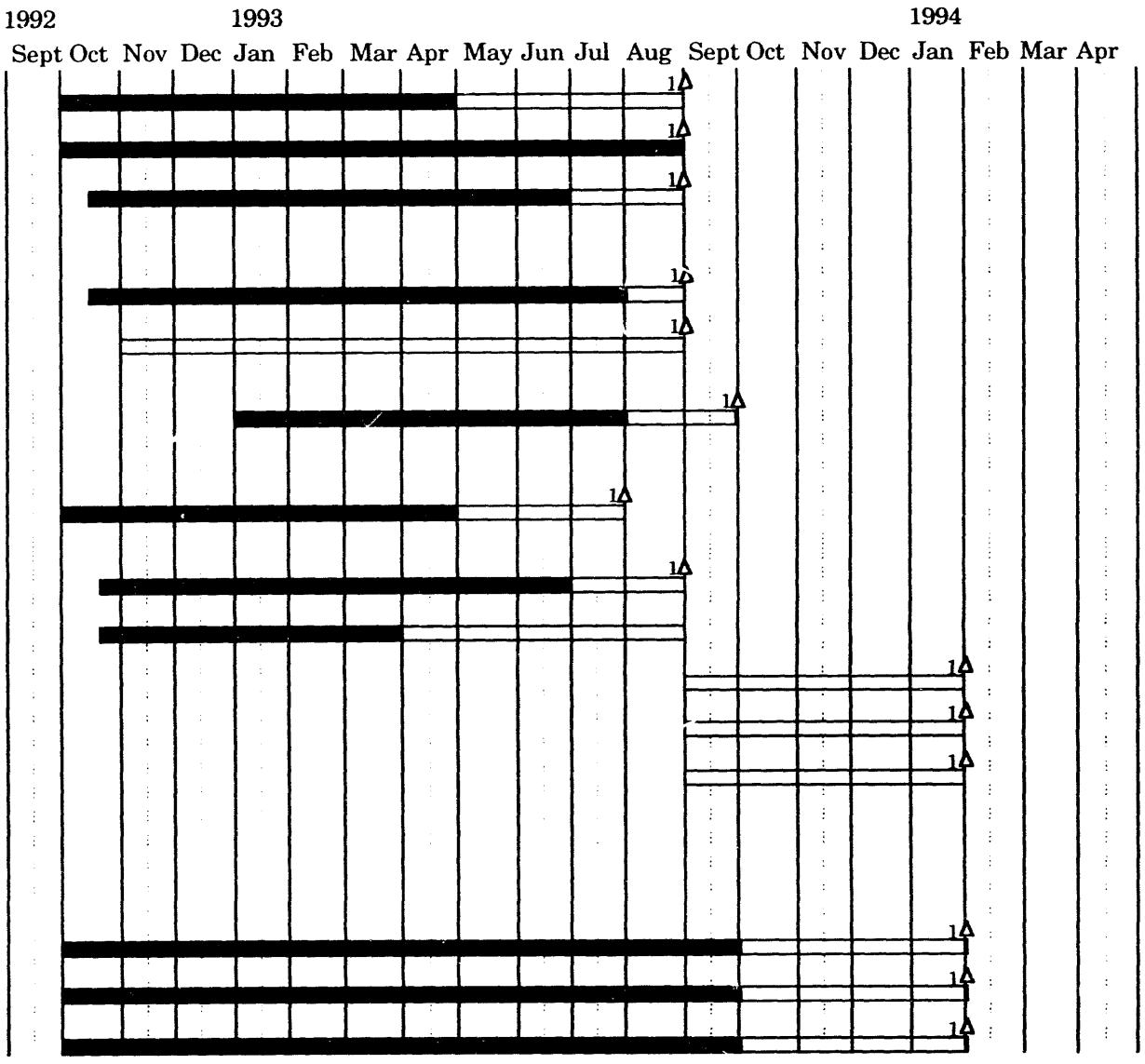

Task 5 - Final Report / Submission of Design Package

Subtask 5.1 Industrial Participants Submission

Subtask 5.2 Penn State Technical Preparation

Subtask 5.3 Report Preparation Support Services

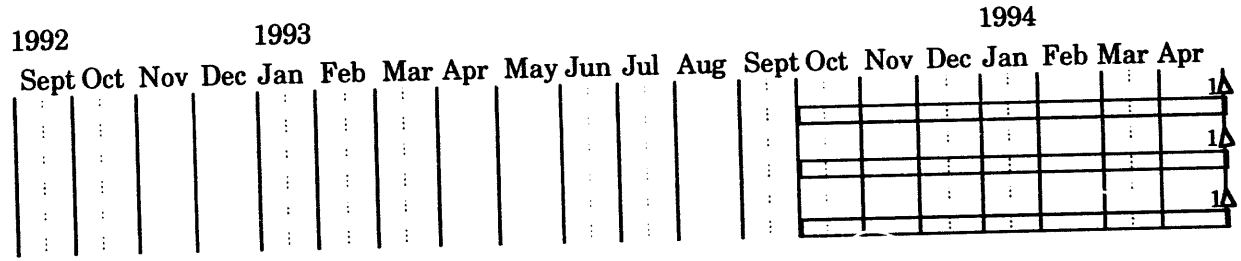

TABLE 1-1. MILESTONE DESCRIPTION

Milestone	Description	Planned Completion Date	Actual Completion Date
Task 1. Coal Beneficiation/Preparation			
Subtask 1.1. Identify/Procure Coals			
Subtask 1.1, No. 1	Establish selection criteria	10/15/92	10/15/92
Subtask 1.1, No. 2	Preliminary list of candidate coals	02/01/93	02/01/93
Subtask 1.1, No. 3	Short list	03/01/93	03/01/93
Subtask 1.1, No. 4	Final list based on boiler selection	05/01/93	08/10/93
Subtask 1.1, No. 5	Procure samples	06/01/93	08/15/93
Subtask 1.2. Determine Liberation Potential			
Subtask 1.2.1.	Conventional Washability Analysis on Type I and Type II Samples		
Subtask 1.2.1, No. 1	Review of published data	06/01/93	06/01/93
Subtask 1.2.1, No. 2	Analysis of Type I complete	06/15/93	07/27/93
Subtask 1.2.1, No. 3	Analysis of Type II complete	09/30/93	
Subtask 1.2.2.	Fine Washability Analysis on Type II and Type III Samples		
Subtask 1.2.2, No. 1	Review of published data	06/01/93	06/01/93
Subtask 1.2.2, No. 2	Analysis of Type II complete	07/01/93	09/30/93
Subtask 1.2.2, No. 3	Analysis of Type III complete	09/30/93	
Subtask 1.3. Produce Laboratory-Scale Quantities of MCWM			
Subtask 1.3.1, No. 1	Identify Cleaning Strategies	10/30/93	
Subtask 1.3.2,	Evaluate Conventional Gravity Separations		
Subtask 1.3.2, No. 1	Test work on Type I complete	09/01/93	09/01/93
Subtask 1.3.2, No. 2	Test work on Type II complete	11/15/93	
Subtask 1.3.2, No. 3	Test work on Type III complete	12/31/93	
Subtask 1.3.3.	Evaluate Fine Gravity Separations		
Subtask 1.3.3, No. 1	Cyclone test rig set-up	11/30/92	11/30/92
Subtask 1.3.3, No. 2	Initiate magnetite classification studies	12/01/92	12/01/92
Subtask 1.3.3, No. 3	Initiate batch centrifuge testing	02/01/93	02/02/93
Subtask 1.3.3, No. 4	Preliminary centrifuge data evaluation	01/31/94	
Subtask 1.3.3, No. 5	Procure continuous centrifuge	08/01/93	07/14/93
Subtask 1.3.3, No. 6	Initiate selectivity studies on Type III coals	06/01/93	06/01/93
Subtask 1.3.3, No. 7	Magnetite classification studies complete	06/15/93	06/15/93
Subtask 1.3.3, No. 8	Procure saturation magnetization analyzer	08/01/93	07/29/93
Subtask 1.3.3, No. 9	Procure variable speed pump	08/01/93	07/29/93
Subtask 1.3.3, No. 10	Preliminary test work complete	04/01/94	
Subtask 1.3.4.	Evaluate Advanced Froth Flotation		
Subtask 1.3.4, No. 1	Reagent selection	06/01/93	06/01/93
Subtask 1.3.4, No. 2	Initiate test work on Type II samples	06/15/93	08/31/93
Subtask 1.3.4, No. 3	Initiate test work on Type III samples	07/01/93	06/15/93

Milestone	Description	Planned Completion Date	Actual Completion Date
Subtask 1.3.4, No. 4	Type II test work complete	10/31/93	
Subtask 1.3.4, No. 5	Type III test work complete	08/31/93	07/31/93
Subtask 1.3.4, No. 6	Data evaluation completed	12/31/93	
Subtask 1.3.5. Evaluate Column Flotation			
Subtask 1.3.5, No. 1	Complete column design	05/01/93	05/01/93
Subtask 1.3.5, No. 2	Procure bubble generators	06/01/93	06/01/93
Subtask 1.3.5, No. 3	Complete column fabrication	07/31/93	09/01/93
Subtask 1.3.5, No. 4	Complete test work	12/31/93	
Subtask 1.3.6. Evaluate Selective Agglomeration			
Subtask 1.3.6, No. 1	Initiate wetting studies	01/15/93	01/15/93
Subtask 1.3.6, No. 2	Initiate 3-phase aggregation studies	01/31/93	01/31/93
Subtask 1.3.6, No. 3	Fabricate test cell	02/15/93	02/15/93
Subtask 1.3.6, No. 4	Complete preliminary test work on Type II samples	11/15/93	
Subtask 1.3.6, No. 5	Complete preliminary test work on Type III samples	09/15/93	09/15/93
Subtask 1.3.6, No. 6	Complete detailed studies on Type II samples	03/01/94	
Subtask 1.3.7. Investigate Solid-Liquid Separations			
Subtask 1.3.7, No. 1	Preliminary evaluation complete	09/30/93	
Subtask 1.3.7, No. 2	Initiate studies on test coals	09/30/93	
Subtask 1.3.7, No. 3	Complete studies on test coals	11/30/93	
Subtask 1.3.8. Select Cleaning Flowsheet(s)			
Subtask 1.3.8, No. 1	Establish flowsheet for Type I sample	12/01/93	
Subtask 1.3.9. Establish Required Size Consist for Slurry Formulation			
Subtask 1.3.9, No. 1	Complete for Type I samples	11/15/93	
Subtask 1.3.9, No. 2	Complete for Type II samples	12/15/93	
Subtask 1.3.9, No. 3	Complete for Type III samples	12/15/93	
Subtask 1.3.10. Investigate Conventional Ball Milling			
Subtask 1.3.10, No. 1	Complete test work for Type I samples	07/31/93	07/31/93
Subtask 1.3.10, No. 2	Complete test work for Type II samples	10/31/93	
Subtask 1.3.10, No. 3	Complete test work for Type III samples	10/31/93	
Subtask 1.3.11. Stirred Media Milling			
Subtask 1.3.11, No. 1	Procure stirred media mill	07/15/93	07/15/93
Subtask 1.3.11, No. 2	Complete test work on Type I samples	11/01/93	
Subtask 1.3.11, No. 3	Complete test work on Type II samples	11/01/93	
Subtask 1.3.11, No. 4	Complete test work on Type III samples	12/01/93	
Subtask 1.3.12. Investigate Attrition Milling			
Subtask 1.3.12, No. 1	Establish test procedure	11/01/93	
Subtask 1.3.12, No. 2	Evaluate preliminary data	12/01/93	
Subtask 1.3.12, No. 3	Complete evaluation	12/31/93	

Milestone	Description	Planned Completion Date	Actual Completion Date
Subtask 1.3.13. Lab-Scale Slurry Production			
Subtask 1.3.13, No. 1	Type I produced	09/15/93	
Subtask 1.3.13, No. 2	Type II produced	10/30/93	
Subtask 1.3.13, No. 3	Type III produced	12/31/93	
Subtask 1.3.14, No. 1	Modify viscosity and sedimentation rate models to account for PSD; compare model predictions to experimental observations	06/30/93	
Subtask 1.3.15, No. 1	Modify viscosity and sedimentation rate models to account for inter-particle attractive forces; compare model predictions to experimental observations	06/30/93	
Subtask 1.3.16, No. 1	Modify models to include effect of polymer additives, oxidation, and aggregate phenomena	03/01/94	
Subtask 1.4. Develop Dry Coal Cleaning Technique			
Subtask 1.4.1. Dry Grinding Studies			
Subtask 1.4.1, No. 1	Procure compressor system	03/15/93	03/15/93
Subtask 1.4.1, No. 2	Set up closed-circuit grinding system	05/15/93	05/15/93
Subtask 1.4.1, No. 3	Procure pilot-scale jet mill	05/30/93	05/30/93
Subtask 1.4.1, No. 4	Procedure established for Type III samples	08/31/93	08/31/93
Subtask 1.4.1, No. 5	Produce micronized product for dry beneficiation studies	11/01/93	
Subtask 1.4.2. Deagglomeration Studies			
Subtask 1.4.2, No. 1	Establish standardized test procedure	11/01/93	
Subtask 1.4.2, No. 2	Initiate humidity and reagent testing	12/01/93	
Subtask 1.4.2, No. 3	Procure laser diagnostic system	10/15/93	
Subtask 1.4.2, No. 4	Complete humidity testing	02/01/94	
Subtask 1.4.3. Dry Separations			
Subtask 1.4.3, No. 1	Procure power supplies	03/01/93	03/01/93
Subtask 1.4.3, No. 2	Fabricate prototype test unit	05/01/93	05/01/93
Subtask 1.4.3, No. 3	Complete preliminary testing	08/31/93	08/31/93
Subtask 1.4.3, No. 4	Complete testing	03/01/94	
Subtask 1.5. Produce MCWMs and Micronized Coal from Dry, Clean Coal			
Subtask 1.5.1, No. 1	Produce Micronized Coal from Dry, Clean Coal	02/01/94	
Subtask 1.5.2, No. 1	Product MCWM from Dry, Clean Coal	03/01/94	
Subtask 1.6. Produce MCWM and Dry, Micronized Coal for the Demonstration			
Subtask 1.6.1, No. 1	Shakedown dry, micronized coal circuit	07/31/93	
Subtask 1.6.2, No. 1	Complete CWM Preparation Facility	07/31/93	
Subtask 1.6.2, No. 2	Procure automated valves	08/31/93	
Subtask 1.6.2, No. 3	Install CWM equipment	09/30/93	
Subtask 1.6.3, No. 1	Shakedown CWM circuit	10/31/93	
Subtask 1.6.4, No. 1	Coal Cleaning	11/30/93	
Subtask 1.6.5, No. 1	Coal Micronizing	12/31/93	
Subtask 1.6.6, No. 1	MCWM Preparation	04/01/94	

Milestone	Description	Planned Completion Date	Actual Completion Date
Subtask 1.7. Project Management and Support			
Subtask 1.7.1, No. 1	Project Management and Technical Advisement	04/01/94	
Subtask 1.7.2, No. 1	Drafting/Technical Secretary Support	04/01/94	
Subtask 1.7.3, No. 1	Budget Management/Project Administration	04/01/94	
Task 2. Combustion Performance Evaluation			
Subtask 2.1. Boiler Retrofit			
Subtask 2.1.1, No. 1	Finalize burner/atomizer design	05/31/93	
Subtask 2.1.2, No. 1	Procure and install burner	08/31/93	
Subtask 2.1.3, No. 1	Optimize burner firing dry, micronized coal	09/30/93	
Subtask 2.1.4, No. 1	Optimize burner firing CWM	12/31/93	
Subtask 2.2. Fuel Evaluation in Research Boiler			
Subtask 2.2.1, No. 1	Test sample of Type I CWM	10/15/93	
Subtask 2.2.2, No. 1	Test sample of Type II CWM	11/30/93	
Subtask 2.2.3, No. 1	Test sample of Type III CWM	01/31/94	
Subtask 2.3. Performance Evaluation of MCWM and Dry, Micronized Coal in Demonstration Boiler			
	Dry, Micronized Coal Testing		
Subtask 2.3.1, No. 1	Procure fire supression system for the baghouse	06/01/93	
Subtask 2.3.1, No. 2	Modify conditioning screw	07/01/93	
Subtask 2.3.1, No. 3	100-hour milestone firing dry, micronized coal	10/22/93	
Subtask 2.3.2, No. 1	200-hour milestone firing dry, micronized coal	10/29/93	
Subtask 2.3.3, No. 1	300-hour milestone firing dry, micronized coal	11/05/93	
Subtask 2.3.4, No. 1	400-hour milestone firing dry, micronized coal	11/12/93	
Subtask 2.3.5, No. 1	500-hour milestone firing dry, micronized coal	11/19/93	
Subtask 2.3.6, No. 1	600-hour milestone firing dry, micronized coal	11/26/93	
Subtask 2.3.7, No. 1	700-hour milestone firing dry, micronized coal	12/03/93	
Subtask 2.3.8, No. 1	800-hour milestone firing dry, micronized coal	12/10/93	
Subtask 2.3.9, No. 1	900-hour milestone firing dry, micronized coal	12/17/93	
Subtask 2.3.10, No. 1	1,000-hour milestone firing dry, micronized coal	12/31/93	
Subtask 2.3.11, No. 1	Technical Advisement by CE	12/31/93	
	MCWM Testing		
Subtask 2.3.12, No. 1	100-hour milestone firing micronized CWM	01/28/94	
Subtask 2.3.13, No. 1	200-hour milestone firing micronized CWM	02/04/94	
Subtask 2.3.14, No. 1	300-hour milestone firing micronized CWM	02/11/94	
Subtask 2.3.15, No. 1	400-hour milestone firing micronized CWM	02/18/94	
Subtask 2.3.16, No. 1	500-hour milestone firing micronized CWM	02/25/94	
Subtask 2.3.17, No. 1	600-hour milestone firing micronized CWM	03/04/94	
Subtask 2.3.18, No. 1	700-hour milestone firing micronized CWM	03/11/94	
Subtask 2.3.19, No. 1	800-hour milestone firing micronized CWM	03/18/94	
Subtask 2.3.20, No. 1	900-hour milestone firing micronized CWM	03/25/94	
Subtask 2.3.21, No. 1	1,000-hour milestone firing micronized CWM	04/01/94	
Subtask 2.3.22, No. 1	Technical advisement by CE	04/01/94	
	Evaluate Erosion/Deposition Characteristics		
Subtask 2.3.23, No. 1	Identify erosion and deposition regimes	11/30/92	11/30/92
Subtask 2.3.24, No. 1	Model simultaneous erosion and deposition	09/30/93	

Milestone	Description	Planned Completion Date	Actual Completion Date
Subtask 2.3.25, No. 1	Procure Zirconia/Platinum sensor/recorder	10/15/93	
Subtask 2.3.25, No. 2	Compare heat transfer surface performance firing micronized dry coal and CWM	02/28/94	
Subtask 2.3.26, No. 1	Develop procedure for determining optimum convective section gas velocity	02/28/94	
Subtask 2.3.27, No. 1	Comparison of performance of three tube materials	03/31/94	
Subtask 2.4. Evaluate Emissions Reduction Strategies			
Subtask 2.4.1, No. 1	Determine emissions from micronized coal testing	12/31/93	
Subtask 2.4.2, No. 1	Determine emissions from CWM testing	04/01/94	
Subtask 2.5. Project Management and Support			
Subtask 2.5.1, No. 1	Project management and advisement	04/01/94	
Subtask 2.5.2, No. 1	Staff supervision, test planning, and quality control	04/01/94	
Subtask 2.5.3, No. 1	Data reduction and interpretation	04/01/94	
Subtask 2.5.4, No. 1	Drafting/technical secretarial support	04/01/94	
Subtask 2.5.5, No. 1	Budget management/project administration	04/01/94	
Task 3. Engineering Design			
Subtask 3.1. Micronized CWM/Dry, Micronized Coal Preparation Facilities			
Subtask 3.1.1, No. 1	Design of micronized CWM preparation facility by Amax	11/15/93	
Subtask 3.1.2, No. 1	Design of dry micronized coal preparation system by EER	10/15/93	
Subtask 3.2. Fuel Handling			
Subtask 3.2.1, No. 1	Design of fuel system by EER	10/15/93	
Subtask 3.2.2, No. 1	Technical support and design of fuel system by PSU	10/15/93	
Subtask 3.3. Burner System			
Subtask 3.3.1, No. 1	Design of burner by CE for selected boiler	09/15/93	
Subtask 3.3.2, No. 1	Design of auxiliary components by EER	11/15/93	
Subtask 3.4. Ash Removal, Handling, and Disposal			
Subtask 3.4.1, No. 1	Design of ash system by EER	09/30/93	
Subtask 3.5. Air Pollution Control			
Subtask 3.5.1, No. 1	Design of emission control by EER	11/15/93	
Subtask 3.6. Integrate Engineering Design			
Subtask 3.6.1, No. 1	Integrate system components	01/15/94	

Milestone	Description	Planned Completion Date	Actual Completion Date
Subtask 3.7. Project Management and Support			
Subtask 3.7.1, No. 1	Project management and technical advisement	01/15/94	
Subtask 3.7.2, No. 1	Penn State technical review	01/15/94	
Subtask 3.7.3, No. 1	Drafting/technical secretarial support	01/15/94	
Subtask 3.7.4, No. 1	Budget management/project administrtaion	01/15/94	
Task 4. Engineering and Economic Analysis			
Subtask 4.1, No. 1	Survey Boiler Population/Identify Boilers for Conversion	08/31/93	
Subtask 4.2, No. 1	Identify Appropriate Cost-Estimating Technologies	05/31/93	
Subtask 4.3, No. 1	Estimate Basic Costs of New Technologies	08/31/93	
Subtask 4.4. Process Analysis of MCWM and Dry, Micronized Coal			
Subtask 4.4.1, No. 1	Penn State Analysis	08/31/93	
Subtask 4.4.2, No. 1	Industrial Participants Assistance/Advisement	08/31/93	
Subtask 4.5, No. 1	Analyze/Identify Transportation Cost of Commercial Sources of MCWM and Cleaned Coal for Dry, Micronized Coal Production	09/30/93	
Subtask 4.6, No. 1	Determine Community Spillovers	07/31/93	
Subtask 4.7, No. 1	Regional Market Considerations and Impacts	08/31/93	
Subtask 4.8. Integrate the Analysis			
Subtask 4.8.1, No. 1	Penn State Review of Industrial Participants Contribution	01/31/94	
Subtask 4.8.2, No. 1	Penn State Integration of the Analysis	01/31/94	
Subtask 4.8.3, No. 1	Industrial Participants Assistance in Preparing, and Review of, the Integrated Analysis	01/31/94	
Subtask 4.9. Project Management and Support			
Subtask 4.9.1, No. 1	Project Management and Advisement	02/01/94	
Subtask 4.9.2, No. 1	Drafting/Technical Secretarial Support	02/01/94	
Subtask 4.9.3, No. 1	Budget Management/Project Administration	02/01/94	
Task 5. Final Report/Submission of Design Package			
Subtask 5.1, No. 1	Industrial Participants Submission to Penn State/Review Final Package	04/30/94	
Subtask 5.2, No. 1	Penn State Technical Preparation	04/30/94	
Subtask 5.3, No. 1	Report Preparation Support Services	04/30/94	

Table 2-1. Characteristics of the test coals.

Sample Designation[a]	I-1	II-1	II-2	III-1	III-2
Seam	Taggart	Lower Kittanning	Indiana VII	Upper Freeport	Pittsburgh
State	Virginia	Pennsylvania	Indiana	Pennsylvania	Pennsylvania
Counties	Wise, Lee	Armstrong, Clarion, Jefferson	Sullivan, Knox	Indiana, Armstrong, Jefferson	Greene, Washington
Etimated Reserves (Million tons)	50	480	400	8000	6000
Proximate Analysis					
Moisture %	1.6	2.1	12.7	1.4	2.6
Volatile Matter %	34.1	33.1	30.4	28.0	34.9
Fixed Carbon %	62.2	55.5	49.4	59.1	55.8
Ash %	2.1	9.4	7.5	11.5	6.7
Total Sulfur %	0.59	0.78	0.42	3.07	1.76
Hardgrove Grindability Index	47	68	51	76	56

[a]The three coal categories are:

- Type I - coals which can meet the specifications at high yield with little or no cleaning.
- Type II - coals which can be cleaned by conventional means and can meet the specifications at fairly high yield.
- Type III - coals which can be cleaned to meet the specifications but only at low yield using conventional cleaning technology.

2.2 Subtask 1.2 Determine Liberation Potential

Test coal samples were subjected to a series of float-sink tests to determine the level of cleaning needed to achieve the required grade of <5% ash and <1% total sulfur. Samples of the Taggart, Lower Kittanning, Upper Freeport and Pittsburgh seam coals were crushed to a nominal -6.35 mm (-1/4") using a jaw crusher followed by screening at 1/4", 28 mesh and 100 mesh. The +1/4", 1/4"x28 mesh, and 28x100 mesh size fractions were separated under gravity using Certigrav solutions of various relative densities, while the -100 mesh fraction was separated using a centrifuge. Separate samples of the Lower Kittanning, Upper Freeport and Pittsburgh seam coal were crushed to a nominal -28 mesh. The ground products were then screened at 100 mesh. The +100 mesh size fraction was separated by gravity float-sink and the -100 mesh fraction was separated using centrifugal float-sink at the same relative densities. Each size/ density fraction was analyzed for ash and sulfur contents. Analyses of four of the five coal samples (except the recently procured Indiana VII seam coal) have been completed and the results are presented in Tables 2.2 - 2.5.

The Taggart seam coal can meet the product specification without any cleaning. However, the float/sink separations were conducted on the -1/4" fraction for completeness. The results indicate that separating the coal at a relative density of 1.3 reduced the ash content from 2.1 to 1.4% with 92% yield, while the sulfur reduction was minimal.

For the Lower Kittanning seam coal, the product specification can be met for the -1/4" coal at a separation density of 1.35 with about a 75% yield (5% ash and 0.80% sulfur). The fine coal washability analysis indicates that by reducing the top size to 28 mesh, the yield can be increased to 82% (5% ash and 0.76% sulfur) at a separation density of 1.37.

Despite the high ash and sulfur contents of the ROM Upper Freeport seam coal, it can be cleaned with a product of 5% ash and 0.98% sulfur at a separation density of 1.37 with a relatively high yield (76%). This indicates that the mineral matter of this coal is well liberated by crushing. Further size reduction to -28 mesh increased the yield to 85% with a cleaner product (5% ash and 0.92% sulfur) at a separation density of 1.45.

The results for the Pittsburgh seam coal showed that the ash specification can be easily met with greater than 90% yield at a separation density of 1.40. However, it would be difficult to obtain a product of <1% sulfur without a significant yield loss. Further liberation studies will be conducted on this coal ground to finer sizes (-100 mesh).

Liberation Modeling

While the function of comminution in this case is to produce an advantageous size distribution that subsequently produces a highly concentrated MCWSF that combusts efficiently, a secondary aspect is the associated liberation of undesirable materials in the coal - *i.e.*, mineral matter that produces particulates and SO_2 upon combustion. If additional liberation is achieved,

Table 2-2. Washability analysis of the Taggart seam coal (Sample I-1) crushed to a nominal -1/4".

Rel. Den.	+1/4"			1/4"x28 Mesh			28x100 Mesh			-100 Mesh			Composite		
	Wt.,%	Ash,%	T.S.%	Wt.,%	Ash,%	T.S.%	Wt.,%	Ash,%	T.S.%	Wt.,%	Ash,%	T.S.%	Wt.,%	Ash,%	
1.3 F	93.8	1.59	0.56	93.7	1.42	0.57	90.5	0.99	0.58	73.8	0.91	0.59	92.5	1.40	
1.4 F	98.9	1.96	0.58	98.9	1.78	0.58	97.5	1.35	0.60	92.7	1.21	0.59	98.5	1.76	
1.5 F	99.8	2.15	0.58	99.6	1.89	0.59	98.7	1.51	0.60	97.7	1.37	0.60	99.5	1.90	
2.0 S	100.	2.18	0.60	100.	2.04	0.59	100.	2.02	0.61	100.	2.66	0.61	100.	2.10	
Wt.,%	25.2			61.5			8.5			4.7			100.		

Table 2-3. Washability analysis of the Lower Kittanning seam coal (Sample II-1).

a) crushed to a nominal -1/4".

Rel. Den.	+1/4"			1/4"x28 Mesh			28x100 Mesh			-100 Mesh			Composite	
	Wt.,%	Ash,%	T.S.%	Wt.,%	Ash,%	T.S.%	Wt.,%	Ash,%	T.S.%	Wt.,%	Ash,%	T.S.%	Wt.,%	Ash,%
1.3 F	49.8	4.37	0.76	62.6	3.83	0.79	59.2	3.00	0.80	28.5	2.98	0.76	56.4	3.67
1.4 F	82.1	7.42	0.80	90.1	6.01	0.83	82.9	4.75	0.81	72.3	5.64	0.78	85.7	5.95
1.5 F	93.6	9.48	0.80	96.1	7.04	0.84	87.8	5.54	0.82	83.9	7.44	0.78	93.0	7.17
1.6 F	98.3	10.6	0.79	98.7	7.69	0.84	89.7	6.26	0.83	88.6	8.50	0.81	96.0	7.94
2.0 F	100.	11.2	0.79	99.5	7.98	0.84	92.7	7.00	0.86	91.6	9.56	0.84	97.6	8.43
2.0 S	100.	11.2	0.79	100.	8.31	0.84	100.	12.8	0.87	100.	16.1	0.99	100.	10.4
Wt.,%	13.7			58.1			16.8			11.4			100.	

b) crushed to a nominal -28 mesh.

Rel. Den.	28x100 Mesh			-100 Mesh			Composite		
	Wt.,%	Ash,%	T.S.%	Wt.,%	Ash,%	T.S.%	Wt.,%	Ash,%	T.S.%
1.3 F	64.4	3.13	0.75	48.6	2.45	0.75	59.8	2.65	0.75
1.4 F	86.8	5.15	0.76	84.3	5.47	0.77	86.1	5.38	0.76
1.5 F	91.9	6.24	0.76	89.4	6.33	0.79	91.2	6.30	0.76
1.6 F	95.7	7.29	0.76	93.8	7.12	0.79	95.2	7.17	0.77
2.0 F	98.1	8.24	0.76	96.3	7.95	0.79	97.6	8.03	0.77
2.0 S	100.	9.47	0.79	100.	10.9	0.90	100.	9.88	0.82
Wt.,%	70.7			29.3			100.		

Table 2-4. Washability analysis of the Upper Freeport seam coal (Sample III-1).

a) crushed to a nominal -1/4".

Rel. Den.	+1/4"			1/4"x28 Mesh			28x100 Mesh			-100 Mesh			Composite		
	Wt.,%	Ash,%	T.S.%	Wt.,%	Ash,%	T.S.%	Wt.,%	Ash,%	T.S.%	Wt.,%	Ash,%	T.S.%	Wt.,%	Ash,%	
1.3 F	33.6	4.61	0.96	57.2	3.62	0.87	63.3	2.64	0.85	45.4	2.83	0.80	53.4	3.57	
1.4 F	74.0	7.05	1.50	85.1	5.26	1.09	83.3	4.00	0.98	73.9	4.64	0.90	82.2	5.30	
1.5 F	80.2	8.10	1.52	89.1	5.80	1.22	87.6	4.61	1.07	83.2	5.42	0.95	87.0	5.95	
1.6 F	85.7	9.41	1.58	91.3	6.24	1.32	89.9	5.07	1.18	89.6	6.85	1.21	90.1	6.61	
2.0 F	93.1	11.7	1.95	94.1	7.02	1.60	92.5	5.86	1.34	93.8	7.90	1.63	93.7	7.64	
2.0 S	100.	16.0	2.61	100.	10.5	2.80	100.	10.7	2.89	100.	12.2	3.21	100.	11.5	
Wt.,%	14.9			62.9			13.2			9.0			100.		

b) crushed to a nominal -28 mesh.

Rel. Den.	28x100 Mesh			-100 Mesh			Composite		
	Wt.,%	Ash,%	T.S.%	Wt.,%	Ash,%	T.S.%	Wt.,%	Ash,%	T.S %
1.3 F	68.0	3.10	0.80	50.0	2.36	0.76	62.5	2.58	0.78
1.4 F	86.0	4.60	0.87	76.7	4.43	0.95	83.2	4.48	0.89
1.5 F	89.5	5.10	0.94	84.4	5.39	1.02	87.9	5.30	0.96
1.6 F	91.7	5.82	0.98	89.1	6.78	1.41	90.9	6.49	1.11
2.0 F	94.0	6.60	1.13	90.6	6.86	1.24	93.0	6.62	1.14
2.0 S	100.	10.37	2.52	100.	12.84	3.66	100.	11.12	2.86
Wt.,%	69.6			30.4			100.		

Table 2-5. Washability analysis of the Pittsburgh seam coal (Sample III-2).

a) crushed to a nominal -1/4".

Rel. Den.	+1/4"			1/4"x28 Mesh			28x100 Mesh			-100 Mesh			Composite		
	Wt.,%	Ash,%	T.S.%	Wt.,%	Ash,%	T.S.%	Wt.,%	Ash,%	T.S %	Wt.,%	Ash,%	T.S %	Wt.,%	Ash,%	
1.3 F	64.0	3.57	1.18	66.3	3.09	1.22	65.5	2.65	1.12	38.2	1.88	1.06	63.0	3.03	
1.4 F	91.8	5.04	1.54	93.5	4.69	1.54	90.9	3.75	1.33	76.8	3.91	1.18	91.2	4.58	
1.5 F	95.6	5.63	1.64	97.0	5.20	1.63	94.7	4.33	1.42	91.7	5.61	1.38	95.9	5.23	
1.8 F	99.5	6.90	1.68	99.2	5.78	1.71	97.3	4.97	1.53	96.4	5.77	1.34	98.8	5.93	
2.0 F	100.	7.09	1.74	99.5	5.91	1.73	97.8	5.30	1.56	98.4	7.42	1.60	99.3	6.24	
2.0 S	100.	7.09	1.74	100.	6.23	1.79	100.	6.76	1.73	100.	8.55	1.89	100.	6.70	
Wt.,%	21.6			57.3			11.5			9.6			100.		

b) crushed to a nominal -28 mesh.

Rel. Den.	28x100 Mesh			-100 Mesh			Composite		
	Wt.,%	Ash,%	T.S.%	Wt.,%	Ash,%	T.S.%	Wt.,%	Ash,%	T.S %
1.3 F	72.2	2.67	1.11	53.3	1.80	1.00	66.5	2.06	1.08
1.4 F	94.8	4.45	1.32	89.1	4.22	1.27	93.1	4.29	1.30
1.5 F	95.5	4.65	1.35	94.5	4.80	1.29	95.2	4.75	1.33
1.6 F	97.4	5.00	1.39	96.4	5.01	1.31	97.1	5.01	1.36
2.0 F	98.8	5.48	1.46	97.5	5.18	1.31	98.4	5.27	1.42
2.0 S	100.	6.26	1.66	100.	6.93	1.77	100.	6.46	1.69
Wt.,%	69.4			30.6			100.		

then the undesirable materials should be separated from the coal prior to combustion. However, taking advantage of the liberation/separation aspect requires proper integration of the fuel preparation system. In order to do this optimally, it is necessary to be able to predict the liberation achieved for the particular devices utilized.

Liberation modeling, unfortunately, is not easily accomplished. From a comminution viewpoint, the liberation model needs to state what fraction of material of composition c_l and size x_k that breaks to size x_i will be of composition c_j. Then the liberation model combined with the appropriate comminution model will predict the washability analysis of the comminuted product -

SIZE INTERVAL:	1	2	—	n
COMPOSITION INTERVAL				
1	$p_{11}a_{11}$	$p_{21}a_{21}$		$p_{n1}a_{n1}$
2	$p_{12}a_{12}$	$p_{22}a_{22}$		$p_{n2}a_{n2}$
-				
-				
-				
m	$p_{1m}a_{1m}$	$p_{2m}a_{2m}$		$p_{nm}a_{nm}$

The p_{ij} values are calculated by

$$p_{ij} = \sum_k \sum_l d_{i;kl}\phi_{j;ikl}f_{kl} \qquad (2\text{-}1)$$

where $d_{i:kl}$ is the comminution model that predicts what fraction of material of size x_k and composition c_l, f_{kl} will break to size x_i, and $\phi_{j:ikl}$ is the liberation model and is calculated as

$$\phi_{j;ikl} = M(c_j;ikl) - M(c_{j-1};ikl) \qquad (2\text{-}2)$$

where $M(c;ikl)$ is the cumulative mass of material of size x_i, created by comminuting material of size x_k and composition c_l, that is of composition c or less. A typical plot of M vs. c, for various degrees of liberation, is shown in Figure 2-1.

If a washability analysis is performed on the size x_i material, then the M vs. c plot is known as the elementary ash curve. Consequently, if the elementary ash curve for materials of size xi, created by comminuting material of size x_k and composition c_l can be predicted, then we have a liberation model.

The a_{ij} values, for example the expected ash content of material in size class i and composition class j, are calculated by

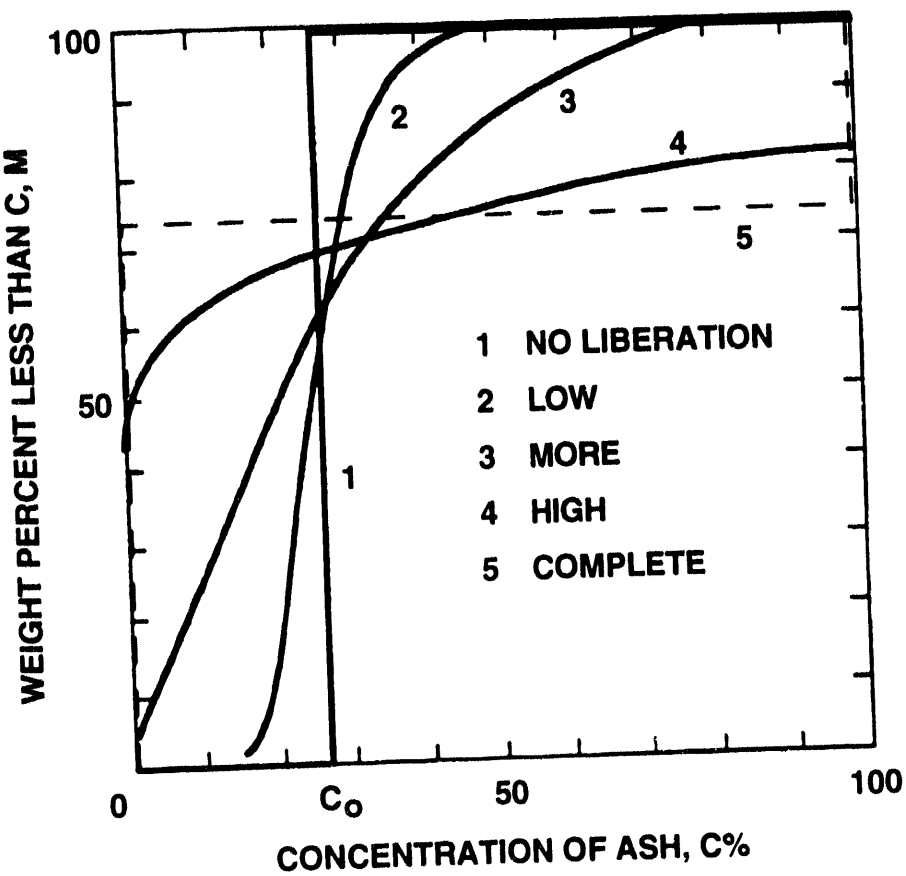

Figure 2-1. Typical M-C plot for various degrees of liberation

$$a_{ij}\, p_{ij} = \sum_{k} \sum_{l} d_{i;k\,l} \alpha_{j;k\,l} f_{k\,l} \qquad (2\text{-}3)$$

where $\alpha_{j;ikl}$ is the ash unit value and is calculated as

$$\alpha_{j;ikl} = A(c_j;ikl) - A(c_{j-1};ikl) \qquad (2\text{-}4)$$

where A(c;ik*l*) is the cumulative ash units of material of size x_i, created by comminuting material of size x_k and composition c_l, that is of composition c or less.

A typical plot of A vs. M for various degrees of liberation is shown in Figure 2-2. This plot is known as the Mayer Curve. Since

$$dA(c;ikl)/dM(c;ikl) = c \qquad (2\text{-}5)$$

it follows that

$$A(c_j;ikl) = \int_0^{c_j} c\, dM(c_j;ikl) \qquad (2\text{-}6)$$

Thus, in order to predict the product washability analysis, it is necessary to predict the M vs. c curves.

Given the above algebra, it is necessary to determine the functional forms for the M vs. c curves. This is a very time consuming process. Starting with a minus 1 1/2" air table product, for example, size and composition samples must be prepared; e.g., 4 mesh x 6 mesh, 30-40% ash (1.60 x 1.80). From a one ton sample, only 500-1,000 gms of this material are obtained. The sample is then comminuted, the product is fractionated on the basis of size and relative density, and the ash contents determined, i.e., a washability analysis is performed. The elementary ash curves are plotted, analyzed and fitted. This protocol is being performed on several such samples.

Initial experimental results following this protocol have indicated that the joint transfer function, dij;kl, must be calculated directly instead of calculating the marginal transfer function, $d_{i;kl}$, and multiplying it by $\phi_{j;ikl}$, in order to get the joint transfer function. This is necessary because, for example, material of size 1 and composition 2 can break to produce material of size 2 and composition 2, which in turn can break to produce material of size 3 and composition 1. Hence,

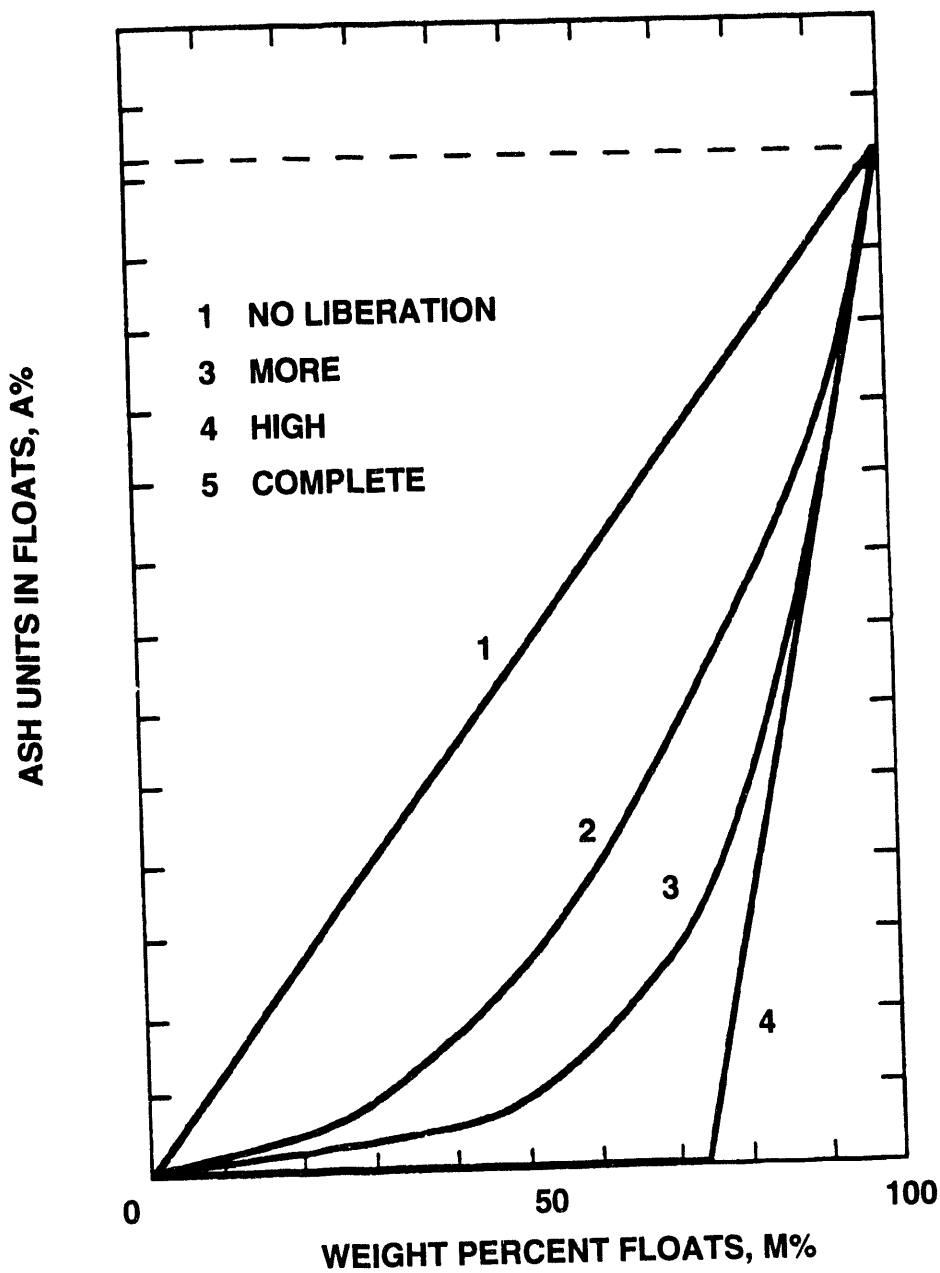

Figure 2-2. Mayer Curves for various degrees of liberation

$$p_{ij} = \sum_{k} \sum_{k} d_{ij;kl}\, f_{kl} \qquad (2\text{-}7)$$

For the roll crusher being used to produce the experimental results,

$$p'_{ij;kl} = \begin{cases} 0 & , i=k,\ j \neq l \\ (1-a_{ij}) & , i=k, j=l \\ (1-a'_{ij})p'_{ij;kl}, & i>k \end{cases} \qquad (2\text{-}8)$$

where

$$p'_{ij;kl} = \begin{cases} 0 & , i \neq k \\ b_{i;kl}\phi_{j;ikl}a_{kl} + \sum_{n} \sum_{m=k+1}^{i=l} b_{i;mn}\phi_{j;imn}a'_{mn}p'_{mn;kl}, & i>k \end{cases} \qquad (2\text{-}9)$$

and a_{ij} and a'_{ij} are the probabilities of material of size i and composition j being broken as it enters the crusher and after being produced from larger materials breaking in the crusher, respectively. Work is continuing using this model.

2.3 Subtask 1.3 Produce Laboratory-Scale Quantities of Micronized Coal-Water Slurry Fuels

Depending on the relative ease of cleaning (Type II or Type III), a general strategy involving appropriate combinations of fine-gravity and surface-based separations has been adopted.

Evaluate Fine Gravity Separations

The prediction of the performance of dense-medium separation devices is difficult due in part to the interaction or compounding of operating variables such as the flow rate, the magnitude of the g-force, turbulence, and the characteristics of the dense medium. The effects of various operating conditions on dense-medium separation using a batch free-settling model have been examined previously (Klima and Luckie 1989, 1990). In this case, the model was based on the assumption that particles separated under free-settling conditions in a medium of constant density within a uniform field. Thus, a pseudo dense-medium liquid, such as a suspension, which is not stable, cannot be accurately simulated because of the density gradients which will exist within the liquid. Furthermore, this model was not able to simulate the effect of a change in solids concentration on separation efficiency.

Recently, a hindered-settling model was developed and used to evaluate the classification behavior of a polydisperse particulate system (Austin et al., 1992). This model was used to investigate the variation of the particle size distribution with time under different settling conditions. Dense-medium separation can be viewed in a similar fashion whereby the dense-medium solids, coal, and refuse, settle in water. Since the principle of separation also depends on the differential settling rate of these particles in the suspension, it should be possible to analyze dense-medium separation using the batch hindered-settling model.

Consider the cylindrical batch device shown in Figure 2-3. If particles are in motion in such a device due to the settling (convection) and mixing (diffusion), it is possible to account for their movement into and out of an element within this device. In a hindered-settling regime, the movement of particles of a particular size and density, due to both convection and diffusion, would be a function of the concentration of these particles in the element. Since the separation occurs primarily in the vertical (z) direction, the separating force (gravity) and the level of mixing are important only in this direction. Thus, if the mixing is characterized by a single eddy-diffusion coefficient, then the rate of accumulation for particles of size x to $x+dx$ and density ρ to $\rho+d\rho$ in an element z to $z+dz$ is given by

$$\frac{\partial \phi(x,\rho,z,t)}{\partial t} = D\frac{\partial^2 \phi(x,\rho,z,t)}{\partial z^2} - \frac{\partial (V(x,\rho,z,t)\phi(x,\rho,z,t)}{\partial z} \qquad (2\text{-}10)$$

The rate of accumulation for the liquid in the same element is given by

$$\frac{\partial (1-\phi(z,t))}{\partial t} = -\frac{\partial (U_f(z,t)(1-\phi(z,t))}{\partial z} \qquad (2\text{-}11)$$

where

$\phi(x,\rho,z,t)$ = volume fraction of particles of size x to $x+dx$ and density $\rho+d\rho$, in the element at position z to $z+dz$ and time t.

D = diffusion coefficient.

$V(x,\rho,z,t)$ = velocity of particles of size x to $x+dx$ and density $\rho+d\rho$ at location z to $z+dz$ and time t, with respect to the wall of the container.

$\phi(z,t)$ = total volume fraction occupied by the solids in the element at position z to $z+dz$ and time t.

$1-\phi(z,t)$ = volume fraction occupied by the liquid in the element at position z to $z+dz$ and time t.

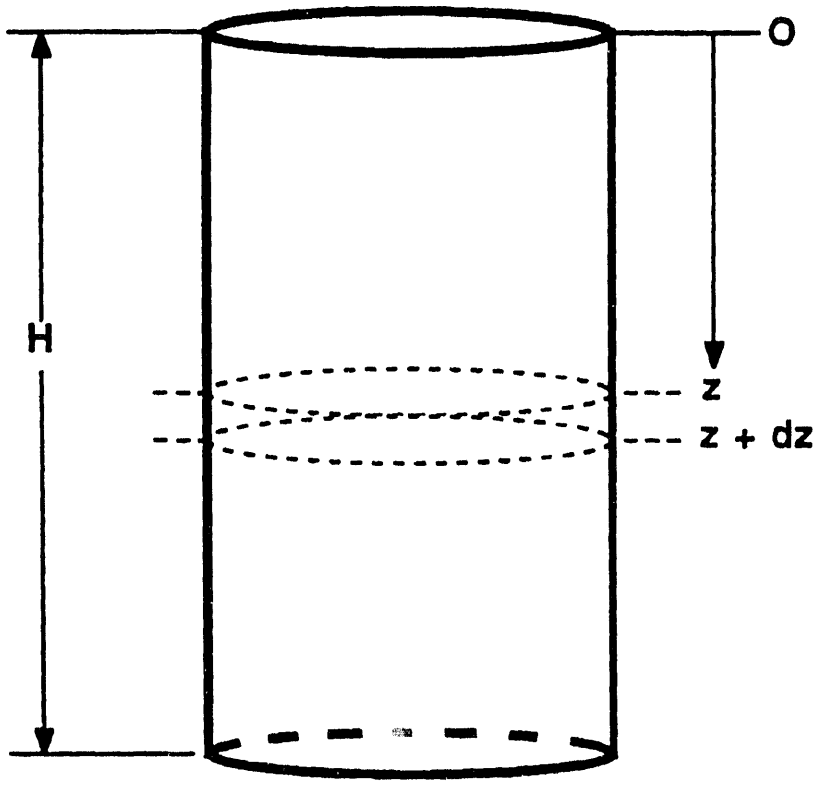

Figure 2-3. Batch settling column

$U_f(z,t)$ = velocity of the liquid with respect to the wall in the element at position z to $z+dz$ and time t.

Now consider the cylinder in Figure 2-3 with particles uniformly dispersed in water. If these particles are allowed to settle for some time t and then the cylinder is cut at some fractional height L/H, the particles below this cut height can be defined as the refuse and the particles above the cut height as the product. Since the particle size/density distribution at any location can be estimated from the solution to Equations 2-10 and 2-11 (Lee, 1989; Austin et al., 1992), the fraction of feed particles of size x and density ρ which reports to the product after time t is given by

$$K(\rho;x,t) = \frac{\int_0^{\frac{L}{H}} \phi(x,\rho,z,t)dz'}{\phi_o(x,\rho)} \qquad (2\text{-}12)$$

where

$\phi_O(\rho,x)$ = initial volume fraction of particles of size x and density ρ.

$\phi(x,\rho,z,t)$ = volume fraction of particles of size x and density ρ at location z of the settling column after time t.

z' = z/H

A plot of a set of values from Equation 2-12 versus ρ for a given particle size is called a fractional recovery (partition) curve. As is common in gravity concentration, this curve can be characterized by a location modulus and a distribution modulus. The location modulus is defined as the density of those particles which have an equal probability of reporting to either the clean coal or to the refuse, *i.e.*, the density corresponding to a fractional recovery value of 0.5. This location modulus for a given size is denoted by $\rho_{50}(x)$ and can be adopted as the separation density for that size (Figure 2-4). A distribution modulus is used to characterize the efficiency of separation. In this case, the probable error (Ecart Probable Moyen) for a given size is defined as

$$E_p(x) = (\rho_{25}(x) - \rho_{75}(x))/2 \qquad (2\text{-}13)$$

where

$\rho_{25}(x)$ = density corresponding to 0.25 on the fractional recovery curve

$\rho_{75}(x)$ = density corresponding to 0.75 on the fractional recovery curve

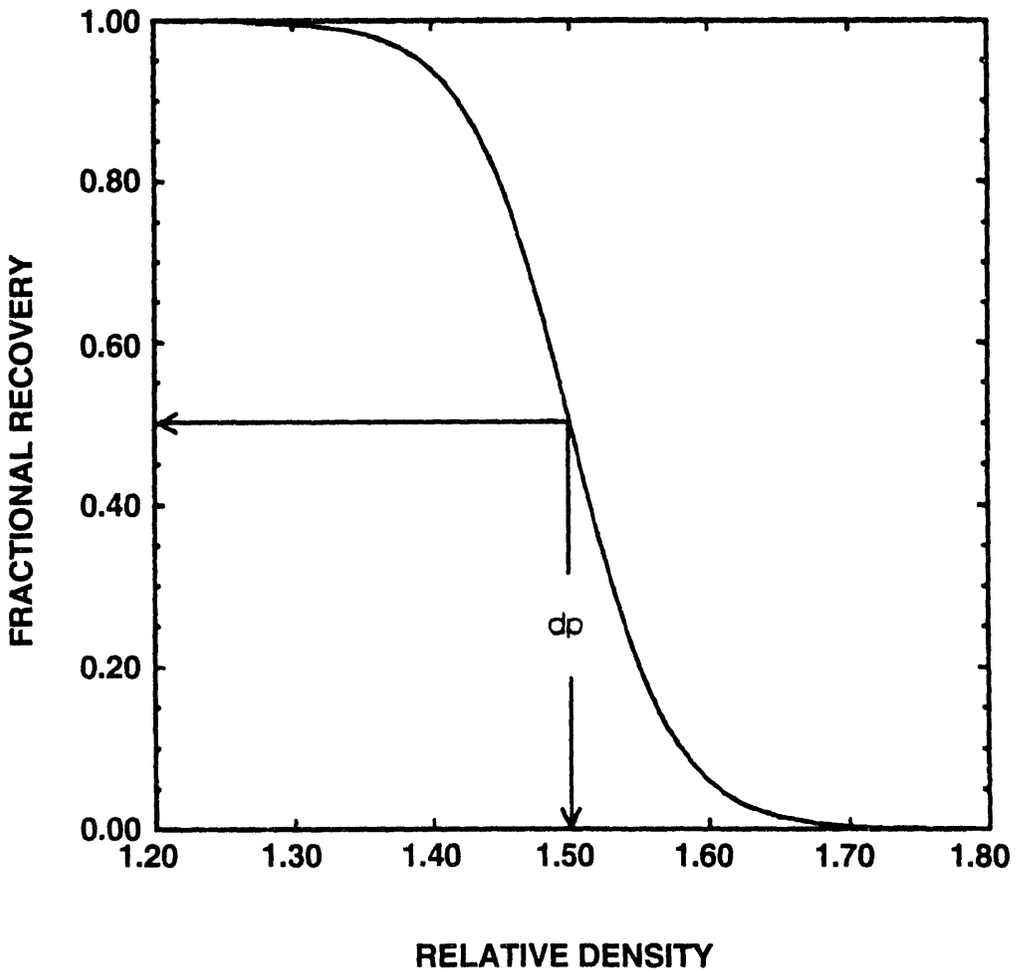

Figure 2-4. Fractional recovery curve showing the relative density of separation

Thus, as $E_p(x)$ approaches zero, the separation approaches ideal, while as $E_p(x)$ approaches infinity, no separation occurs, but rather the particles are split in the ratio *L/H*. The fractional recovery values can be fit to a mathematical function (model) from which the characteristic parameters can be obtained. One such model that has been shown to fit dense medium data is the logistic function given by (Meloy, 1979; Klima and Luckie, 1986; Napier-Munn, 1991)

$$K(\rho;x) = \frac{1}{1+exp[(1.099/E_p(x))(\rho-\rho_{50}(x))]} \qquad (2\text{-}14)$$

The parameters $\rho_{50}(x)$ and $E_p(x)$ can be found by using a nonlinear optimization routine.

Cyclone Separations

In order to produce an acceptable yield for the Type II or Type III coals (See Table 2.1 for a description of the coal types), the range of particle sizes to be processed must to be extended to fine sizes. Currently, most coal cleaning facilities treat coal down to about 28 mesh, and in some cases, down to 100 mesh, utilizing dense-medium cyclones. It is likely that cleaning of the 28x100 mesh size fraction would be required for a Type II coal to produce an acceptable yield of low ash, low sulfur material and even finer sizes would be required for a Type III coal. Because of the ability to make low density separations, with the capability of processing coals containing large amounts of near-gravity material, dense-medium separation would be the likely choice in these cases. Using the batch-settling model, an analysis of the change in the separation efficiency for a wide variety of conditions can be made. Appropriate parameters can be used to describe the cyclone operation in terms of retention time, number of g's, etc. (as discussed in Miller et al., 1993a), the feed washability (*i.e.*, the size and density distribution), and the dense medium characteristics.

Simulations were performed to investigate the separation of 28x100 mesh coal in a conventional (36 cm) diameter cyclone using a suspension of magnetite and water at a medium density of 1.28 g/cm^3. The corresponding set of simulation conditions are given in Table 2-6. The fraction of each coal species which reported to the product (Equation 2-12), was calculated by the batch hindered-settling model. Figure 2-5 shows the variation of the fractional recovery curves with particle size. As would be expected, sharper separations (i.e., lower $E_p(x)$ values) were obtained for the coarser particles. If this treatment is extended to finer sizes, *i.e.*, 100x400 mesh size fraction, the curves in Figure 2-6 are obtained. In this case, the fractional recovery curves are much flatter. Consequently, longer separation times and/or higher g's are needed to improve the separation (as discussed in Miller et al., 1993a).

Table 2-6. Simulation conditions for the dense-medium cyclone.

Total Height	18.0 cm
Relative Cut Height	0.6
Number of g's	120.0
Retention Time	1.75 s
Diffusion Coefficient	16.0 cm^2/s

Size/density distribution of the coal particles

	495 μm	351 μm	246 μm	175 μm	Composite
1.25 g/cm^3	0.145	0.204	0.185	0.142	0.676
1.35 g/cm^3	0.026	0.031	0.022	0.012	0.091
1.45 g/cm^3	0.014	0.014	0.010	0.007	0.045
1.55 g/cm^3	0.015	0.015	0.010	0.006	0.046
1.70 g/cm^3	0.010	0.010	0.007	0.004	0.031
2.30 g/cm^3	0.037	0.039	0.023	0.013	0.112
Composite	0.247	0.313	0.256	0.184	1.0

Characteristics of the dense medium.

Medium Density	1.28 g/cm^3
Med.-to-Coal Ratio	5:1
Magnetite	
Density, g/cm^3	4.8
Size	95%<53 μm
Vol. Fraction	
Solids	0.074
Water	0.926

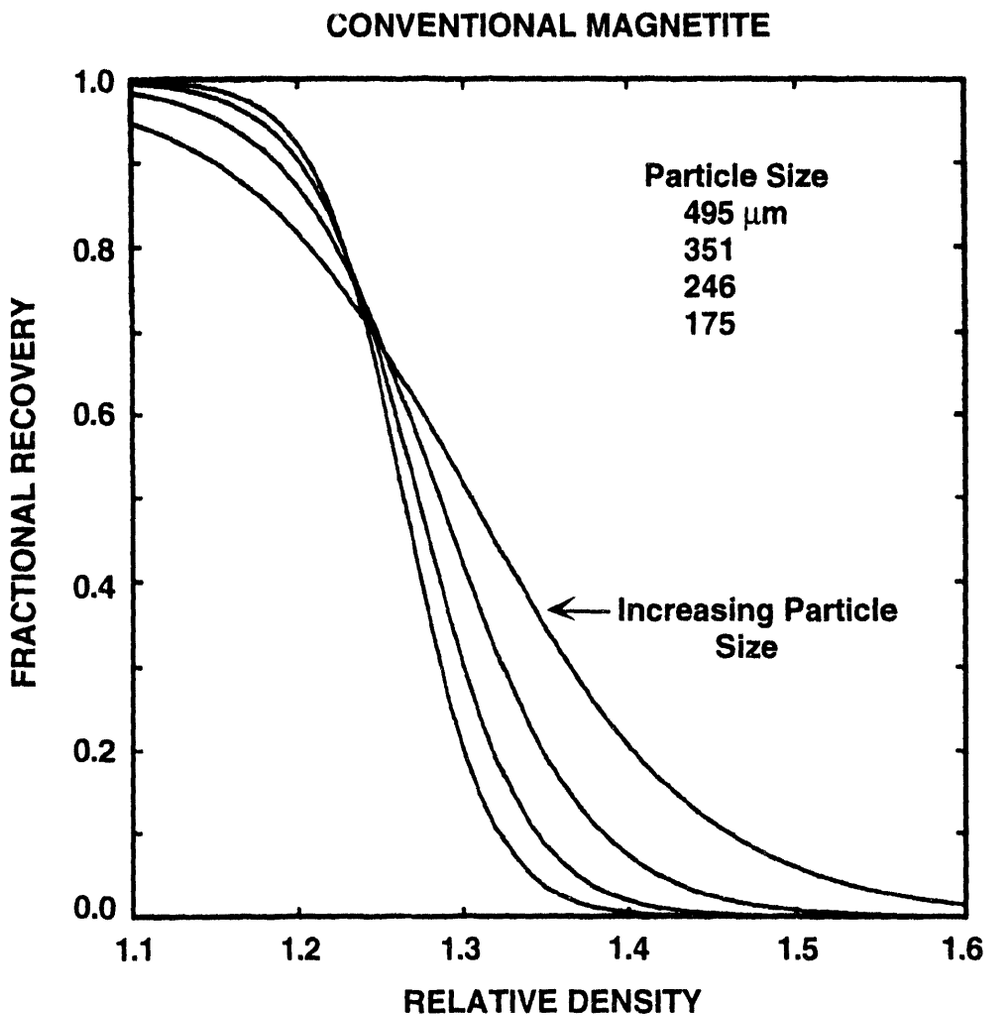

Figure 2-5. Variation of the fractional recovery curves with particle size for the 28 x 100 mesh size fraction

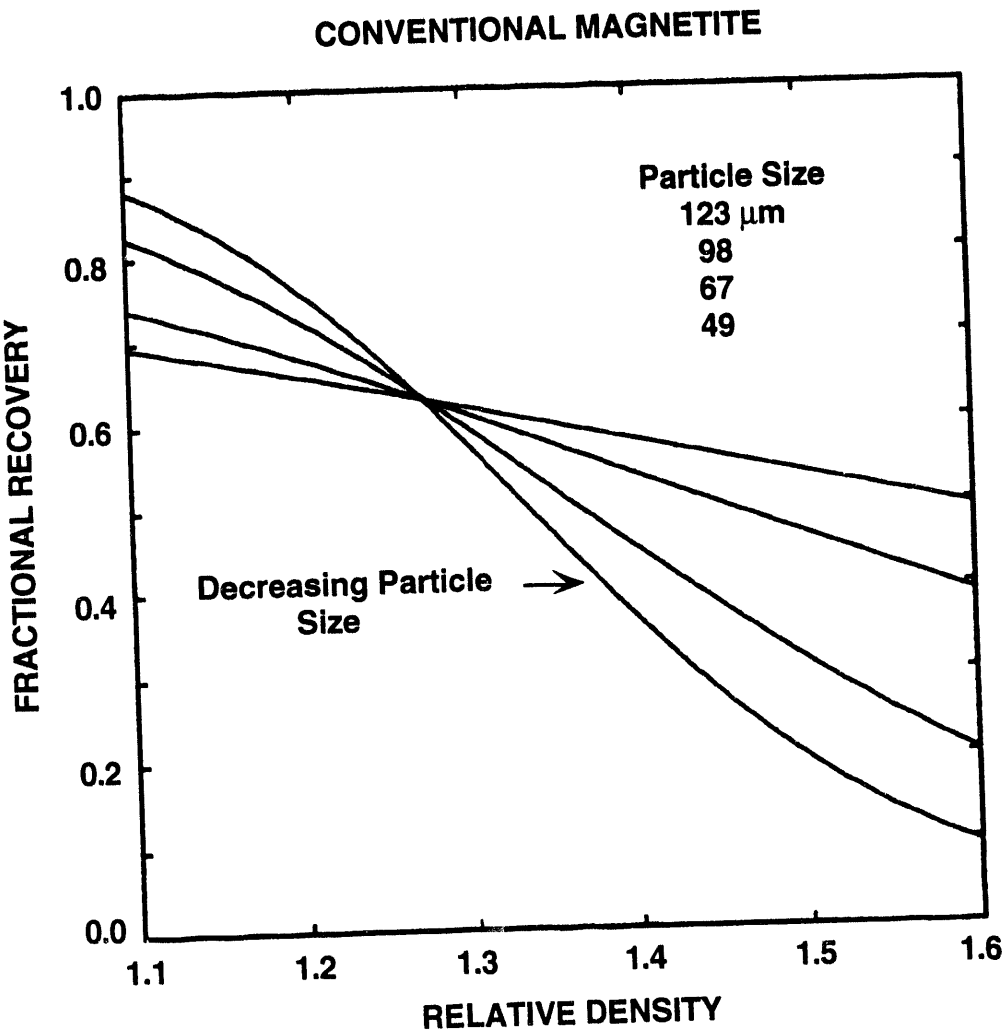

Figure 2-6. Variation of the fractional recovery curves with particle size for the 100 x 325 mesh size fraction

Work is continuing in this area investigating the effects of variable interactions on separation efficiency. Likewise, the effects of medium characteristics on cyclone performance are also being investigated, including the size distribution of the dense-medium solids.

Centrifuge Separations

Although dense-medium cyclones will likely be used to clean coal down to 100 mesh and perhaps even 400 mesh when utilizing an ultrafine (micronized) magnetite-based process, certain coals will require grinding to top sizes of 100 mesh or finer to achieve liberation. Such grinding would invariably create a large fraction of -400 mesh material. Under these conditions, it may not be practical to utilize dense-medium cycloning since smaller diameter (*i.e.*, lower capacity) units may be required to generate a sufficient number of g's. Also, because of the trade-off between the number of g's and the retention time, it may not be possible to separate the -400 mesh coal efficiently even using a smaller diameter cyclone. Alternatively, it should be possible to use a continuous solid-bowl centrifuge for dense-medium separation, also employing an ultrafine-magnetite/water suspension. Because of the ability to control independently the mean retention time and the number of g's, it should be possible to separate much finer particles compared to a cyclone. In addition, the amount of turbulence that occurs in a centrifuge should be lower since high inlet pressures are not required as is the case in a cyclone. Also, by changing the scroll speed, it may be possible to vary the pulp split independently, and in turn, change the relative density of separation at a constant medium relative density. The batch hindered-settling model will be used to investigate these variables.

Another potential advantage of the solid-bowl centrifuge is that can be used to classify particles at very fine sizes. In fact, these devices have been used in the minerals industry to separate particles less than 10 μm (Scheffler and Zahr, 1980). The capability to classify in this range would be very valuable in producing "custom" size distributions for the MCWSFs.

The baseline testing of the "batch" centrifuge with a Type III coal (Upper Freeport) was initiated. The nominal -6.35 mm coal was crushed to -100 mesh, followed by wet screening at 500 mesh (25 μm). The +500 mesh material was then used for the centrifuge testing. A suspension of ultrafine magnetite and water was used as the dense medium at a relative density of 1.30. The magnetite was obtained from the Pea Ridge Iron Ore Company of Sullivan, Missouri. This material is much finer than that used in commercial coal preparation facilities being nearly 100%<15 μm, with approximately 75%<5 μm. A medium-to-coal ratio of approximately 15-to-1 was used.

For each test, the coal/dense-medium mixture was mixed in a several liter tank. The slurry was then pumped through the centrifuge feed pipe near the top of the cylinder. After the feed was started, the overflow (clean coal) and underflow (refuse) streams were sampled simultaneously by applying a vacuum on each of the product streams. Each product sample was wet

screened at 500 mesh to separate the coal from the magnetite. The results from these tests indicated that some of the higher-ash fraction of the coal was being retained in the separator. To minimize this effect, the overall length of the separator was reduced from 152 to 76 mm.

Subsequent tests were run to develop a sampling strategy for the separator. This involved setting the discharge pipes and sampling time. One of the problems encountered during sampling was the difficulty in balancing the suction (discharge) rates with the feed rate using a single vacuum pump. The addition of a positive displacement pump seems to have eliminated this problem. Testing of this system is continuing.

The high-g, solid-bowl centrifuge has been ordered. This unit will allow continuous testing of dense-medium centrifugation and of ultrafine classification. The results from this study can be scaled to a larger diameter unit that can be used in a production facility.

Magnetic Fluid Separation

As an alternative to using a suspension of solids and water as a dense medium, it is possible to utilize a ferro (magnetic) fluid as the separating medium. These fluids consist of a colloidal suspension of sub-micron magnetite particles and dispersant in water. The fineness of the magnetite particles prevents the solids from settling in the fluid. When a magnetic field is applied to the fluid, the particles align themselves in the direction of the field. The result of this alignment is that a "buoyant " or "levitation" force is produced, allowing the particles to be separated according to the density difference between the particles and the fluid, similar to that in float-sink separations. When the magnetic field is removed, the particles return to a random orientation. Consequently, no magnetic flocculation occurs. The strength of the buoyant force can be regulated by changing the strength of the magnetic field and/or concentration of the fluid.

A commercially available separator that uses a rotating magnetic fluid is the Magstream separator (Walker et al., 1990). One of these units has been obtained recently on loan from the U.S. Department of Energy and is currently being installed. It will be used to evaluate the application of this technology to fine coal separations.

Evaluate Surface-Based Cleaning Processes

Advanced Froth Flotation

Block co-polymers consisting of hydrophobic polypropylene oxide (PPO) and hydrophilic polyethylene oxide (PEO) groups were selected to improve the efficiency of separation. These reagents were selected based on previous experience with such reagents. A list of the surfactants used in this investigation and their characteristics is given in Table 2-7. Other reagents to selectively disperse ash-forming minerals and depress sulfur-bearing minerals will be used if needed.

Flotation testing was initiated for two Type III coals from the Pittsburgh and Upper Freeport seams. The specific objective was to enhance the separation efficiency of the fine

Table 2-7. Selected properties of the surfactants used in this study

Surfactant	Surfactant Code	Number of Hydrophobic PPO Groups	Number of Hydrophilic PEO Group	M.W	HLB	Surface Tension @ cmc, dyne/cm
Ethylene oxide propylene oxide block copolymers	BC1			2700	2.1	36.0
	BC2	30	26	2650	11	43.0
	BC3	56	39	4950	9	34.0
	BC4	56	60	5900	13	33.0

PPO: Polypropylene oxide
PEO: Polyethylene oxide

particles using a surfactant. Several methods are available to enhance separation efficiency. These include:

- Aiding capture of fine particles by small bubbles
- Increasing the hydrophobicity to increase rate of flotation by the use of a surfactant.
- Increasing the hydrophobicity of particles which might increase the extent of hydrophobic aggregation.
- Aiding capture of fine particles by oil droplets followed by flotation of aggregates.
- Selective Agglomeration to produce larger 'particles' which can be floated readily.

A comprehensive approach is being used in this project to exploit some or all of the above methods.

Standard procedures were used to conduct tests and suitable models were used to determine the rate of, and the ultimate recovery.

Flotation Kinetics Models

Flotation rate data are essential for design of flotation systems. Flotation tests are being conducted to obtain the relevant information. The first step in the evaluation of flotation results was to select a model to evaluate the flotation kinetics. Approximately 25 models in the literature were reviewed, and they are grouped as:

First-order models

Second-order models

Miscellaneous models: Froth flow, gas adsorption, two phase, law of proportionality, etc.

The Classical First-Order (CFO) model together with rectangular (FRD) and sinusoidal (FSD) distributions of floatabilities were reviewed in Miller et al., 1993a. Various first-order flotation models and a few others were evaluated and a new model was developed because the exiting models were deemed to be unsatisfactory. It was established that some of the models gave a good fit for certain conditions, whereas others were better under different conditions. The reasons for this are not clear, however. Based on this experience, a new model was developed and it is described in the following paragraphs.

A First-Order Flotation Kinetics Model with Normal Distribution of Floatabilities. In this model the rate of flotation is assumed to be a normal distribution about a mean value. This model is capable of fitting the rate data under a wide variety of flotation conditions and the fitting errors were found to be small in the cases tested thus far.

The general form of the first-order rate equation with a floatability distribution f(k) is:

$$R_{(t)} = R_i\left\{1-\int_0^{\infty} f(k)e^{-kt}dk\right\} \qquad (2\text{-}15)$$

Where R(t) is the recovery at time t, and R_i is the ultimate recovery.
If a normal distribution of floatabilities is assumed, then

$$f(k) = \frac{\exp\{-(k-\mu)^2/2\sigma^2\}}{\sigma\sqrt{2\pi}} \qquad \text{where } 0<k<\infty \qquad (2\text{-}16)$$

and

$$R = R_i\{1 \quad 0.5\, e^{-A}(erf\, B - erf\, C)\} \qquad (2\text{-}17)$$

where μ is the mean and σ is the standard deviation of the normal distribution curve. The quantities A, B and C are defined by the following equations:

$$A = -\mu t + 0.5\, \sigma^2 t^2 \qquad (2\text{-}17a)$$

$$B = (t\sigma + \mu/\sigma)/\sqrt{2} \qquad (2\text{-}17b)$$

$$C = (t\sigma - \mu/\sigma)/\sqrt{2} \qquad (2\text{-}17c)$$

Model Evaluation. The results of the flotation kinetics tests were presented previously (Miller et al., 1993a). The frequency distributions fitted to the kinetics data are given in Figure 2-7 for the Upper Freeport seam coal and in Figure 2-8 for the Pittsburgh seam coal. The experimental conditions are given in the figure captions. The results of fitting four different models are given. It can be seen that the predicted values of the floatabilities are strongly model dependent, making it necessary to select the model which most accurately represents the actual distribution of floatabilities. The floatability distributions vary with coal type and conditions of flotation, as expected. The model fitting errors are given as mean residual square (MRS) errors in the inserts in the respective figures. For the Upper Freeport coal the MRS increased in the order:

$$FND < FRD < FSD < CFO \qquad (2\text{-}18)$$

and, for the Pittsburgh seam coal, it increased in the order:

$$FND \sim CFO < FRD < FSD \qquad (2\text{-}19)$$

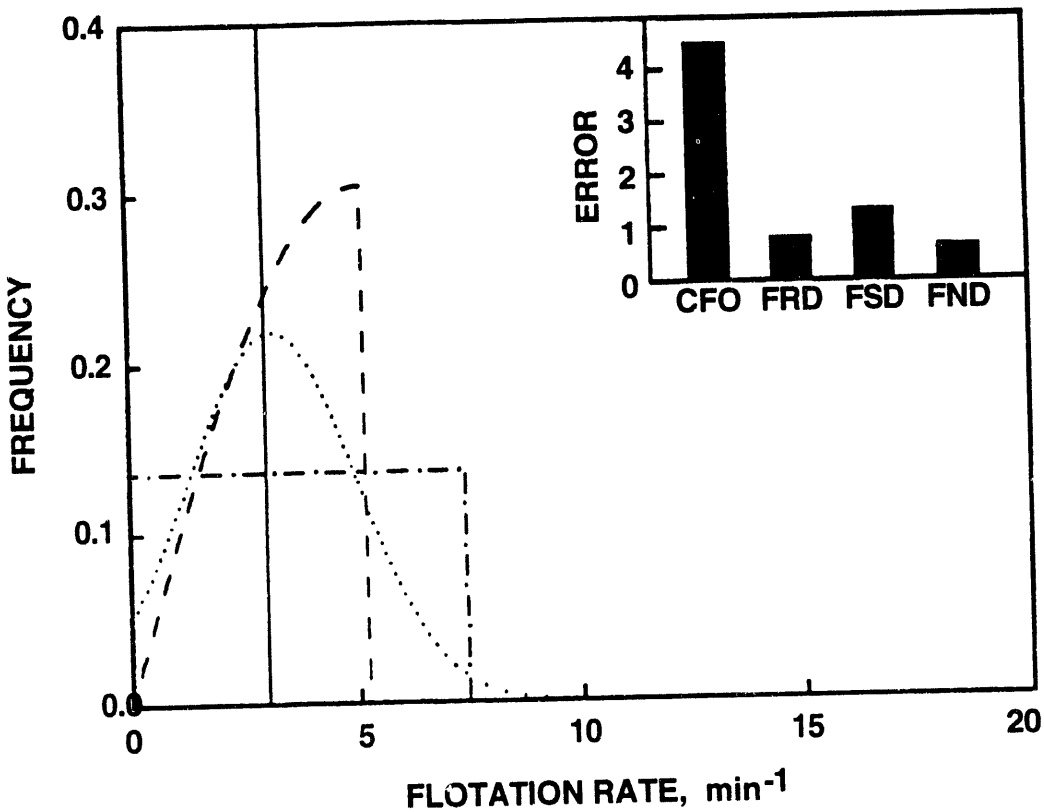

Figure 2-7. Frequency distributions of flotation rates of the overall sample predicted by various first-order flotation kinetics models for the Upper Freeport coal. Inset: The mean residual square error of the fits for various models. Frother: 0.33 kg/T MIBC; Collector: 1.3 kg/T Dodecane. Model: CFO (—); FRD (- · -); FSD (—); FND (···)

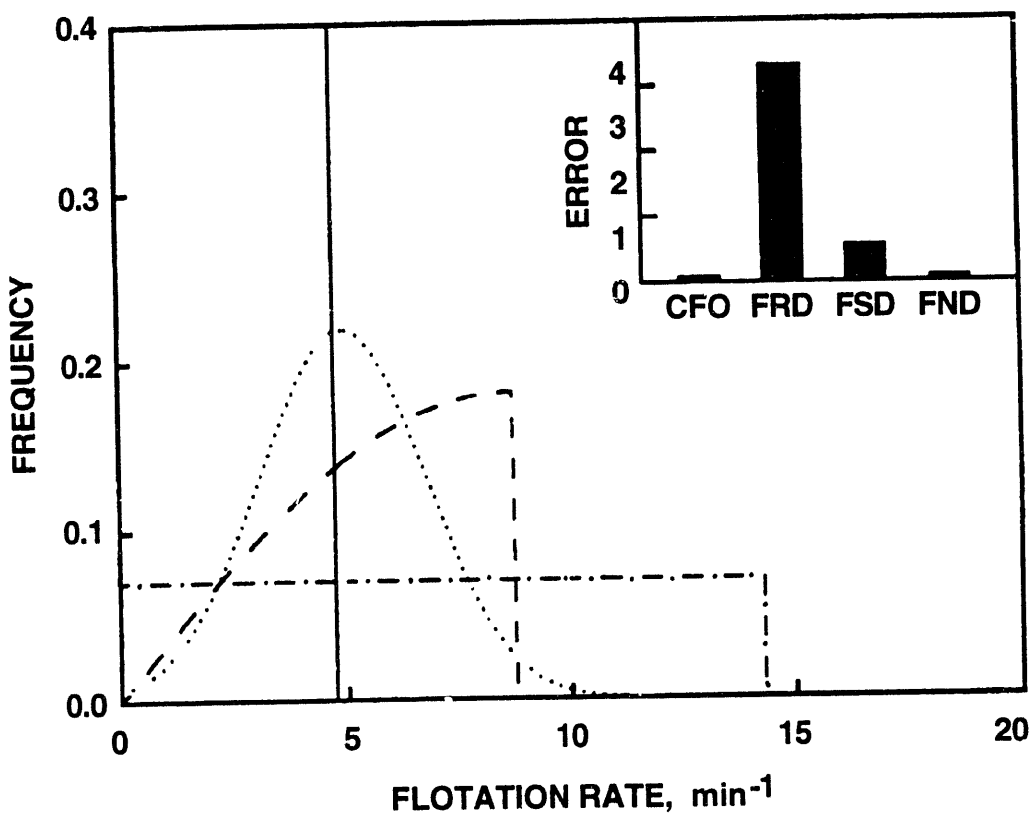

Figure 2-8. Frequency distributions of flotation rates of the overall sample predicted by various first-order flotation kinetics models for the Pittsburgh coal. Inset: The mean residual square error of the fits for various models. Frother: 0.33 kg/T MIBC; Collector: 1.3 kg/T Dodecane. Model: CFO (—); FRD (- · -); FSD (—); FND (···)

For both of the coals, errors were least for the FND model. This model is being evaluated further using the flotation results for other test conditions. Specifically, the effect of particle size is being determined. The effect of particle size on flotation is well recognized but the specific data for a given coal are generally not available. To determine the flotation response of individual size fractions, the flotation products were fractionated by sieving, weighed and analyzed for ash and sulfur. From this data the flotation rate distributions will be determined for particles in individual size fractions using the flotation models described above.

Role of Surfactants. Preliminary flotation tests conducted in the presence of selected reagents clearly demonstrated that substantial benefits are realized in coal cleaning when appropriate surfactants are used in small quantities. Our prior studies have shown that block co-polymers containing ethylene oxide-propylene oxide groups were found to be very effective in flotation of some coals. To determine their effectiveness for the coals chosen for this project, studies were carried out to determine the effect of

- Surfactant concentration, and
- Surfactant type.

The results were analyzed using the total combustible matter recovery (CMR) and % ash in the clean product and the results are presented in Figure 2-9. The corresponding ash recovery curves are given in Figure 2-10. The data for flotation in the absence of surfactant are given for comparison. In this figure the results of pre-agglomerating the coal are also included but they will be discussed in the section on Selective Agglomeration. Based on these results the following observations were made:

- For the BC2 surfactant, 1x10-4 kg/T (the lowest concentration tested) gave the best results with 80% CMR and 3.1% ash.
- For the BC4 surfactant, a higher concentration was required to obtain low ash (3%) but the CMR decreased to 67%.
- At low surfactant concentrations, the surfactant with fewer ethylene oxide groups gave lower ash at a CMR of about 80%.
- Except at very low concentrations, the increase in number of ethylene oxide groups decreased the ash by about 0.5% and the CMR by about 10%.

The surfactants can improve the efficiency of separation in two ways:

1. They make the coal more hydrophobic thereby increasing the rate of flotation.
2. They emulsify the oil to produce fine droplets. The fine droplets might act as collectors for coal or as liquid bridges. In both cases, an increase in flotation rate is expected but the effect on quality of the product might be more complex.

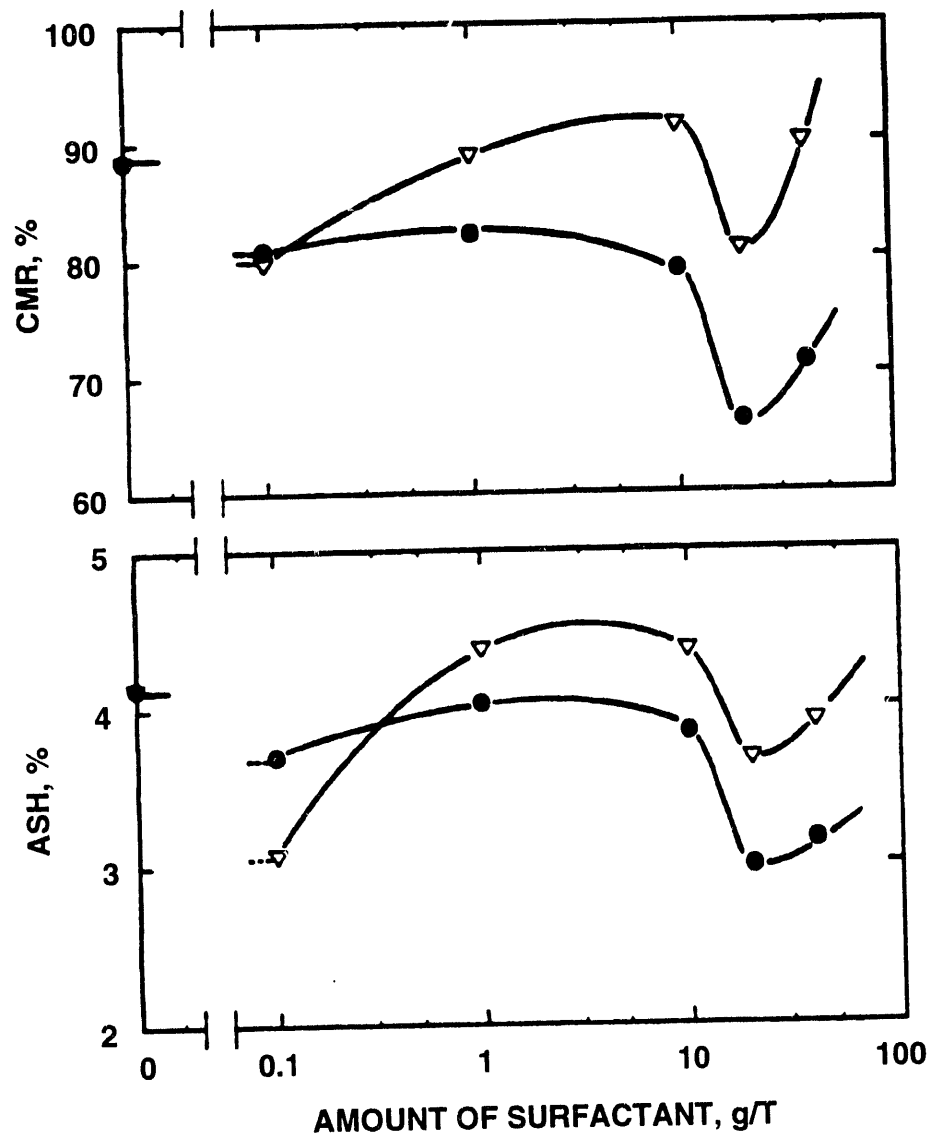

Figure 2-9. Effect of surfactant concentration on the combustible matter recovery (CMR) and Ash % for the Pittsburgh coal. Frother: 0.5 kg/T MIBC; Collector: 0.07 kg/T Dodecane. (∇ - BC2; ● - BC4)

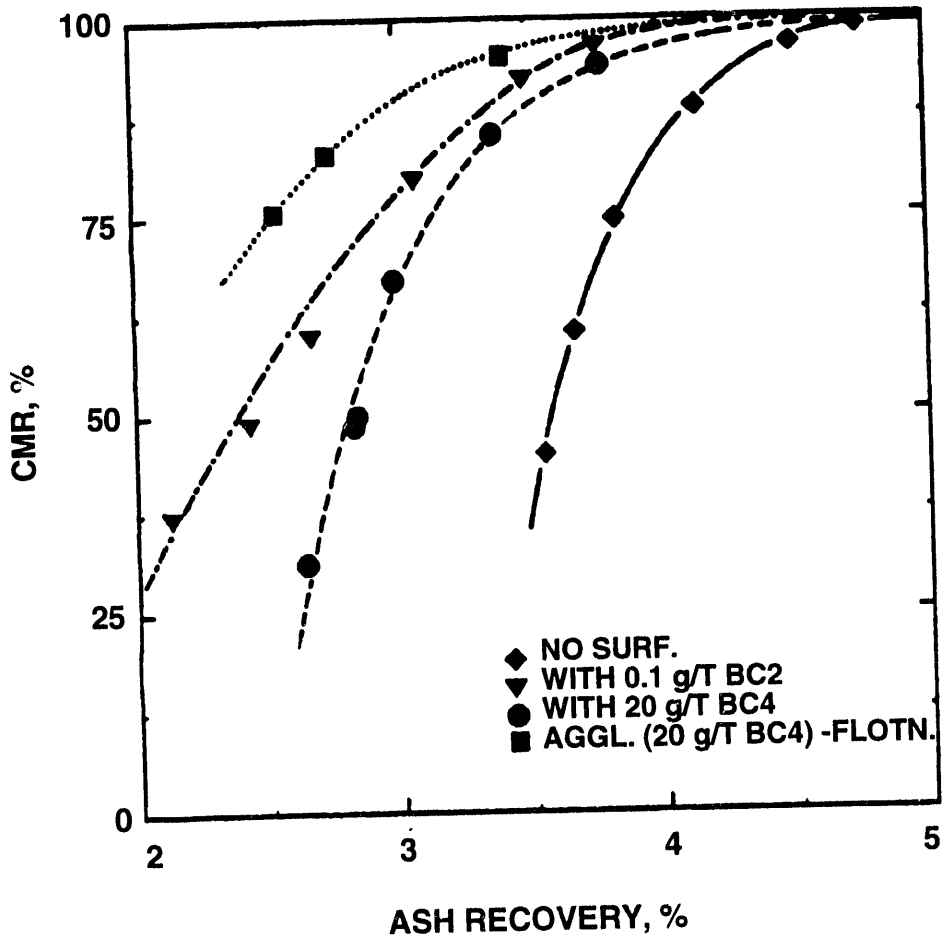

Figure 2-10. Performance of flotation under various conditions for Pittsburgh Seam coal. Frother: 0.5 kg/T MIBC; Collector: 0.07 kg/T Dodecane. (◆ - no surfactant; ▼ - 0.1 g/T BC2; ● - 20 g/T BC4; ■ - Preagglomeration with 20 g/T BC4)

To delineate the above effects, contact angle and emulsification studies are being conducted. This part of the work is being performed in coordination with studies under a separately-funded DOE project (DE-FG22-92PC92543, "Micro-agglomerate flotation for deep cleaning of coal," PI's: S. Chander and R. Hogg).

Column Flotation

In the previous semiannual progress report (Miller et al., 1993a), a new mass transfer approach to flotation column design was presented. The validity of this approach was tested using literature data from a variety of applications. In the present approach to column design, the bubble surface area emerges as a key design and scale-up variable. However, the parameters controlling the availability of bubble surface are the gas rate and bubble generator design. Thus, knowledge of the maximum gas velocity for column flotation, and how it changes with the scale of the column is required for design and scale-up.

The maximum gas flow rate for column flotation has been shown to be in the bubbly flow regime (Ityokumbul, 1992). Using dimensional analysis, the maximum gas velocity for column flotation was recently determined to be (Ityokumbul, 1993):

$$Ug_{,max} = 0.11 D_c^{0.5} \qquad (2\text{-}20)$$

In the previous report, it was shown that the height of a transfer unit, HTU, for pyrolusite flotation was higher than the corresponding value for fluorite. For the 0.064 m flotation column used by Ynchausti et al. (1988), the pyrolusite and fluorite flotations were carried out at gas velocities above and below the maximum value predicted by Equation 2-20. Analysis of published data revealed that in most large diameter flotation columns ($D_c > 0.5$ m), the operational gas velocities were less than 40% of the maximum value predicted by Equation 2-20 (see Figure 2-11). This may partially explain the low carrying capacities observed in large diameter columns. In addition, the optimum recovery zone heights determined were considerably shorter than conventional column designs and agreed rather well with those of the first column installations at Inspiration Copper Company, Ltd.

The fabrication of the laboratory flotation column has been completed. Most of the items ordered for the column instrumentation have been received. Assembly of the column has commenced. As designed, the height of the collection zone (and column) may be readily changed to permit the evaluation of the design parameters. Cominco R and Mott Metallurgical R bubble generators have been procured. The former employs high external shear to generate fine bubbles while the latter forces air though a porous medium with an average pore opening of 2 μm. Schematic diagrams of the experimental set-up and the two bubble generators are shown in Figures 2-12 and 2-13, respectively. Upon completion of the column assembly, the characteristics of the

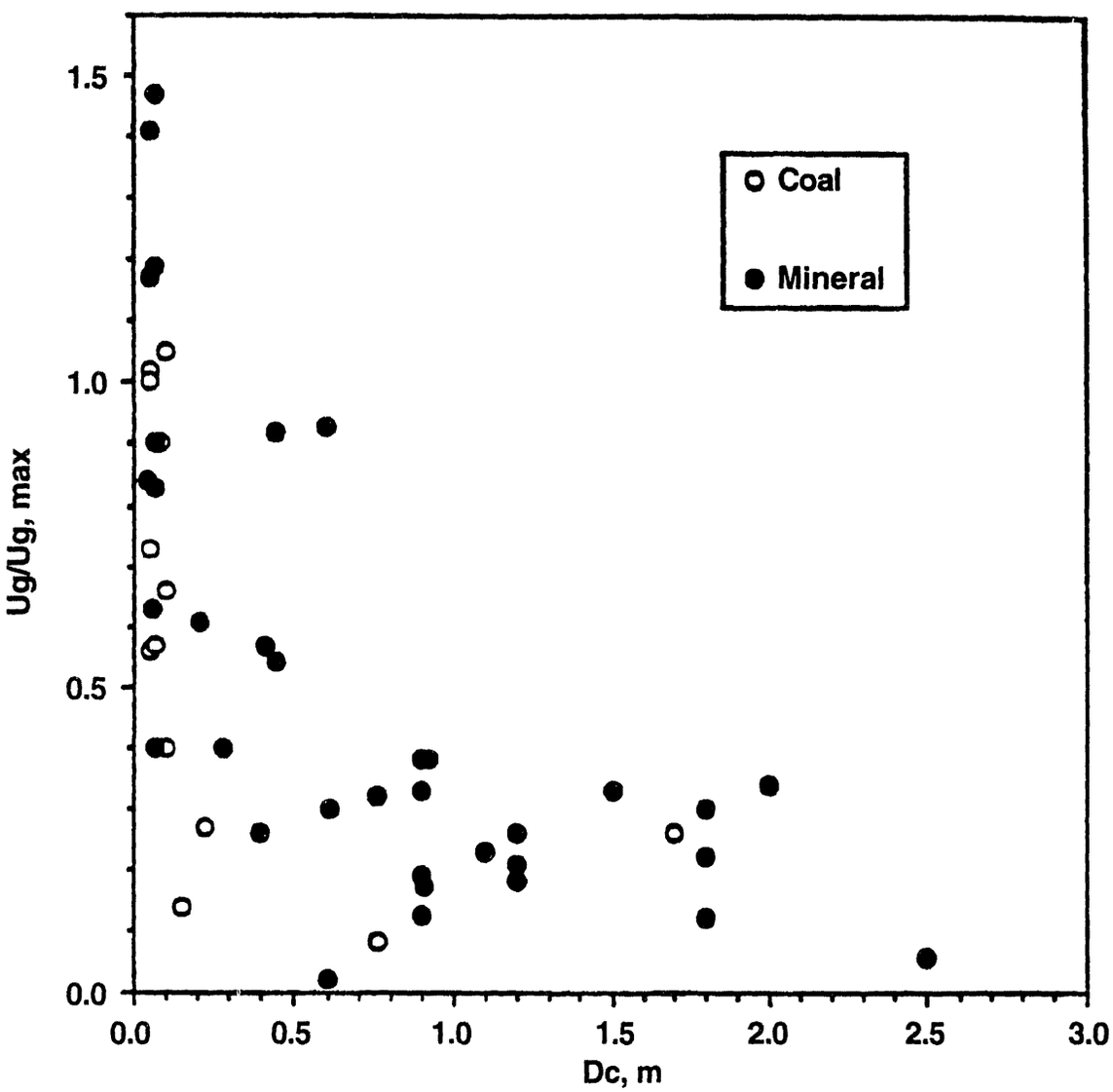

Figure 2-11. Comparison of operational to the theoretical maximum gas velocities in column flotation

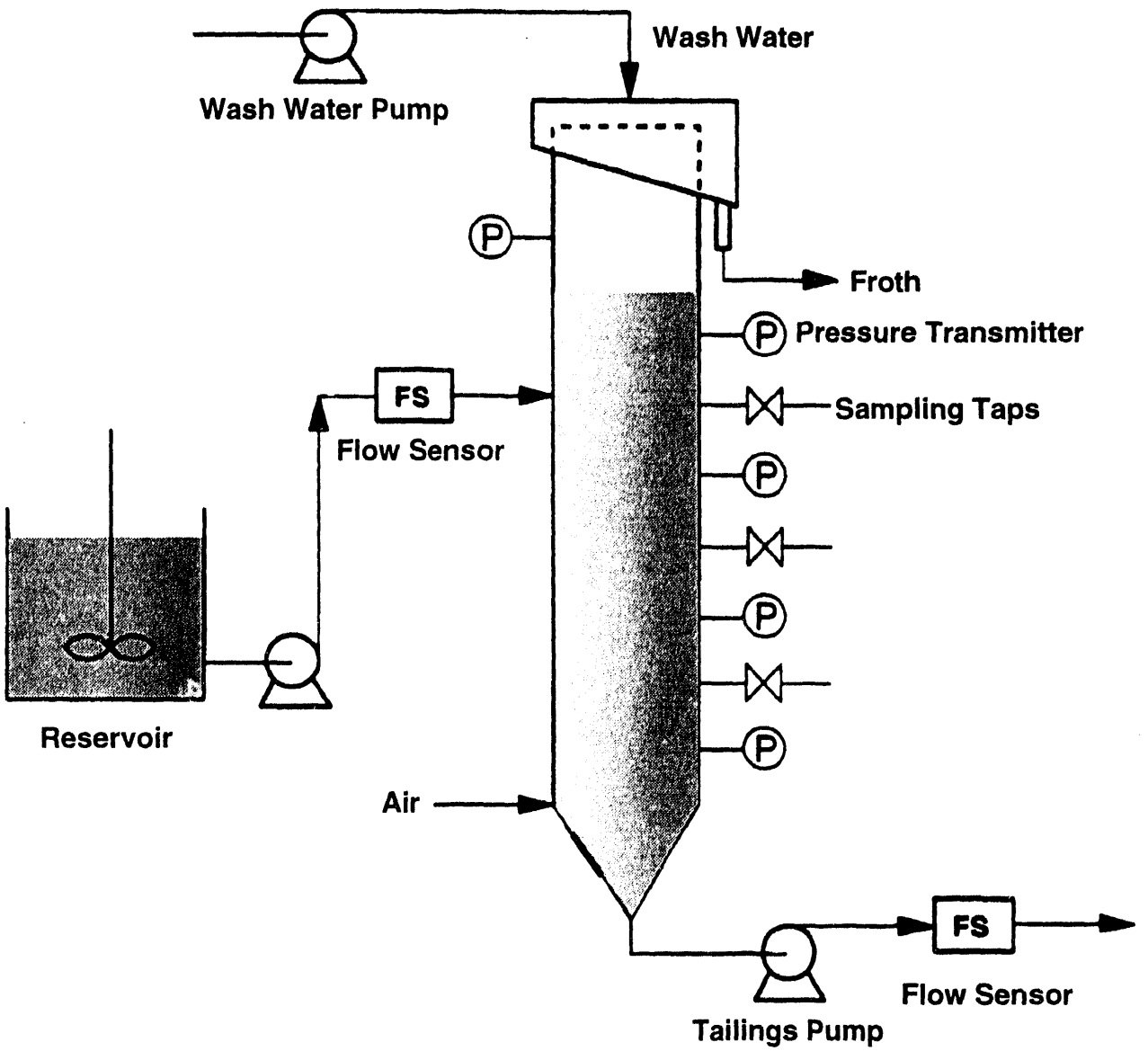

Figure 2-12. Schematic diagram of the flotation column set-up

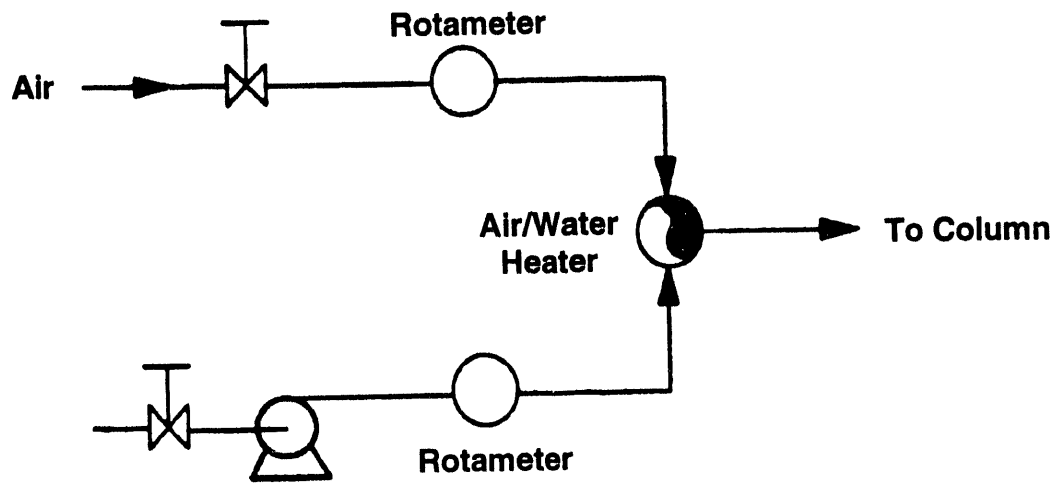

Cominco Sparger

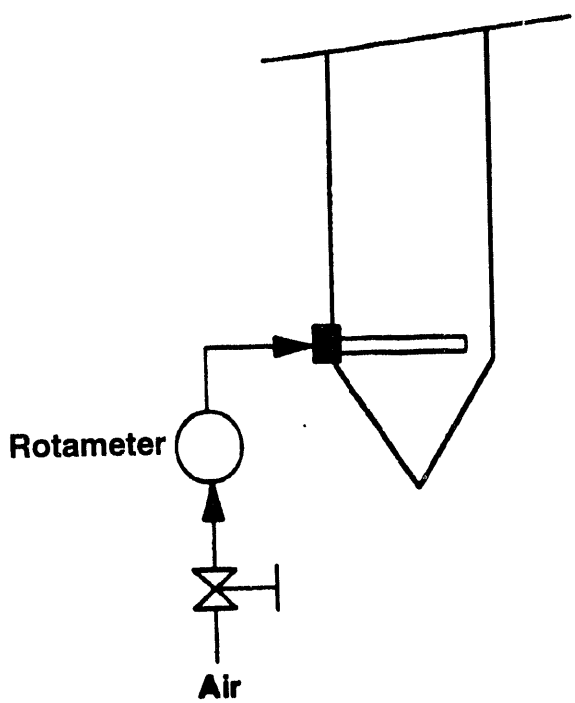

Static Sparger

Figure 2-13. Schematic diagram of the procured bubble generators

bubbles produced by these gas spargers will be studied in air-water and air-water-frother systems. This study will form the basis for preliminary evaluation of the effectiveness of both gas spargers in fine coal cleaning.

Selective Agglomeration

The addition of small quantities of oil to a coal-water slurry promotes the selective agglomeration of hydrophobic coal particles leaving liberated (hydrophilic) ash minerals dispersed in the aqueous phase. The oil-agglomeration process has been the subject of numerous laboratory and pilot-scale studies (Mehrotra et al., 1983; Capes et al., 1990; Pawlak et al., 1989; Simmons and Keller, 1986) but has not found wide commercial application. The process does, however, have considerable potential for deep cleaning of coal at fine sizes, especially for applications in coal-water slurry fuel technology so as to avoid the problems of dewatering the fine, clean-coal product. The process is particularly attractive for use in combination with froth flotation to enhance recovery of the agglomerated material.

The use of oil agglomeration, at very low oil-addition levels, for sulfur and ash rejection in fine (-200 mesh) coal is being investigated. Under a separate DOE-sponsored project, the wetting phenomena which provide the driving force for agglomerate formation and the growth of agglomerates in three-phase (oil-water-coal) systems are being studied.

Wetting behavior is being evaluated in terms of the various contact angles (solid-liquid-liquid and solid-liquid-gas) which define the attachment of oil droplets to solid surfaces in an aqueous medium. A technique known as interface partitioning, which has recently been developed (Wei et al., 1992), is being used for determining contact angles on small particles at liquid-gas and liquid-liquid interfaces. Agglomerate growth is being studied by in-situ measurement of particle/agglomerate size in agitated coal-water slurries with small quantities of added oil. Following preliminary, baseline studies on "pure" (coal-water-oil) systems, the role of surfactants in wetting and agglomerate formation will be investigated in some detail.

Studies of combined agglomeration flotation are also being carried out. Pre-agglomerated coal has been separated by flotation and the results are given in Figure 2-10. A substantial increase in separation efficiency was observed. Additional studies are in progress to determine the effect of key variables on the separation efficiency.

Establish Required Size Consist for Slurry Formulation

The size distribution of the solid particles is a critical factor in the production of high-density MCWSF with acceptable viscosity. It is generally accepted that broad size distributions are desirable since they afford the most opportunity for efficient packing of the particles. However, there seems to be little agreement over the "optimum" size distribution, and trial-and-error methods involving changes in the fine-grinding procedure are usually adopted. The size-consist

requirements in terms of the role of packing and particle interaction forces in determining slurry characteristics are being reevaluated.

Particle Interactions

Solid particles dispersed in water are subject to forces of interaction which become increasingly important as particle size is reduced.

van der Waals Forces act between any pair of molecules and, by extension, between any particle and its neighbors. The term van der Waals force is generally applied to the interaction between either permanent or induced dipoles in a pair of molecules. Typically, the energies of interaction are associated with an inverse sixth power variation with molecular separation. The forces are always attractive. The interaction between particles can be estimated by summing the pair-wise molecular interactions (Hamaker, 1936). Analytical expressions have been derived for a variety of particle geometries (plate-plate, sphere-sphere, sphere-plate, etc.). A useful approximation for the attractive force between dissimilar spheres of composition i and j and diameter x_i and x_j immersed in a fluid medium k is:

$$F_{ijk} = \frac{A_{ijk} x_i x_j}{12(x_i+x_j)\, H^2} \qquad (2\text{-}21)$$

where H is the surface-to-surface separation of the particles and A_{ijk} is known as the Hamaker constant for interaction between materials i and j in medium k. More exact expressions, including corrections for electromagnetic retardation effects at large separations are available in the literature (Schenkel and Kitchener, 1960; Clayfield and Lumb, 1971; Gregory, 1981).

The overall, effective Hamaker constant for a given interaction can be estimated from

$$A_{ijk} = (\sqrt{A_i} - \sqrt{A_k})(\sqrt{A_j} - \sqrt{A_k}) \qquad (2\text{-}22)$$

where A_i, A_j and A_k refer to interactions of the separate components in vacuum. For identical particles (i = j), A_{ijk} is always positive and the net force is always attractive. On the other hand, for dissimilar particles ($i \neq j$), A_{ijk} can be positive or negative depending on the values of the individual constants and it is possible for the net force to be a repulsion. Typical values of Hamaker constants A_{ii} for common solids and liquids are available in publications by Visser (1972) and Fowkes (1964).

Electrical Forces result from electrochemical equilibrium between particles and ionic species in liquid (especially aqueous) solutions. The charged particles attract oppositely charged ions from solution leading to the establishment of an electrical double layer at the solid-liquid interface. Interaction forces arise as the electrical double layers surrounding two particles over-

lap. The magnitude and range of the interaction force depend on the electrical potential difference between the solid and liquid phases and on the ionic strength of the solution - which controls the extent of the double layer away from the particle surface.

Electrical double layer interaction forces have been studied at length by colloid scientists, and numerous theoretical expressions, appropriate for a variety of conditions, are available to describe their magnitude (Overbeek, 1952). A useful, general relationship for estimating the double layer interaction was given by Hogg, Healy and Fuerstenau (1966). Based on this work, the force can be expressed as:

$$F_{ij} = \frac{\varepsilon\kappa x_i x_j}{4(x_i+x_j)} \frac{e^{-\kappa H}}{1-e^{-2\kappa H}}\left[(\zeta_i^2 + \zeta_j^2)e^{-\kappa H} - 2\zeta_i\zeta_i\right] \qquad (2\text{-}23)$$

where x_i and x_j are equivalent sphere particle diameters, ε is the dielectric constant for the medium and κ is the Debye-Huckel reciprocal thickness parameter defined by

$$\kappa^2 = \frac{8\pi e^2 I}{\varepsilon kT} \qquad (2\text{-}24)$$

in which e is the electronic charge, I is the ionic strength of the medium, k is Boltzmann's constant and T is the absolute temperature.

The quantity ζ in Equation (2-23) is the so-called Zeta Potential of the particles which provides an estimate of the electrical potential drop across the mobile part of the double layer. In general, the zeta potential depends on the composition of the solid and solution phases; for aqueous systems it varies in particular with the pH and ionic strength of the solution. A detailed discussion of the zeta potential and its significance in colloidal systems has been published by Hunter (1981).

The force due to the double layer interaction can represent either attraction or repulsion depending on the relative sign and magnitude of the zeta potentials. For identical particles with finite zeta potential ($\zeta_1 = \zeta_2$), the force is invariably repulsive, for particles with zeta potentials of opposite sign it is always attractive, while for particles whose zeta potentials have the same sign but different magnitude, the force can change from repulsion at large separation to attraction as the particles come into contact (Hogg, Healy and Fuerstenau, 1966; Overbeek, 1988).

Chemical Forces due to the formation of chemical bonds between particles in contact can contribute to the strength of agglomerates. However, such forces are of extremely short range and play little or no role in the production and properties of coal-water slurry fuels.

Solvation Forces are a result of interaction between particle surfaces and a liquid medium. The formation of structured layers of either solvent molecules or adsorbed solute species can contribute to these effects. Soluble polymers can have very significant effects on particle

interactions. Complete coating of particle surfaces by adsorbed polymer typically leads to strong repulsion between particles (Napper, 1983) while partial coatings can promote aggregation by polymer bridging from one particle to another (Smellie and La Mer, 1958).

Hydrophobic Forces have recently been postulated as a distinct class (Israelachvili, 1985), but should perhaps be more properly regarded as a special case of salvation forces.

Attractive, van der Waals' forces and repulsive, electrical double layer and steric interaction forces due to adsorbed, dispersant layers probably assume a dominant role in coal-water slurry fuels. In the absence of repulsion, the attractive forces lead to particle aggregation and network formation with a corresponding increase in apparent viscosity. The presence of repulsive forces gives rise to the development of repulsive energy or force barriers between particles which prevent their coming into actual contact. Typically, these barriers lead to minimum particle separations in the range of 0.01 to 0.1 μm.

By preventing aggregation or network formation, the development of repulsive barriers generally contributes to the reduction of CWSF viscosity. On the other hand, the barrier itself represents an additional excluded volume which increases the effective solids volume in suspension. Such effects can become significant for very fine particles. For particles of size x with minimum separation H_m, the effective solids volume fraction ϕ is increased to

$$\phi_{eff} = \phi\left(1 + \frac{H_m}{2x}\right)^3 \qquad (2\text{-}25)$$

For 0.1 μm particles with a minimum separation of 0.05 μm, this would correspond to almost a doubling of the effective solids concentration.

Particle interactions also play a role in another important characteristic of coal-water slurry fuels: sediment consolidation. Practical coal-water slurry fuels are inevitably subject to some settling during long-term storage. This becomes a problem if the resulting sediments are highly consolidated ("hard-packed") and not easily redispersed by agitation. Network formation due to net attraction between particles generally promotes settling but opposes consolidation by forming rigid but relatively open structures which can easily be broken down by agitation. Very strong repulsive interactions can also inhibit consolidation by preventing close approach of particles. Both of these conditions can, however, contribute to increased slurry viscosity.

Particle Packing

It has long been recognized that particles of uniform size, arranged at random, pack to a solids volume fraction of about 0.6. These packing densities can be increased substantially by the addition of smaller particles which can fit into the interstices between the original particles.

For CWSF applications, it is convenient to consider the reverse (but entirely equivalent) situation of adding coarser material to a suspension of fine particles.

Consider a suspension of particles of size x_1 with solids concentration ϕ_1. If coarser particles (size x_2) are added, each particle (initially) adds its own solid volume to the suspension. Thus

$$V = V_1/\phi_1 + V_2 \tag{2-26}$$

where V is the total slurry volume, V_1 and V_2 are the respective solid volumes.

By definition, the slurry concentration (volume fraction) is

$$\phi = \frac{V_1 + V_2}{V} \tag{2-27}$$

and the fraction of coarse particles is

$$Q = \frac{V_2}{V_1 + V_2} \tag{2-28}$$

It follows that

$$\phi = \frac{\phi_1}{1-Q(1-\phi_1)} \tag{2-29}$$

which describes the increase in solids loading due to the addition of coarse material. Obviously, such an increase in loading canno continue indefinitely. Eventually, the coarse particles cease to act independently; they begin to disturb the packing of the finer material and finally reach a packing limit of their own.

The maximum possible loading occurs when there is just enough fine-particle slurry to fill the voids in a bed of close-packed coarse particles. In this case,

$$V = V_2/\phi_2^* \tag{2-30}$$

where ϕ_2^* is the maximum packing fraction for the coarse material (typically about 0.6). The void volume V_v (available to fine-particle slurry) is

$$V_v = \left(1-\phi_2^*\right)V \tag{2-31}$$

It follows that the maximum loading occurs when the fraction of coarse particles in the mixture is Q_m such that

$$Q_m = \frac{\phi_2^*}{\phi_1\left(1 - \phi_2^*\right) + \phi_2^*} \qquad (2\text{-}32)$$

The corresponding maximum solids loading is

$$\phi_m = \phi_2^*\left(1 - \phi_1\right) + \phi_1 \qquad (2\text{-}33)$$

Some examples of calculated solids loadings for coarse-particle/fine-slurry mixtures are shown in Figure 2-14. The substantial increases in loading which can, potentially, be achieved can be seen clearly. It is also apparent that a range of options is available for producing a CWSF with a given loading. Thus, a loading of 50% solids overall can be accomplished by adding about 30% coarse particles to a 40% slurry or 70% coarse particles to a 20% slurry. Obviously, the rheological and settling characteristics of these different (but same-density) CWSFs would not be expected to be the same.

In principle, further increases in solids loading could be obtained by the addition of a third, still finer or coarser component in the appropriate amount. However, experience with powders suggests that such improvements are not generally achieved in practice (Cross, 1985).

In order to obtain the optimum packing from binary mixtures, it is necessary that the size ratio x_2/x_1 be as large as possible. In real CWSFs, however, there are practical limits on this ratio. Combustion and burner requirements generally limit the upper size, x_2 to less than about 100 μm. Grinding costs and, to some extent, rheology constraints place limits on the finer size x_1.

The ability to achieve high packing density is largely determined by the ratio of the average separation H_2 of the large particles to the size of the fine material. For a "dilute" (non close-packed) coarse fraction, assuming an average cubic arrangement, the mean particle separation can be estimated as follows:

The volume of slurry associated with an average (size x) particle is

$$v_s = k_v\, x^3/\phi \qquad (2\text{-}34)$$

where k_v is the column shape factor ($=\pi/6$ for spheres). For a cubic arrangement, the average center-to-center separation is

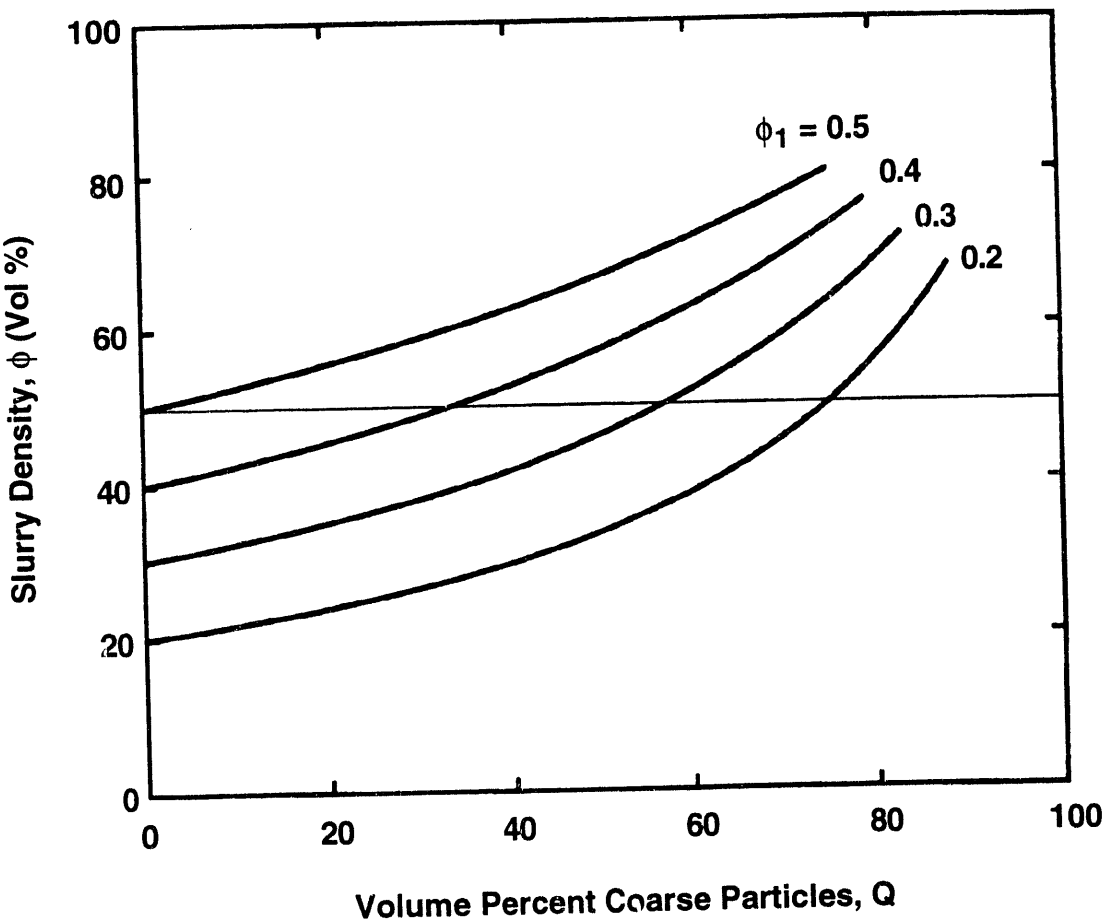

Figure 2-14. Slurry preparation from binary mixtures

$$v_s^{\frac{1}{3}} = \left(k_v/\phi\right)^{\frac{1}{3}} x \qquad (2\text{-}35)$$

and the average surface-to-surface separation for the coarse component is:

$$H_2 = \left[\left(k_v/\phi_2\right)^{\frac{1}{3}} - 1\right] x_2 \qquad (2\text{-}36)$$

The excluded-volume effect noted above restricts the size (x_1) of the fine-particle fraction. For stabilized particles, the minimum separation H_m (see Equation 2-25) is essentially constant and independent of particle size. Thus, as size x is reduced, the excluded volume effect described by Equation 2-25 becomes increasingly important and places an upper limit on the concentration ϕ_1.

The particle size limitations can be illustrated by considering a hypothetical CWSF prepared at 50% solids by weight from various combinations of coarse and fine particles. The packing effect is described by the ratio of the coarse-particle separation H_2 to the fine-particle size x_1. A large value indicates that the fine-particle slurry can readily fill the space between coarse particles. The excluded volume effect is reflected by the effective fine-particle concentration $(\phi_1)_{eff}$ as defined by Equation 2-25. High values would be expected to correspond to high CWSF viscosity.

The results of such calculations, based on a coarse-particle size x_2 of 75 μm and a minimum separation of the fine particles of 0.05 μm, are given in Table 2-8. It can be seen that the packing effect becomes critical when the fine-particle component is dilute and relatively coarse. As expected, the excluded volume effect becomes significant when the fine-particle component is concentrated and extra fine.

These calculations also demonstrate the value of using a true bimodal size distribution for CWSF formulation. The presence of intermediate sizes in a broad but continuous distribution will invariably lead to reduced values of H_2/x_1 and correspondingly reduced packing efficiency for a given solids loading.

The packing model can also be used to estimate the rheological behavior of binary (coarse + fine) coal-water slurries. Provided the coarse particles are sufficiently widely spaced (dilute), such systems can be modelled as suspensions of coarse particles (concentration ϕ_2) in a medium consisting of fine particles at concentration ϕ_1. The advantage of this approach is that the relatively simple relationships which have been developed for suspensions of uniform particles can be used to estimate the viscosity of the fine-particle medium and the overall slurry. Typically, such expressions are of the form:

Table 2-8. Packing ratio and excluded volume effect for binary slurries at 50% solids by volume (Based on 75 μm coarse particles). Shaded figures represent conditions where coarse-particle separation would be expected to limit fine-particle packing.

Fine-Particle Size X_1 (μm)	Packing Ratio H_2/x_1				Excluded Volume Effect (Effective Fine-Particle Concentration)				
	ϕ_1=0.1	0.2	0.3	0.4	ϕ_1=0.1	0.2	0.3	0.4	0.5
0.5	8.4	17.7	33.6	69.7	0.116	0.232	0.347	0.463	0.579
1	4.2	8.8	16.8	34.8	0.108	0.215	0.323	0.431	0.538
2	2.1	4.4	8.4	17.4	0.104	0.208	0.311	0.415	0.519
5	0.8	1.8	3.4	7.0	0.102	0.203	0.305	0.406	0.508
10	0.4	0.9	1.7	3.5	0.101	0.202	0.302	0.403	0.504

$$\mu = \mu_0 f(\phi) \qquad (2\text{-}37)$$

where μ is the viscosity of the suspension and μ_0 is that of the medium. Thus, for the binary coal-water slurry, the viscosity can be estimated by successively applying Equation 2-37, first to the fine-particle "medium", and then to the suspension of coarse particles in that medium. An example, using the Dougherty-Krieger relationship (see next section, Equation 2-65), is given in Table 2-9. The results indicate an optimum composition (minimum viscosity) consisting of relatively coarse (> 2 μm) fine particles at about 30% solids by volume with an appropriate addition of the coarse fraction (also about 30% by volume) in order to provide the desired overall solids content (50% in this example).

Stabilization of Coal/Water Suspensions

Work that has been completed to date on this aspect of the project includes: (1) the construction of a modified form of the Dougherty-Krieger equation describing the dependence of CWSF viscosity on coal particle concentration and size distribution and (2) obtaining some initial models for the sedimentation or settling of the particles in a CWSF using an "effective medium approximation" (*i.e.* the viscosity expression obtained using the modified form of the Dougherty-Krieger equation).

In addition, the dynamics of settling and the equilibrium density profiles that are to be expected in various types of systems were examined. The approach used was systematic in the sense that what would be expected in a system of non-interacting particles (i.e. neglecting van der Waals and Coulombic interactions, but not the "hydrodynamic interactions" (i.e. steric repulsions) that are characteristic of a concentrated slurry) were first considered. The next step is to add various types of interactions to the model and calculate the effect of these forces. The recent work has focused on Coulombic interactions and this is described in the following section.

The Settling of Charged Coal Particles - Description of Results

During the last reporting period (Miller et al., 1993a), the general equations describing the equilibrium profile $\phi(h)$ of the settled CWSF, where $\phi(h)$ is the volume fraction of coal particles at a depth h, were formulated. Knowing the interparticle forces the dependence of the coal volume fraction ϕ on the depth h after the CWSF has settled can be calculated. It was calculated that for the simplest situation, where the only interaction force is the steric repulsion between coal particles, the density profile has a sharp transition from clear water to the close packing limit, ϕ_m as illustrated in Figure 2-15. In other words, the CWSF is completely "settled". Evidently, Brownian motion and steric repulsion alone cannot ensure a good stabilization of a CWSF. This is, of course, to some degree intuitively obvious, but it is the essential starting point for any model of coal sedimentation.

Table 2-9. Estimated viscosity for binary slurries at 50% solids by volume. Shaded figures represent impractical packing conditions (see Table 2-8).

Fine-Particle Size X_1 (μm)	Estimated Viscosity (cp)				
	ϕ_1=0.1	0.2	0.3	0.4	0.5
0.5	12.3	10.5	11.3	18.0	211.9
1	11.9	9.8	9.7	12.8	38.4
2	11.8	9.5	9.1	11.1	24.7
5	11.7	9.3	8.8	10.3	20.0
10	11.7	9.3	8.7	10.0	18.8

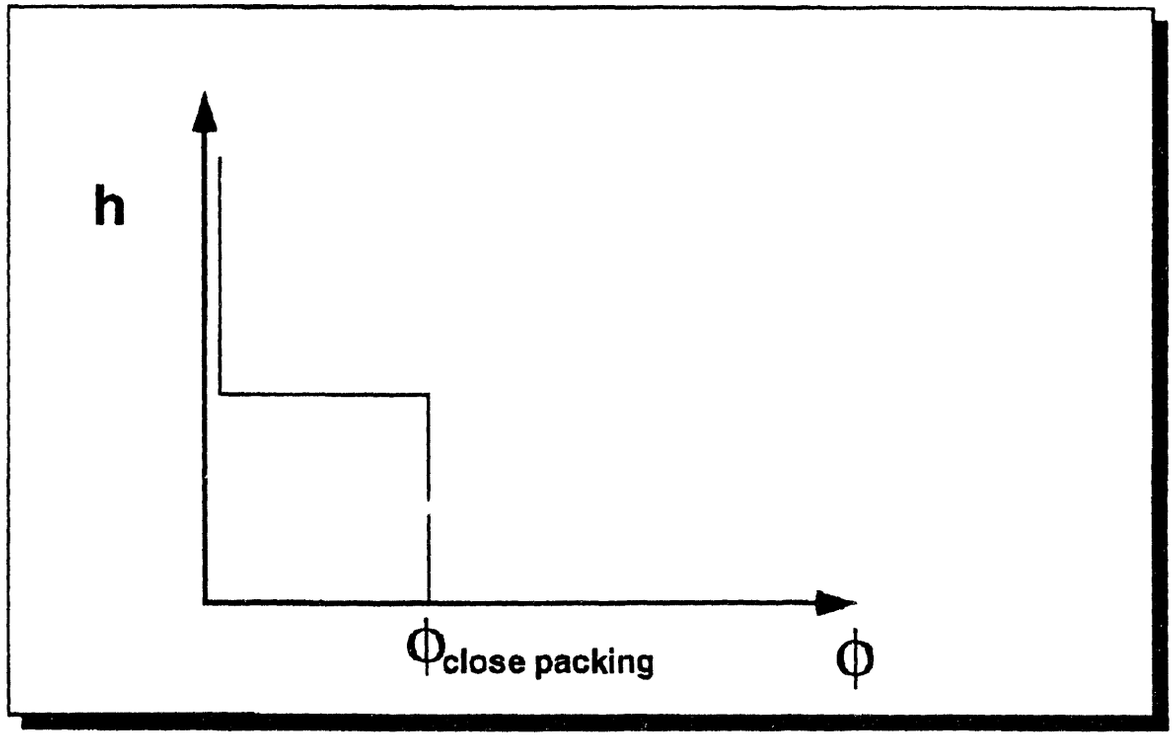

Figure 2-15. Equilibrium profile - nonstabilized coal particles

It was decided that the next logical step is a consideration of the effect of Coulombic interactions because:

1) These are expected to be repulsive and hence aid in CWSF stabilization (there are some complications here, however)
2) Charged groups can be readily introduced onto the surface of coal particles
3) Such groups are also "naturally" introduced as a consequence of oxidation.

Because the chemical group that is most commonly formed during oxidation is carboxylic acids, attention was focused on species of the form

$$-AH \leftrightarrow A^- + H^+ \qquad (2\text{-}38)$$

so that the surface of the particles can become negatively charged and an electrical double layer forms around each particle, as two double layers repel one other, there will be repulsion between particles. This is illustrated schematically in Figure 2-16.

The thickness of the double electric layer is, roughly speaking, the Debye length r_D. If the water contains various ions of valences z_i ($i = 1, 2, \ldots$), and of concentrations n_i, then

$$r_D = \left(\varepsilon \varepsilon_0 kT/\Sigma e^2 z_i r_i \right)^{1/2} \qquad (2\text{-}39)$$

In water solutions the usual range of the Debye length is between 1 and 100 nm and can be altered within this range by varying the concentration of surface charged species, the pH and ionic strength of the suspending medium (water), etc. Equations that describe the dependence of coal concentration ($\phi(h)$) on the Debye length were obtained and for simplicity of presentation the mathematical development of the model is not described here, rather it is contained in the following section. Here, the key features of the results will be summarized.

The equilibrium concentration (volume fraction) profile for coal particles with a Debye length of 1, 10 and 100 nm were calculated. For each of these cases, particles where 1%, 10% and 20% of their surface areas consisted of charged species such as COO^-, which are formed as a result of oxidation, were considered. For a small Debye length of 1 nm, the profile shown in Figure 2-17 is calculated. A maximum (close packing) volume fraction of $\phi = 0.67$ was assumed and it can be seen that for all coverages the equilibrium profile is essentially close packed, with a sharp transition or interface between the settled slurry and the clear water supernatant. In other words, the electrical repulsive forces between the coal particles are, in this case, too short-range to prevent settling. There is a crucial point here that is worth noting, however. The concentration transition is not quite as sharp as in slurries without charged species (see Figure 2-15) and

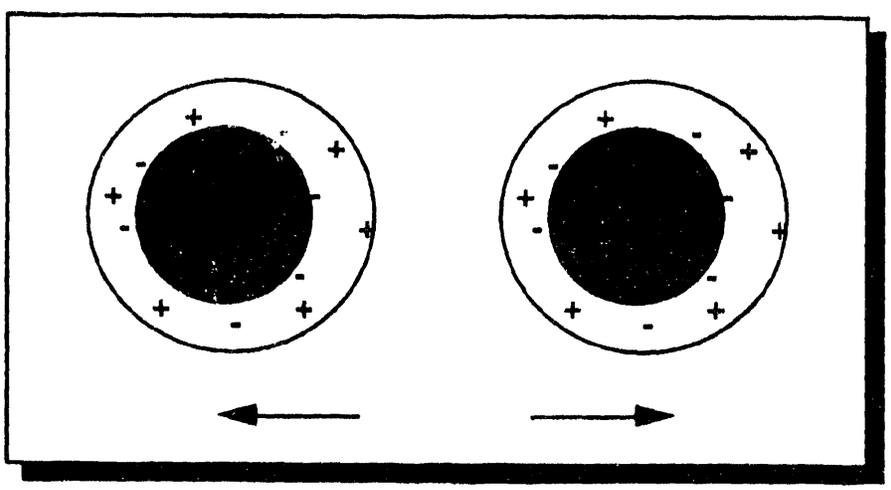

Figure 2-16. Repulsion between charged surface groups (electrical double layer)

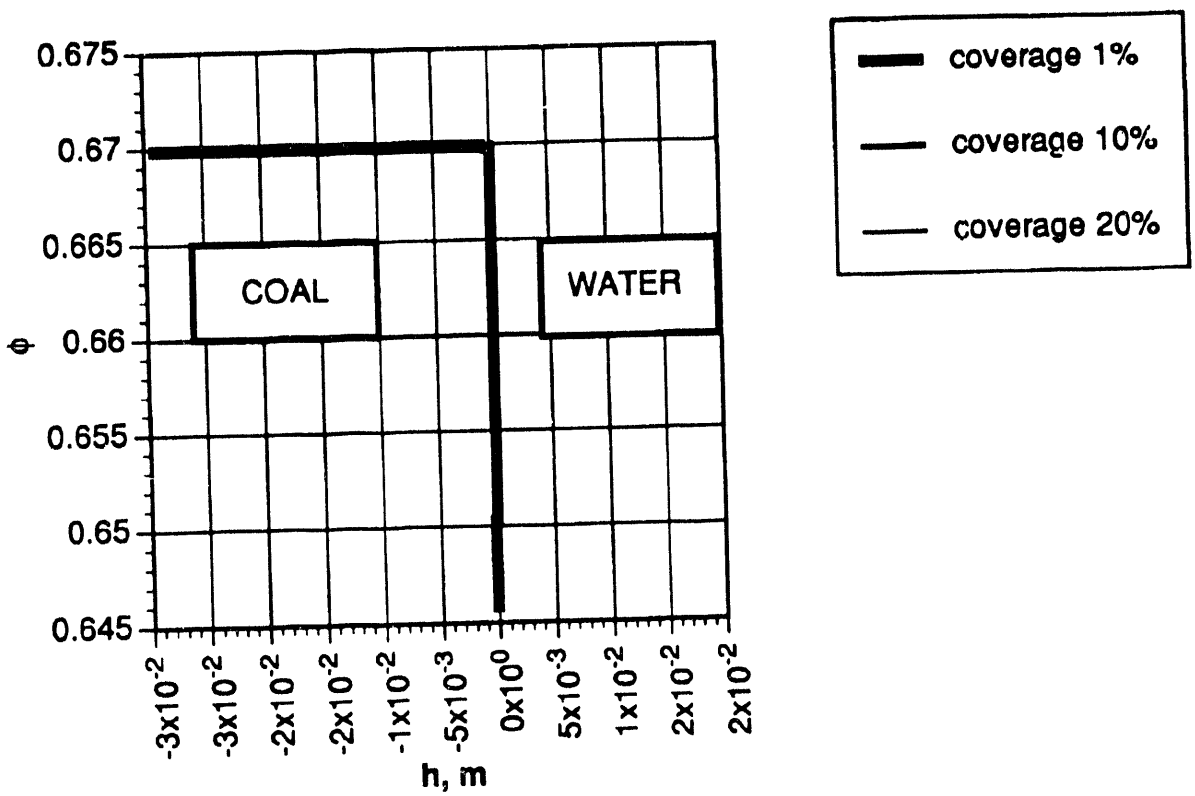

Figure 2-17. Coal volume fraction profile
Debye radius = 1 nm

even a small concentration deviation from maximum packing can lead to a dramatic drop in viscosity (typical viscosity profiles were described in Miller et al., 1993a). Accordingly, a plot of viscosity ratio K (= η^*/η_s, Miller et al., 1993a) shows that at 20% coverage there is a "manageable" viscosity that extends a few centimeters into the settled slurry (Figure 2-18). This suggests that it should be possible to "move" a settled slurry of this type by continually "sweeping away" the surface layer using a flow of water. The slurry will attempt to establish a new surface layer equilibrium that in turn will also be swept away.

If, by adjusting the pH of the slurry or adding electrolytes, the Debye length is extended to about 10 nm, then the interface between the "settled" portion of the slurry and the clear water overlayer becomes more diffuse and a region of manageable (*i.e.* non infinite) viscosity extends further into the slurry, as illustrated in Figures 2-19 and 2-20. Unfortunately, as the Debye length is increased beyond 10 nm this stabilization is lost as the electrical double layer becomes too diffuse and the repulsive forces too weak to stabilize the slurry. Figures 2-21 and 2-22 show the return of the sharp settled slurry/clear water interface for slurries with a Debye length of 100 nm.

These results clearly show that arranging slurry conditions so that the Debye length is about 10 nm produces optimum results (at any coverage of charged species), but this alone is insufficient to prevent settling. As a result, additives must be used such a polymer stabilizers and in Phase II of the program the affect of stabilizers on viscosity and sedimentation will be investigated.

The Settling of Charged Coal Particles - Derivation of Equations

To calculate the density profile, the equations described in Miller et al. (1993a) are used as the starting point. The profile $\phi(h)$ is determined by the set of equations:

$$h/L_0 = - \int_{\phi(0)}^{\phi(h)} d(\Gamma(\phi)\phi)/d\phi \; d\phi/\phi \qquad (2\text{-}40)$$

$$\phi(0)\,\Gamma(\phi(0)) - \phi(H)\,\Gamma(\phi(H)) = (H/L_0)\,\phi_{init} \qquad (2\text{-}41)$$

Note that Equation 2-41 is slightly different to that given in the previous report (Miller et al., 1993a), because the surface of the slurry is now defined as the zero point. In Equations 2-40 and 2-41

$$L_0 = kT/V_0 g(\rho_c - \rho_w)) \approx 10^{-11}\ m \qquad (2\text{-}42)$$

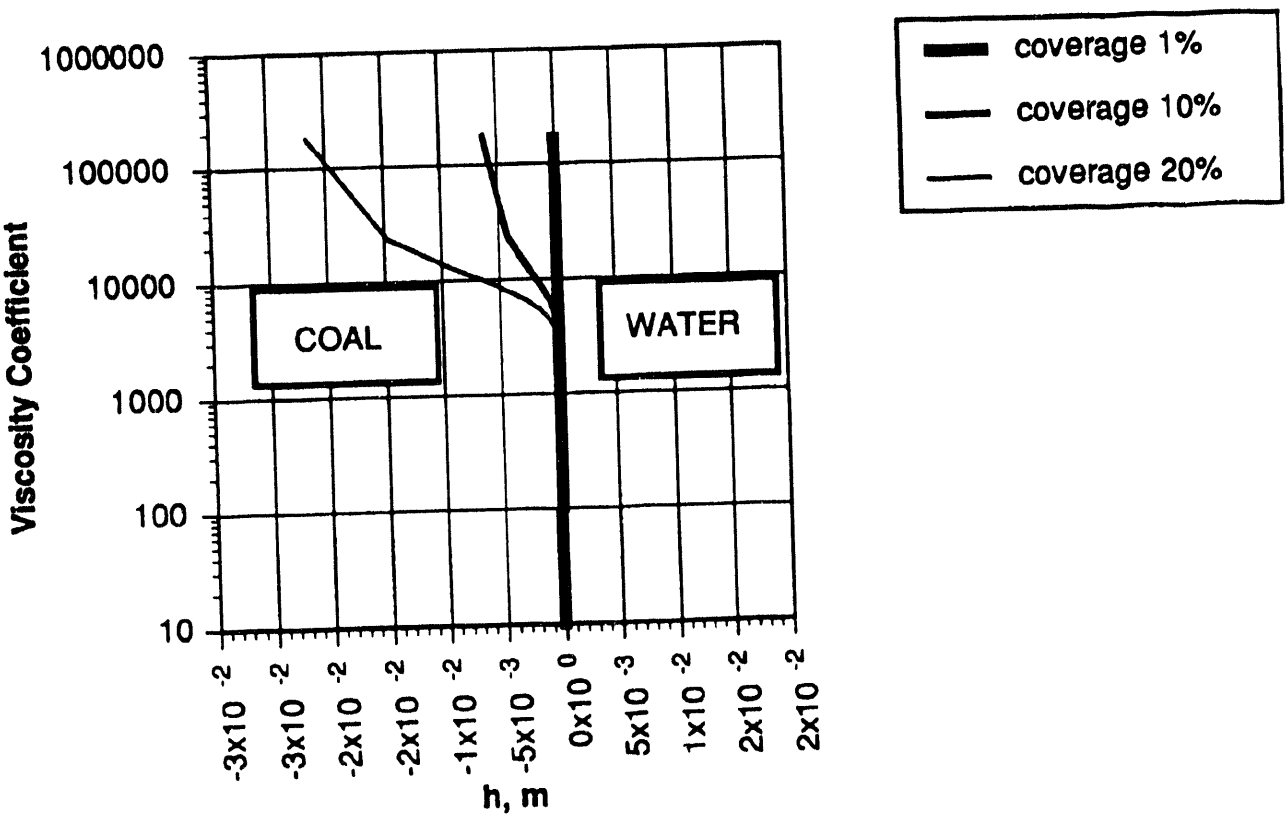

Figure 2-18. Viscosity profile
Debye radius = 1 nm

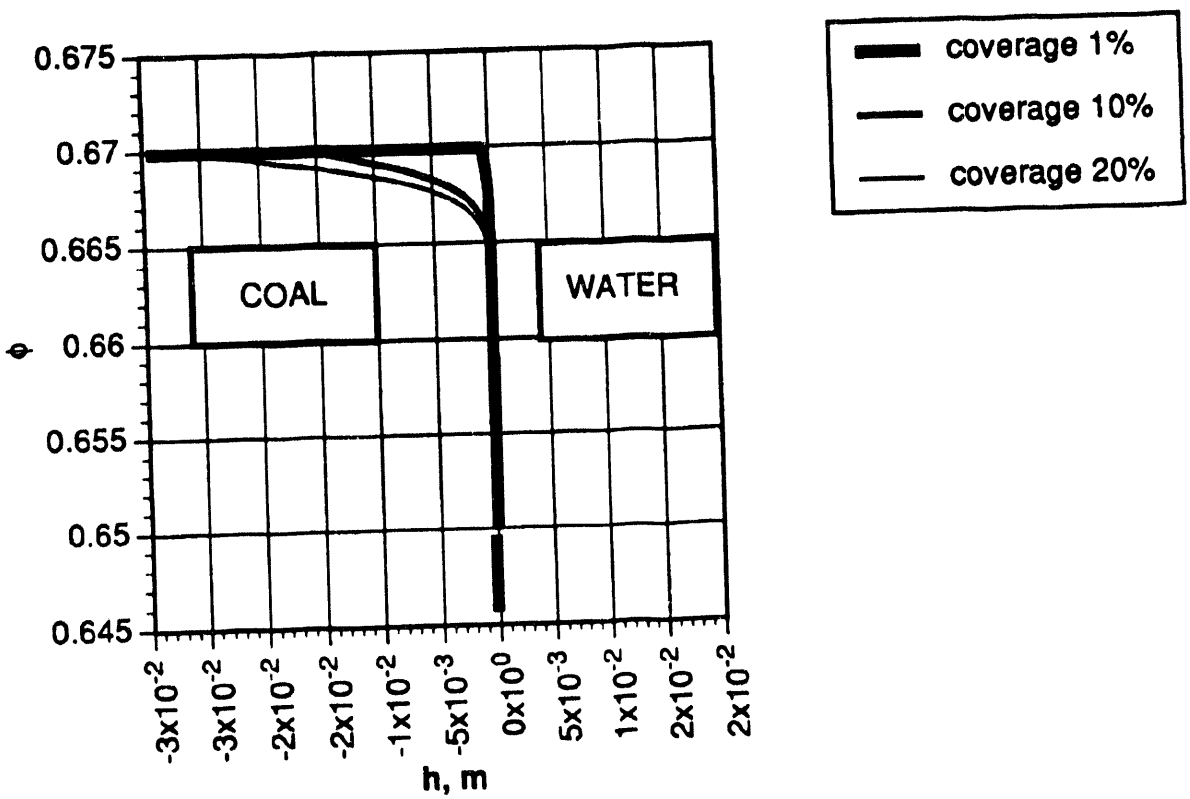

Figure 2-19. Coal volume fraction profile
Debye radius = 10 nm

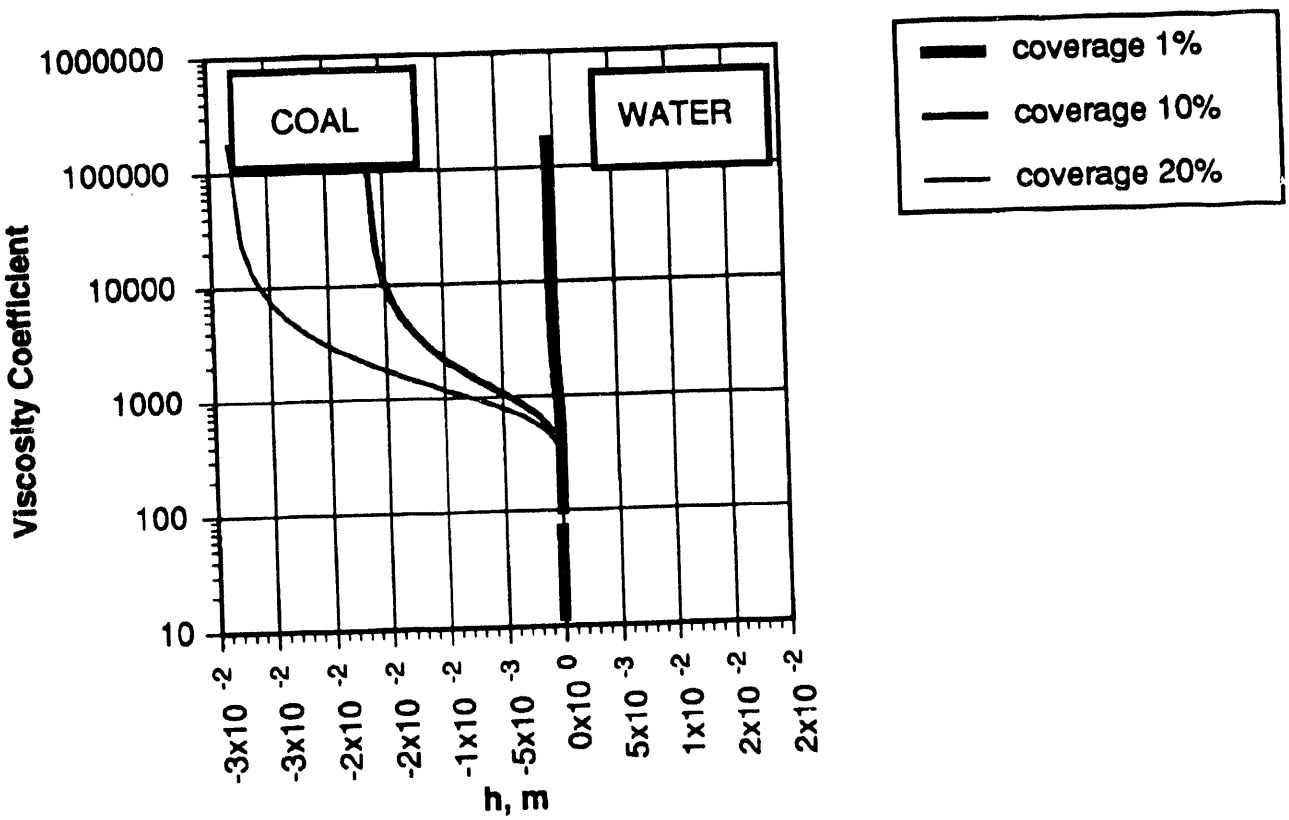

Figure 2-20. Viscosity profile
Debye radius = 10 nm

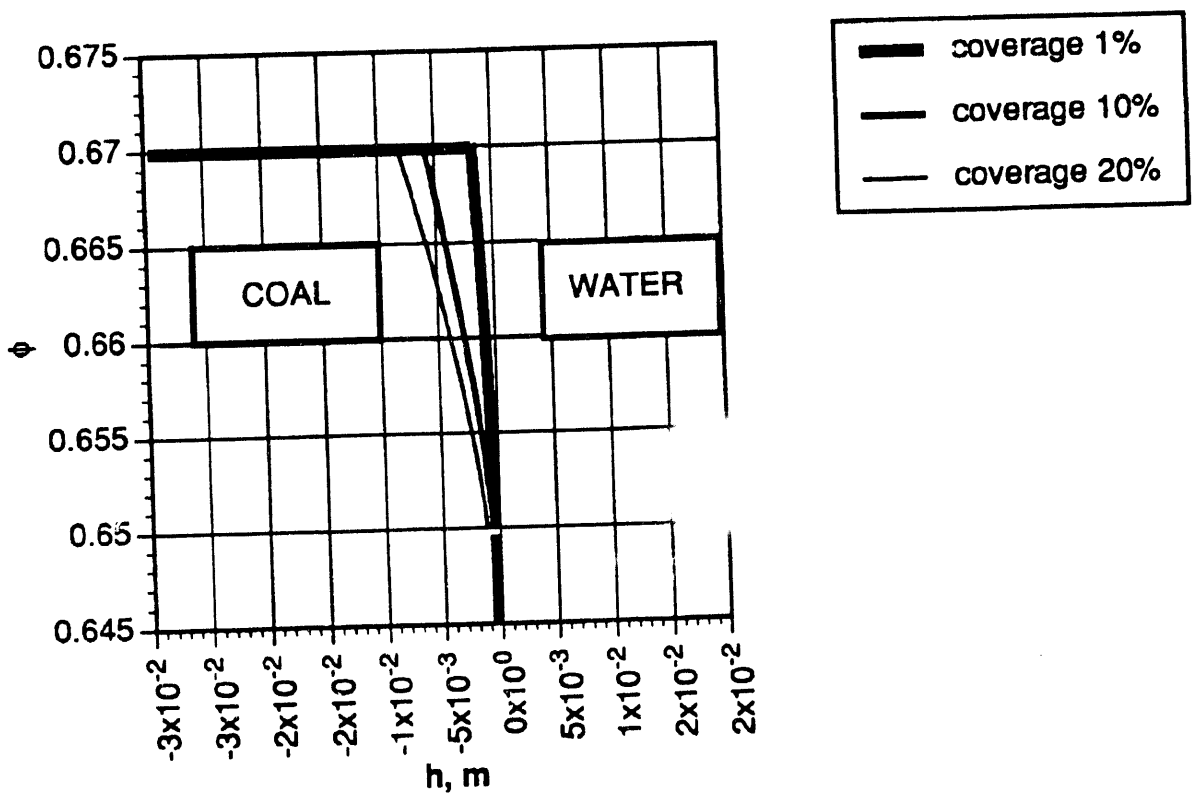

Figure 2-21. Coal volume fraction profile
Debye radius = 100 nm

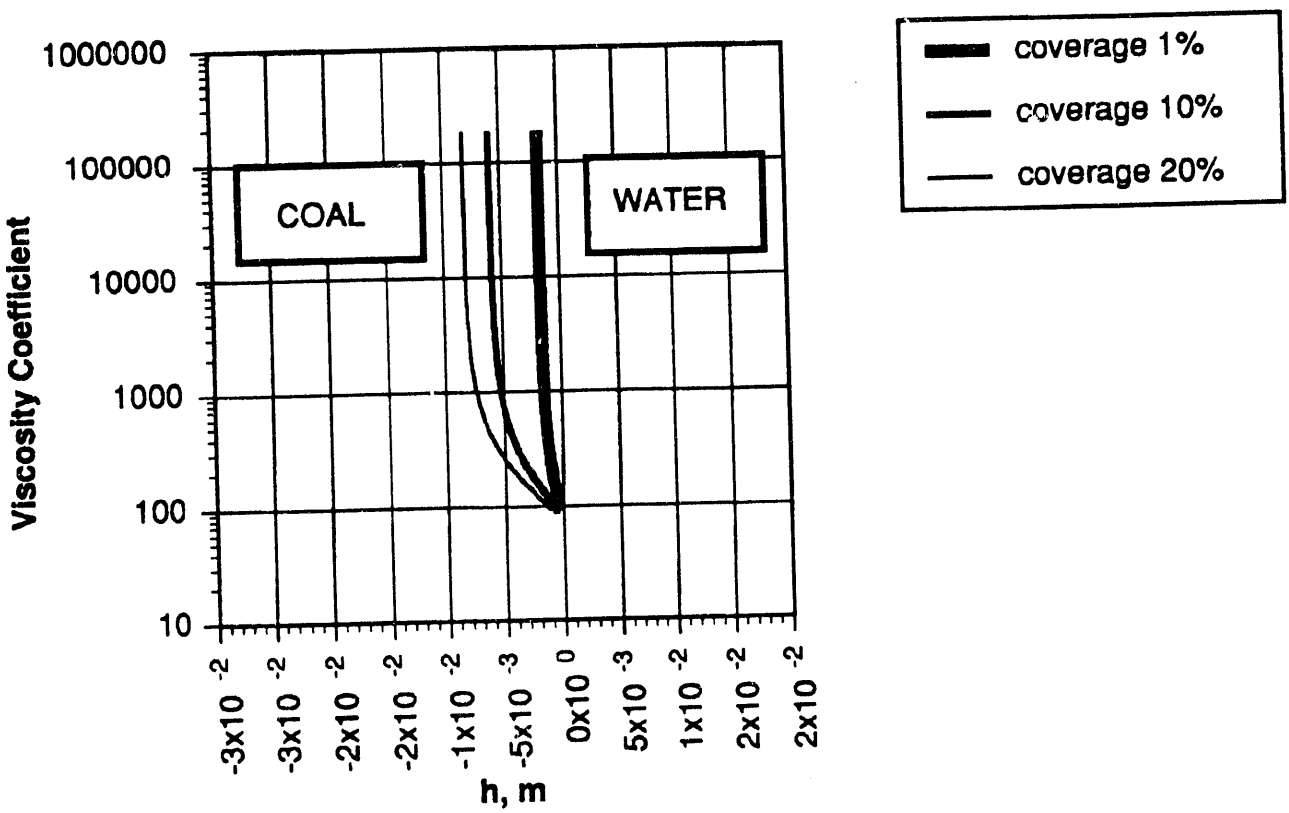

Figure 2-22. Viscosity profile
Debye radius = 100 nm

where ρ_c and ρ_w are densities of coal and water, respectively, V_o is the volume of a coal particle, g is the gravitation constant, H is the height of the vessel, ϕ_{init} is its initial coal volume fraction (assumed to be uniform), and the function Γ is determined by

$$\Gamma(\phi) = (V_o/\phi kT)\ \pi(\phi) \tag{2-43}$$

where $\pi(\phi)$ is the osmotic pressure of the coal particles.
For the electrically stabilized slurry it can be written

$$\pi(\phi) = \pi_o + p_{el} \tag{2-44}$$

where π_o describes steric repulsion only, as discussed previously (Miller et al., 1993a). The π_o term gives;

$$\Gamma_o = 1.85/(\phi_{close} - \phi) \tag{2-45}$$

The electric contribution is

$$p_{el} = -\ \partial F_{el}/\partial V \tag{2-46}$$

where F_{el} is the free energy of the interaction between the electrical double layers.

To calculate F_{el} the fact that the electric double layers are thin is used. Therefore, it can be assumed that the particles packing structure is close to the close packing limit. In other words, imagine that each particle is surrounded by a thin 'coat' of thickness s, so that in effect the slurry can be modeled as a system of close-packed particles of radius a + s, where a is the true radius. In this case

$$\partial F_{el}/\partial V = (\partial F_{el}/\partial s)\ (\partial s/\partial V) \tag{2-47}$$

and for close-packing

$$((a+s)/a)^3 = \phi_{close}/\phi) \tag{2-48}$$

and, since

$$\phi = 4/3\ \pi\ a^3N/V \tag{2-49}$$

where N is the number of particles, gives

$$\partial s/\partial V = (a + s)/3V \qquad (2\text{-}50)$$

To calculate F_{el} the fact that s<<a is used, so that only nearest neighbors have overlapping layers. If each particle has an average of l neighbors (for random close packing $l \approx 10$), and the repulsive force between two neighboring particles is P(s), then

$$\partial F_{el}/\partial s = - (Nl/2)\, P(s) \qquad (2\text{-}51)$$

In the Derjaguin approximation the force P(s) is then

$$P(s) = 2\pi\, \varepsilon\, \varepsilon_o\, (kT/e)^2\, (a/r_D)\, (\Psi_S)^2\, \exp(-2s/r_D) / (1 + \exp(-2s/r_D)) \qquad (2\text{-}52)$$

where Ψ_s is the dimensionless parameter, determined by the electric potential ψ_s of the particles surface. For a monovalent group (e.g. COO^-)

$$\Psi_s = e\psi_s/kT \qquad (2\text{-}53)$$

The potential of the coal surface is determined by three factors:

1) the constant K_i of the ionization reaction (Equation (2-38))
2) the concentration of the ions $[H^+]_o$ in the solution.
3) the concentration $n = [A^-]$ of the anchored groups on the coal particles surface.

The Guoy-Chapmen model is used to calculate Ψ_s. The equilibrium condition on the surface of the particles can be written as

$$[A^-]\,[H^+]_s = K_i\,(n - [A^-]) \qquad (2\text{-}54)$$

Therefore the surface charge is

$$Q = e[A^-] = (eK_i\, n)/(K_i + [H^+]_s) \qquad (2\text{-}55)$$

If the bulk concentration of H^+ ions is $[H^+]_o$, then the surface concentration is

$$[H^+]_s = [H^+]_o \cdot \exp(-\Psi_s) \qquad (2\text{-}56)$$

Accordingly, this gives three variables: $[H^+]_s$, Q and Ψ_s and two Equations 2-55 and 2-56. To obtain solutions, an independent relationship between the surface charge and the surface potential is required. This relationship can be obtained using the Loeg, Overbeek and Wiersema approximation for $a/r_D >> 1$. This approximation gives

$$Q = 2 (\varepsilon \varepsilon_o kT \Sigma z_i n_i)^{.5} \cdot \sinh (- 1/2 \Psi_s) \qquad (2\text{-}57)$$

From equations 2-55 to 2-57 it then follows that

$$(K_i n/(K_i + [H^+]_o \exp (-\Psi_s)) = (2 \varepsilon \varepsilon\alpha\upsilon kT/e^2 r_D) \sinh [-1/2 \Psi_s] \qquad (2\text{-}58)$$

For $K_i >> [H^+]_o \exp (-\Psi_s)$ (i.e. the surface groups are almost completely ionized) this equation gives

$\Psi_s = -2 f(, 2 \varepsilon \varepsilon\tau)$ (2-59)

The density profile then becomes;

$$h = - L_o \int_{\phi(o)}^{\phi(h)} (d(\Gamma_o(\phi)\phi)/d\phi) (d\phi/\phi) - L_1 \int_{\phi(o)}^{\phi(h)} (d(\gamma_{el}(\phi) \phi)/d\phi) (d\phi/\phi) \qquad (2\text{-}60)$$

where L_o and Γ_o are given by Equations 2-42 and 2-45 and

$$L_1 = (\varepsilon \varepsilon\alpha\upsilon \Psi\sigma \, l/bag \, (\rho_c - \rho_w) \, r_D) \, (kT/e)^2 \qquad (2\text{-}61)$$

$$\gamma_{el} (\phi) = \exp (- 2 s (\phi)/r_D) / (1 + \exp (- 2s(\phi)/r_D)) \qquad (2\text{-}62)$$

and $s(\phi)$ is determined by Equation 2-47. Inside the transition layer ϕ is near ϕ_{close}. Therefore

$$d(\Gamma A \Phi)/d\phi) \approx \phi \, (dg/d\phi) \text{ and } (d(\gamma\phi)/d\phi) \approx \phi \, (d\gamma/d\phi) \qquad (2\text{-}63)$$

Then using Equation 2-40 and supposing $\Gamma_o (0) \approx 0$, $\gamma_{el} (0) \approx 0$ gives

$$h = H (\phi_{init}/\phi_{close}) - \Gamma_o (\phi) L_o - \gamma_{el} (\phi) L_1 \qquad (2\text{-}64)$$

The most interesting parameter for the CWSF is the viscosity coefficient $K = \mu/\mu_o$. As ϕ goes to ϕ_{close}, K goes to infinity. In the Dougherty-Krieger approximation

$$K = (1 - (\phi/\phi_{close}))^{-\rho\,\phi_{close}} \qquad (2\text{-}65)$$

where $\rho \approx 2.67$.

The profiles $\phi(h)$ and $K(h)$ for various values of r_D are described in the preceding section. In performing the calculations it was assumed that the factor n describing the concentration of groups on the coal surface can be calculated in terms of the fraction of surface area occupied by the charged species and that COO^- groups cover approximately $100Å^2$ each.

The Optimal Packing of Particles

Recently a critical review of a widely used theory of particle packing due to Furnas has been completed. There are some problems with this approach that are a consequence of a fundamental assumption, namely that in a set of particles with a distribution of sizes there is a large difference in diameter between successive particle sizes in the distribution. In recent work this assumption has been abandoned and a new model has been constructed. At this time there are some "loose ends" however, so that a full description will be presented in the next report.

2.4 Subtask 1.4 Develop a Dry Coal Cleaning Technique:

The equipment for assembling the dry grinding circuit was received. The circuit consists of an opposing jet, fluid-energy mill in closed circuit with a Donaldson Acucut classifier (Figure 2-23). The compressed air (@~760 kPa) for the jet mill is supplied by a rotary screw compressor, while the flow of air through each jet is monitored with a differential pressure gauge. This circuit will be capable of providing a range of particle size distributions for TriboElectrostatic separation and will be used primarily to produce micronized coal. In order to produce the coarser ("PC") material, stage crushing using a hammermill and a high-speed pulverizer will be used. A typical size distribution of the coal generated by this procedure is shown in Figure 2-24.

Dry Beneficiation

Work is continuing on the development of a dry beneficiation process based on TriboElectrostatic Separation (Link et al., 1990). The electrostatic separator was modified by adding a series of flow straighteners (~5 mm diameter by ~100 mm long plastic tubes) at the feed end to the separator whereby sweep air could be drawn through the tubes (Figure 2-25). An air cyclone was added to the exhaust portion of the separator. This will allow those particles that were not collected on the plates to be recovered. Previously, this fraction of coal was lost into the vacuum system. Also, the feed system was modified to ensure a more uniform solids distribution along the width of the separator.

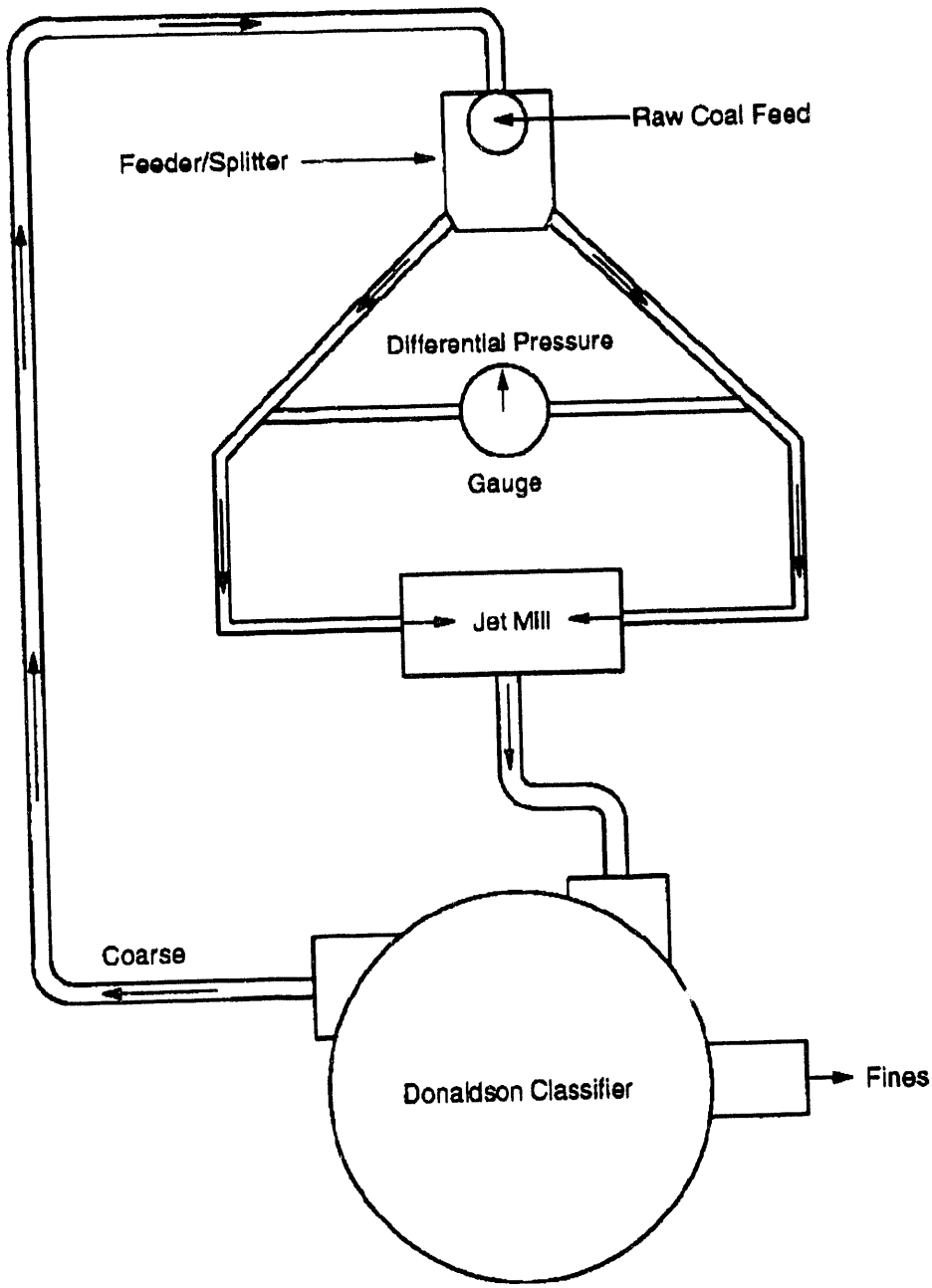

Figure 2-23. Schematic diagram of the dry grinding circuit

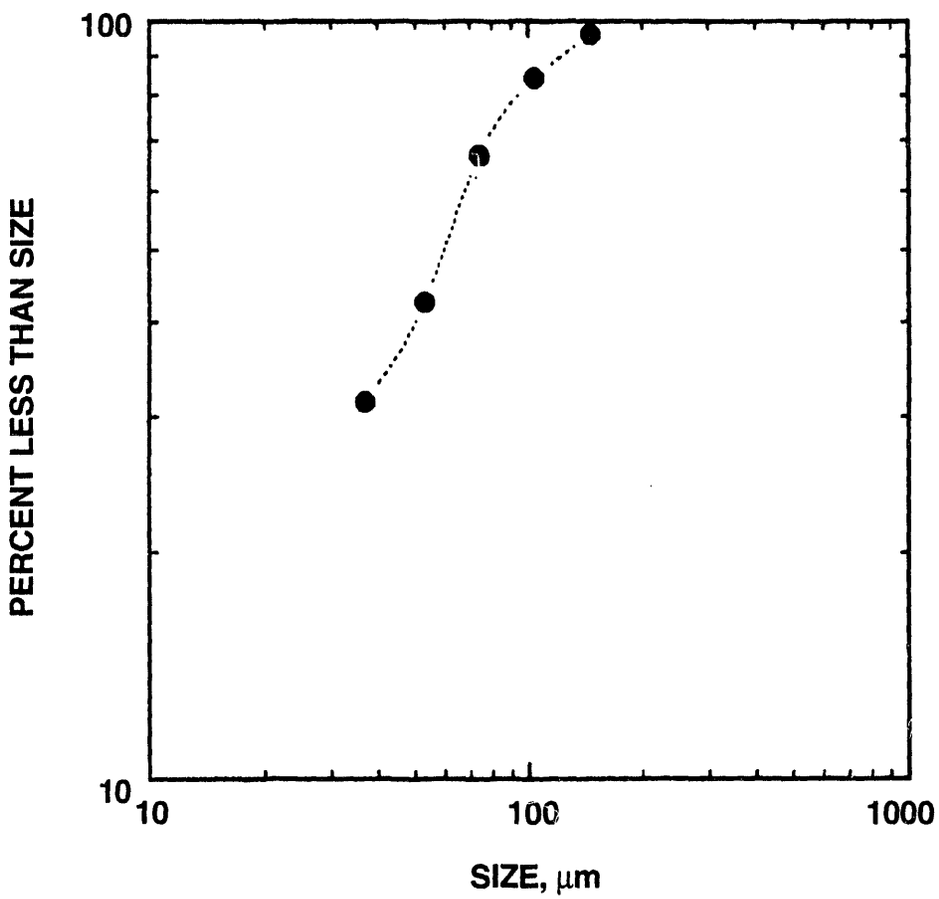

Figure 2-24. Size Distribution of the coarse ground coal

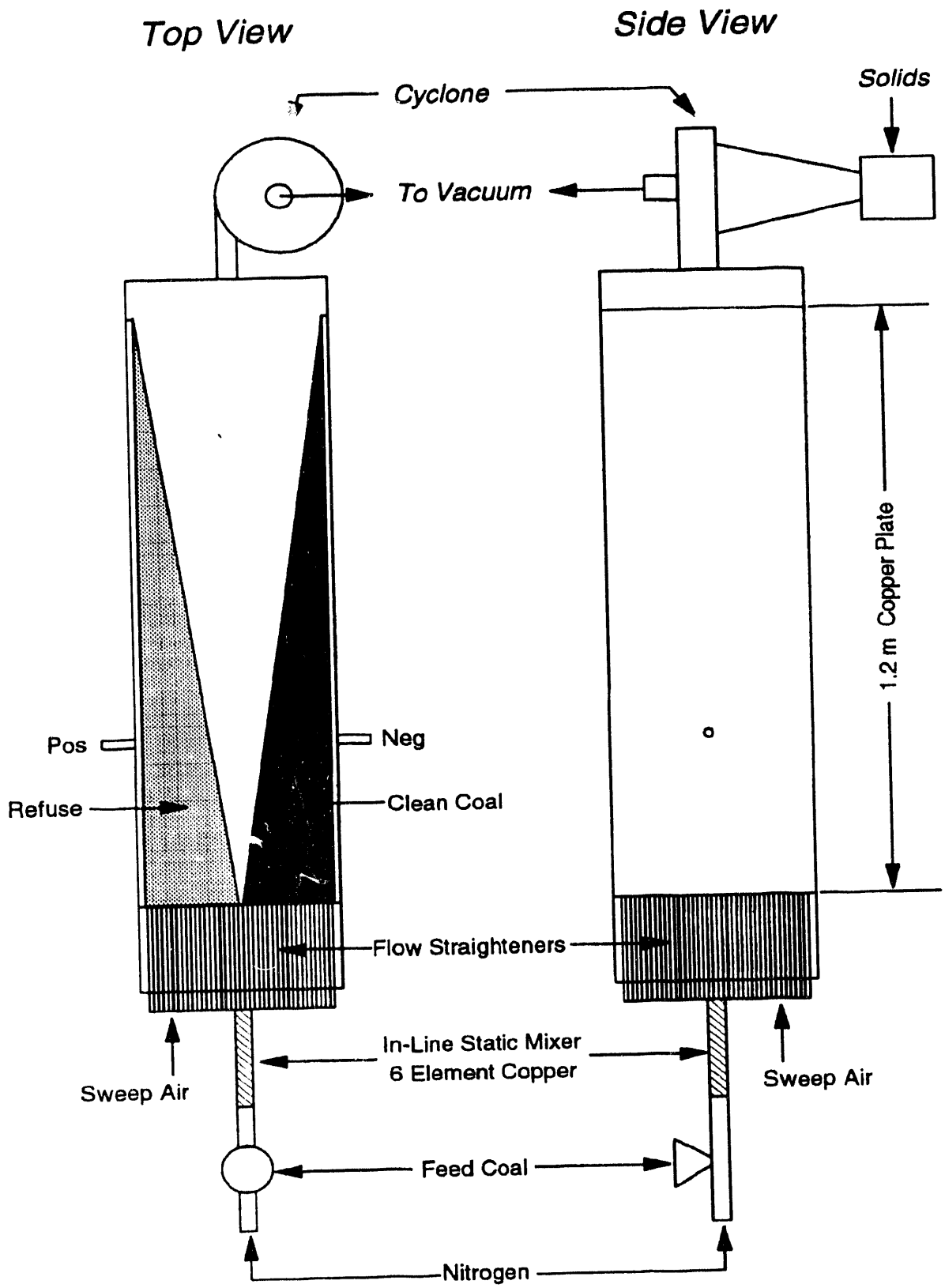

Figure 2-25. Schematic diagram of the TriboElectrostatic Separator

The testing was initiated using the Upper Freeport coal to develop the proper operating and sampling procedures. A 50 g sample of the coal was fed over a 10 minute period. Initially, dried, compressed air was used as the aerosolizing stream, although bottled nitrogen is now being used. The gap between the separator plates was set at 115 mm, with a voltage drop across the plates of approximately 52 kV (±26 kV). After the separation was completed, the plates were removed and the coal and refuse fractions were separated at spaced increments along the length of each plate. The samples were weighed to determine the yield at each point and then analyzed for ash and total sulfur content. The complete set of results at the above test conditions is given in Table 2-10 and Figures 2-26 through 2-30.

2.5 Subtask 1.5 Produce MCWMs and Micronized Coal from Dry, Clean Coal

No work was scheduled or performed in Subtask 1.5 this reporting period.

2.6 Subtask 1.6 Produce MCWM and Dry, Micronized Coal for the Demonstration Boiler

Fuel Preparation Facility

Work on this subtask focused on completing the fuel preparation facility (containing MCWSF and DMC preparation circuits) associated with the demonstration boiler (15,000 lb steam/h boiler). The facility is complete and has been turned over to Penn State (from the construction managing company). Figure 2-31 is a plan view of the demonstration boiler site. The boiler is located adjacent to Penn State's East Campus Steam Plant (ECSP) in the boilerhouse labeled 'new addition'. Details of the ECSP, demonstration boiler and ancillary components, and a chronology of Penn State's previous efforts in coal-water slurry fuel research can be found elsewhere (Miller et al., 1993b; Miller and Scaroni, 1990 a,b). In addition, the baghouse, the 15,000 gallon CWSF storage tank, the CWSF transfer station, the diagnostics laboratory trailer, and the future emissions control systems site are shown in Figure 2-31.

A schematic diagram of the equipment train in the fuel preparation facility is shown in Figure 2-32. There are two circuits in the facility, one for producing dry, micronized coal and one for producing MCWSF.

Dry, Micronized Coal Preparation Circuit

The dry, micronized coal preparation circuit is complete. The 25-ton coal hopper, coal crusher, metal detector, reddler elevator, 5-ton surge bin, screw feeder, booster fan and TCS mill (pulverizer) have been installed. A dual-control system has been installed to allow operation of the circuit from either the coal preparation facility or the demonstration boiler. This system is currently undergoing shakedown.

Table 2-10. Results for the Triboelectrostatic Separation of Upper Freeport Coal. (Size: 80% < 200 m, Voltage Drop: 56KV, Separator Gap: 115 mm, Humidity: 50%).

	Direct						Cumulative					
	Positive			Negative			Positive			Negative		
Distance, cm	Wt %	Ash %	Total Sulfur %	Wt %	Ash %	Total Sulfur %	Wt %	Ash %	Total Sulfur %	Wt %	Ash %	Total Sulfur %
0-3	1.1	45.7	1.0	1.7	1.7	0.7	1.1	45.7	1.0	1.1	1.7	0.7
3-4	1.7	37.0	2.0	2.7	2.0	0.8	2.8	40.4	1.6	3.8	1.9	0.8
4-6	2.8	31.1	3.4	5.4	2.3	0.8	5.6	35.7	2.5	9.2	2.1	0.8
6-8	3.1	25.8	4.2	5.6	2.5	0.8	8.7	32.2	3.1	14.8	2.3	0.8
8-12	4.2	22.2	5.2	10.4	3.1	0.8	12.9	28.9	3.8	25.2	2.6	0.8
12-16	3.8	20.1	5.4	9.1	4.3	1.0	16.7	26.9	4.2	34.3	3.1	0.8
16-25	6.0	18.7	5.8	9.4	6.0	1.3	22.7	24.7	4.6	43.7	3.7	0.9
25-35	3.3	16.3	5.5	5.0	8.2	1.7	26.0	23.6	4.6	48.7	4.1	1.0
35-80	3.3	12.6	4.1	3.9	9.1	2.1	29.3	22.4	4.6	52.6	4.5	1.1
80-120	0.7	10.6	2.5	0.8	9.7	2.8	30.0	22.1	4.6	53.4	4.6	1.1

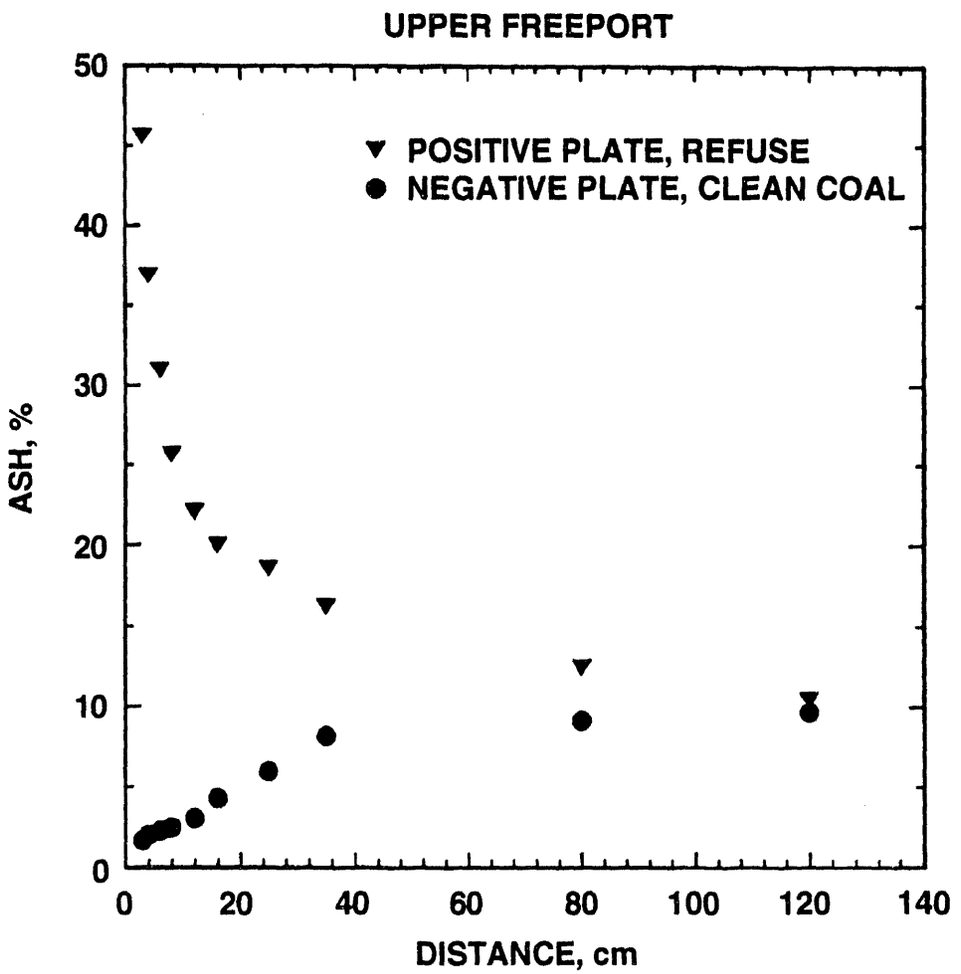

Figure 2-26. Direct ash values as a function of separator length

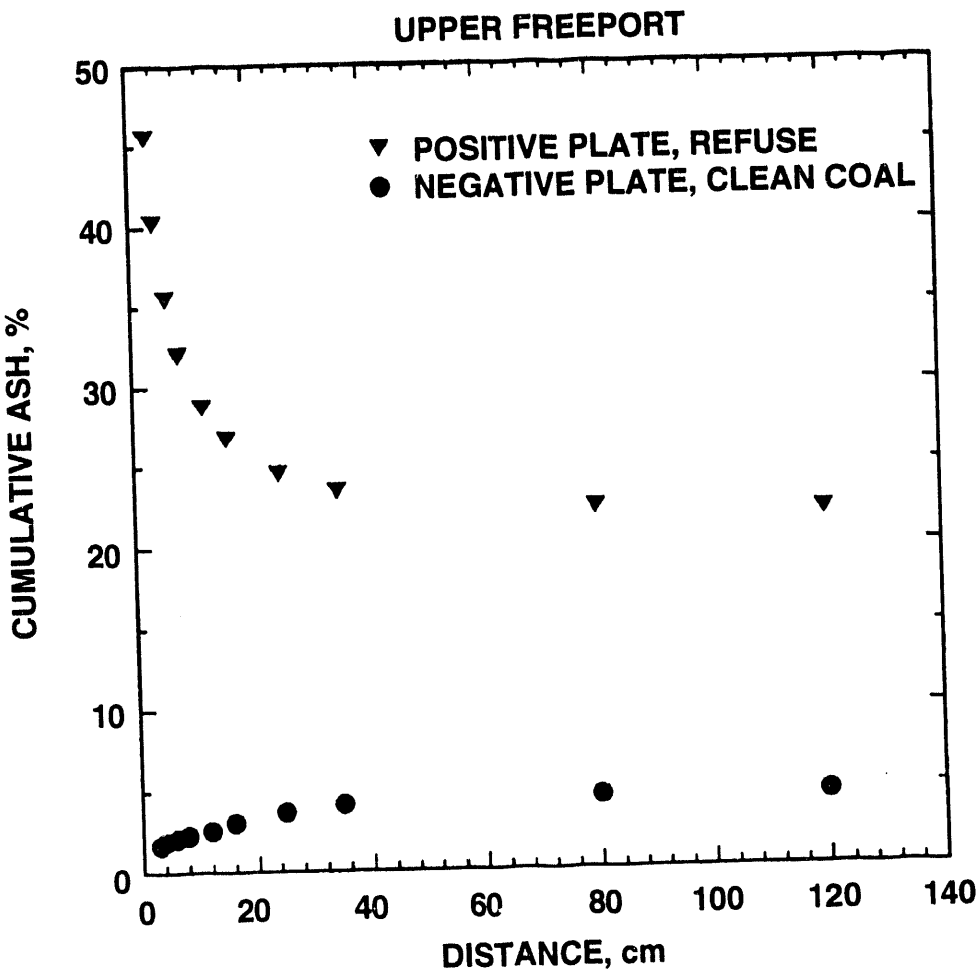

Figure 2-27. Cumulative ash as a function of separator length

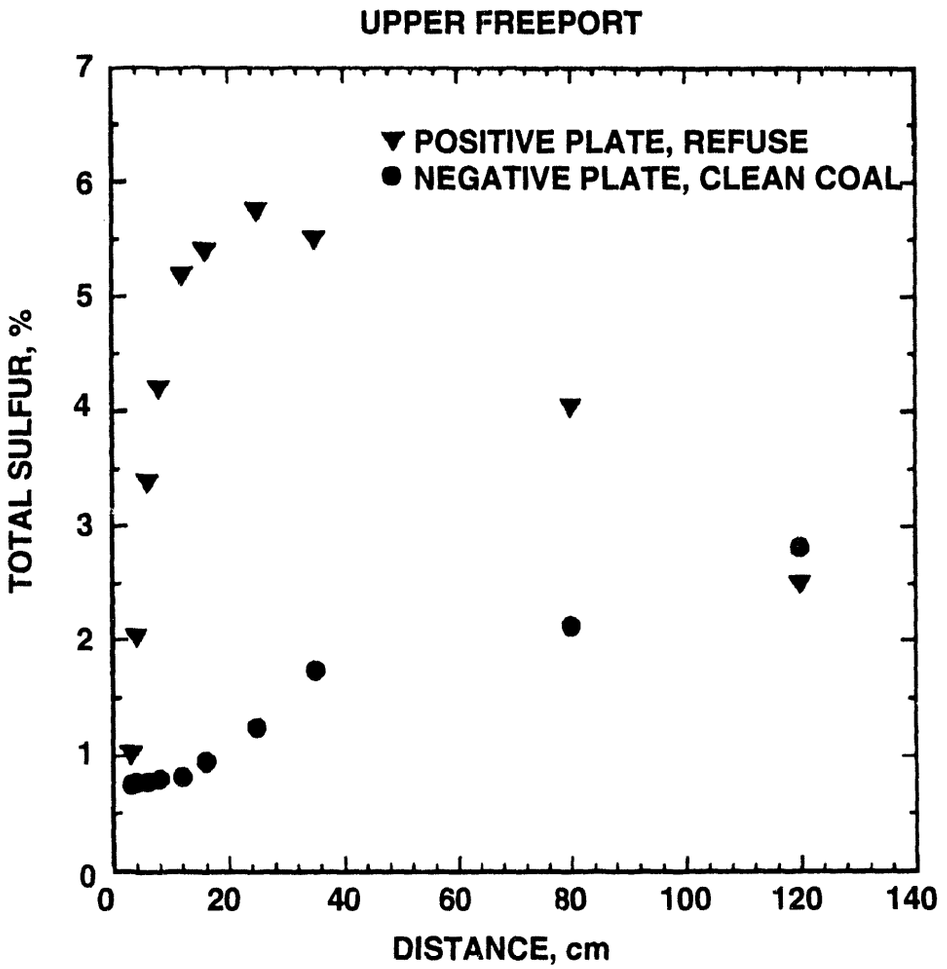

Figure 2-28. Direct total sulfur values as a function of separator length

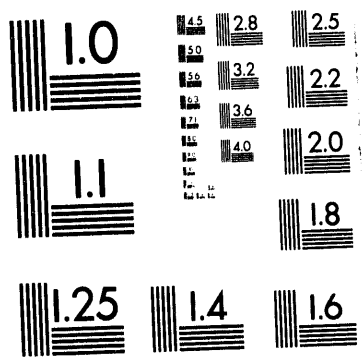
1.0
1.1
1.25
1.4
1.6
1.8
2.0
2.2
2.5
2.8
3.2
3.6
4.0
4.5
5.0
5.6
6.3
7.1

2 of 2

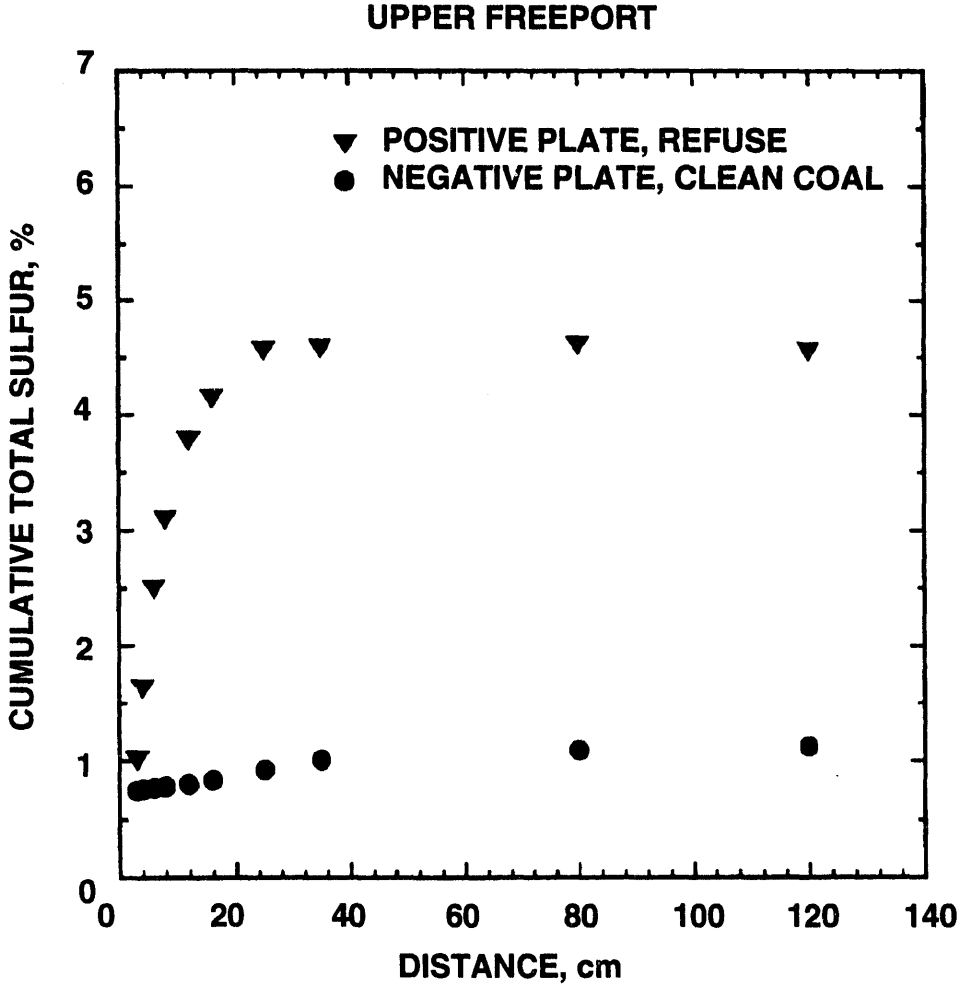

Figure 2-29. Cumulative total sulfur as a function of separator length

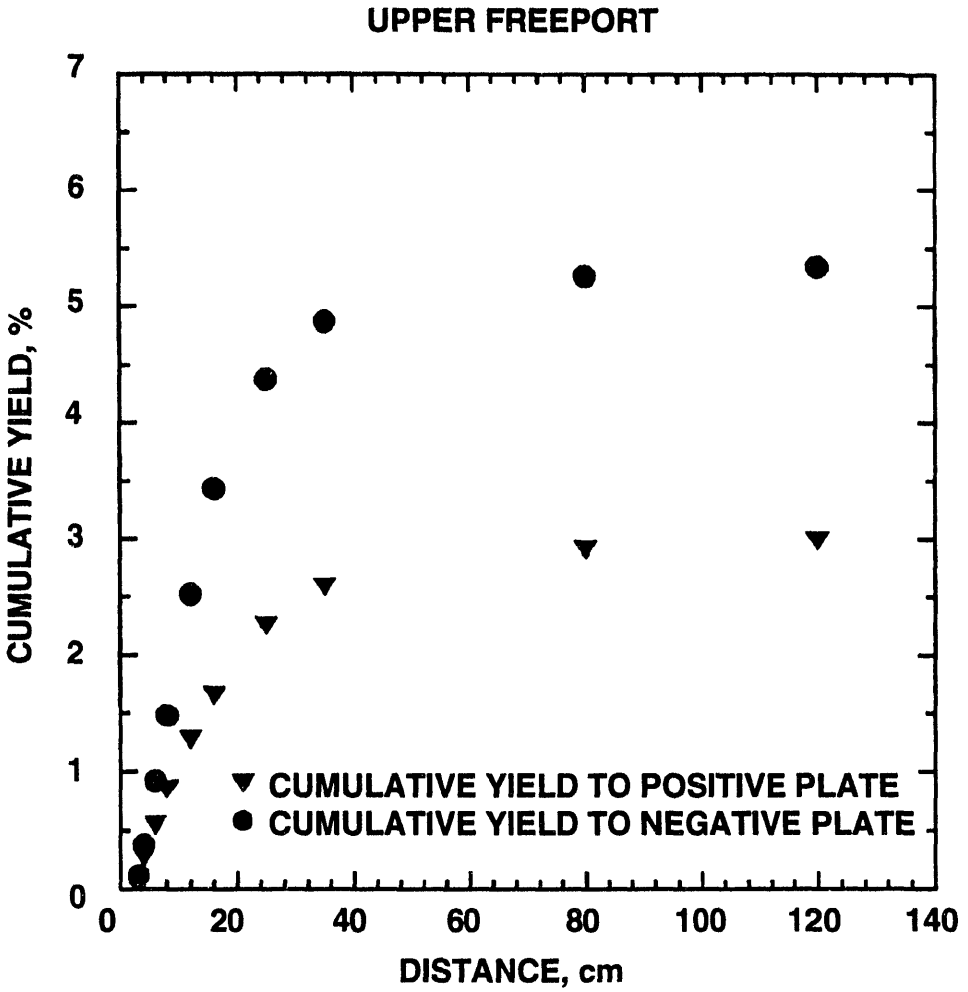

Figure 2-30. Total yield as a function of separator length

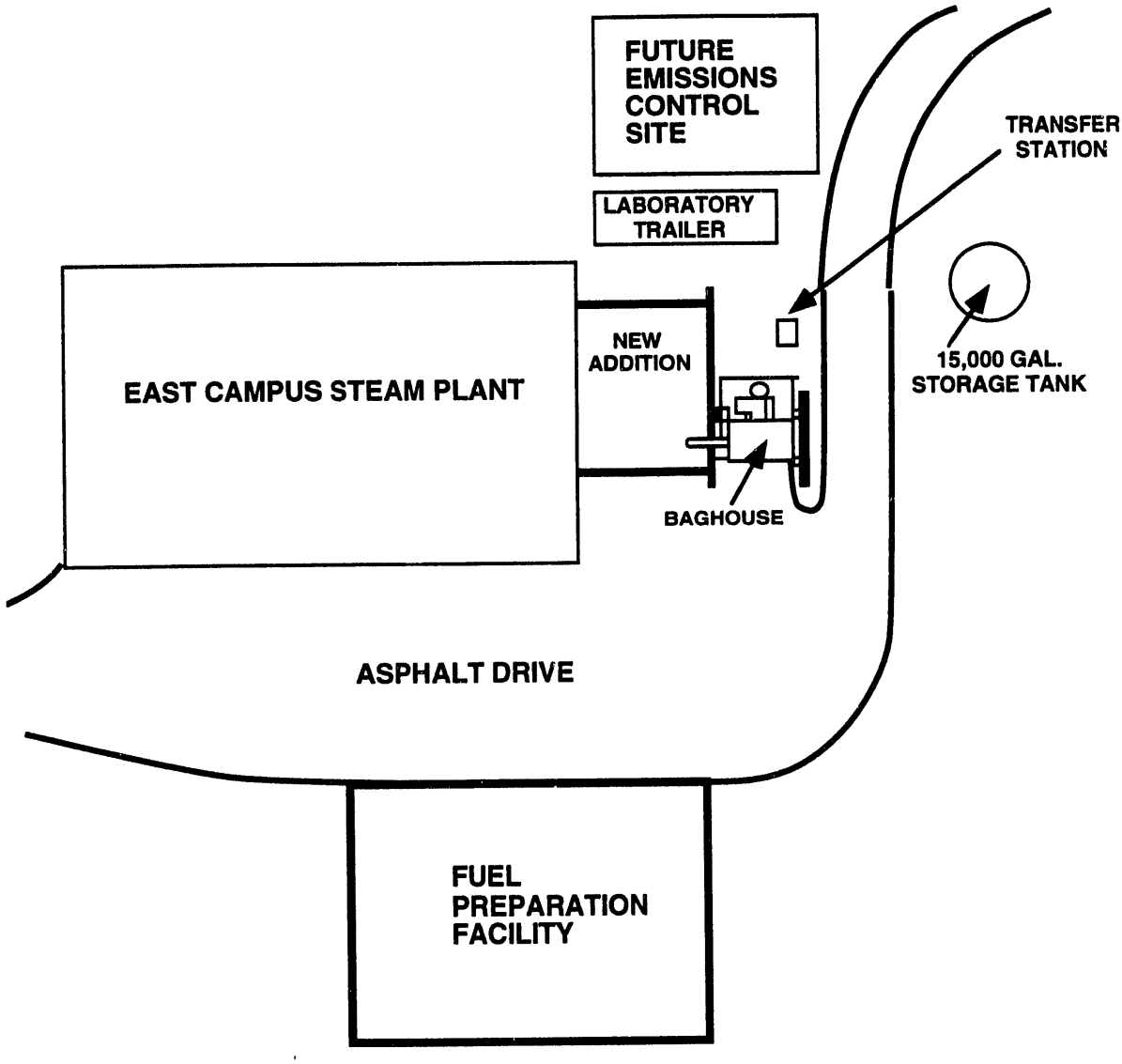

Figure 2-31. Overall site view showing the location of the fuel preparation facility and future emissions control site

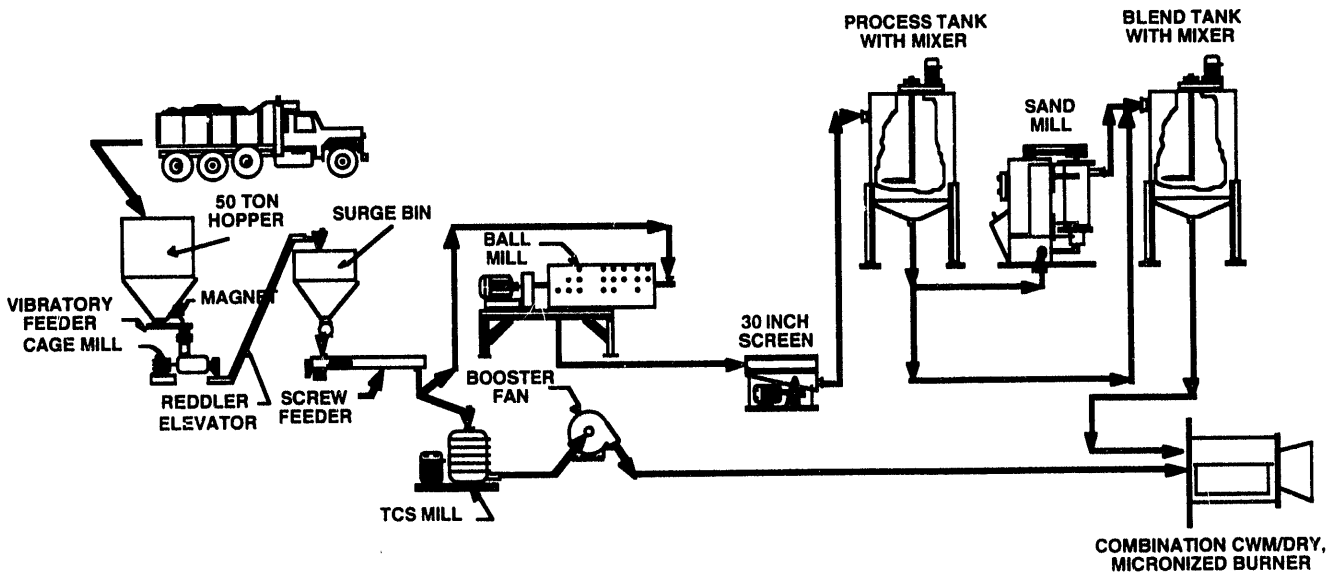

Figure 2-32. Schematic diagram of the equipment train in the fuel preparation facility

MCWSF Preparation Circuit

Work is currently underway setting up the MCWSF preparation circuit. The 25-ton coal hopper, reddler elevator 5-ton surge bin, and screw feeder are common to the dry, micronized coal and MCWSF circuits. The ball mill has been delivered, cleaned (a used mill was donated by Allis Minerals Systems), leveled, and anchored. It is being modified in that the motor is being relocated underneath the mill due to space constraints. In addition, the hydraulic system and feed screw (screw located in the ball mill inlet hopper) are being rebuilt. The ball mill has been deflaked and painted and associated piping and pumps will be installed.

The MCWSF preparation circuit includes several moyno progressive cavity displacement pumps, a 30-inch screen, several tanks (process, blend, waste water), a sand mill, and a plate filter press. The pumps and sand mill were donated by CE, as part of the cost-sharing component of the program, and were part of their pilot-scale coal-water mixture preparation facility. Penn State personnel inspected each piece of equipment, disassembled it, and determined its operability. Equipment that was in, or near working condition was cleaned, reassembled, in some cases rebuilt, and painted. A list of the equipment that has been reconditioned was previously reported (Miller et al., 1993a). Installation of this equipment will begin in the next reporting period.

The goal is for the overall site (boiler and MCWSF preparation facility) to be a zero-discharge facility. Consequently, Penn State's Mineral Processing Section is designing a system to process waste water. This includes water that is generated from flushing lines, off-specification MCWSF, and water used to clean the facility (equipment and floors). The solid material will be removed from the water, and the water will be reused in the production of MCWSF. The system will contain either a filter press or rotary filter.

3.0 TASK 2: COAL COMBUSTION PERFORMANCE

3.1 Subtask 2.1 Boiler Retrofit

No work was conducted this reporting period. CE is still negotiating with Penn State regarding contract language; therefore, the burner and atomizer (for the MCWSF testing) designs have not been finalized.

A High Efficiency Advanced Coal Combustor (HEACC), developed by CE under another DOE program (DE-AC22-91PC91160), was installed on the demonstration boiler. Penn State is the host site for demonstrating the HEACC. The burner is currently undergoing shakedown and a test program will be conducted for CE prior to the start of the DOD testing (MCWSF and DMC). The testing for CE is anticipated to be completed by November 1993.

3.2 Subtask 2.2 Fuel Evaluation in the Research Boiler

In this subtask, candidate fuels will be evaluated in Penn State's 1,000 lb steam/h research boiler. Details of the boiler and auxiliary components were previously presented (Miller et al., 1993a).

Mulled Coal Testing

During this reporting period, three combustion tests were conducted to evaluate a coal-based fuel produced by Energy International, Inc. (EI). The fuel, called mulled coal, was tested on an as-received basis and as a coal-water slurry fuel.

Results

Mulled coal is produced from filter cake obtained from coal cleaning processes. Two mulled coal combustion tests were originally planned, one using the as-received material (fired in suspension) and one with the mulled coal produced into a CWSF. However, because the high moisture content of the first shipment (~41-42 wt.%) caused operability problems when fired in suspension (as discussed below), EI air dried a sample of the mulled coal (labeled Sample #3 by Penn State) until the moisture content was ~18 wt.% and then shipped it to Penn State. This sample was then fired in suspension.

Analyses of the mulled coal samples that were shipped to Penn State are given in Table 3-1, which contains the proximate and ultimate analyses, calorific value, and particle size distributions. Samples #1 and 2 were obtained from the first shipment while Sample #3 was taken from the second shipment.

A discussion of the test results is contained in the following sections. Table 3-2 contains a summary of the combustion tests.

Test #1

Tests #1 and 2 were conducted on March 23, 1993 with representatives of EI in attendance. The mulled coal was to be first fired as received and then as a CWSF. The procedure that was used when firing the mulled coal in suspension was as follows:

1) The boiler was preheated firing natural gas at a rate of ~2 million Btu/h until the quarl reached a predetermined temperature.
2) The natural gas-fired preheater was started and the secondary air was preheated to 190-230°F.
3) The pulverized coal entrainment air was started and the coal feeder turned on, introducing the mulled coal.
4) The mulled coal feed rate was increased while the natural gas was decreased.

Test #1 was conducted firing the mulled coal in pulverized form for only 15 minutes. Handling of the mulled coal was a problem as the screw feeder did not feed it consistently. This resulted in slugging into the boiler and the flame pulsated between yellow-white and black. Consequently, the natural gas flow could not be eliminated and was retained at a high level (50% of the thermal input into the boiler) for safety reasons.

The pulsing also caused other problems. When slugs of coal were fed into the boiler, there was insufficient oxygen available for complete coal combustion. This resulted in the

Table 3-1. Mulled Coal (MC) Analysis

	Mulled Coal (As Received)		MC Produced into CWSF		MC Tested on April 7, 1993	
	As Det.	Dry Basis	As Det.	Dry Basis	As Det.	Dry Basis
PROXIMATE ANALYSIS (wt.%)						
Moisture	40.7	–	42.5	–	17.7	–
Volatile Matter	21.9	37.0	21.7	37.8	30.2	36.7
Fixed Carbon	36.3	61.2	34.9	60.7	50.8	61.7
Ash	1.1	1.9	0.9	1.5	1.3	1.6
ULTIMATE ANALYSIS (wt.%)						
Carbon	–	–	49.4	85.9	70.6	85.8
Hydrogen	–	–	3.2	5.6	4.8	5.8
Nitrogen	–	–	0.9	1.5	1.2	1.5
Sulfur	–	–	0.3	0.6	0.5	0.6
Oxygen	–	–	2.8	4.9	3.9	4.7
Ash	–	–	0.9	1.5	1.3	1.6
Calorific Value (Btu/lb)	8,889	14,990	8,748	15,215	12,617	15,330
Particle Size[a] (μm)		–		33.3		42.4
D(v, 0.9)		–		12.0		13.7
D(v, 0.5)		–		4.1		4.4
D(v, 0.1)						

[a]Particle size was measured using a Malvern 2600C Particle and Droplet Sizer. Particle sizes refer to volume fractions that are less than the indicated size

Table 3-2. Summary of Test Results

Date of Test:	March 22, 1993	March 22, 1993	April 7, 1993
Test Number:	1	2	3
Fuel Form Tested:	Pulverized Coal	CWSF	Pulverized Coal
Combustion Air Preheat Temperature (°C)	88.6	110.8	92.2
Economizer Temp. (°C)	318.5	268.5	229.4
Thermal Input (%)			
Coal	50	0	100
Natural Gas	50	0	0
CWSF	0	100	0
Selected Air Flow Rates (scfm)			
Primary	5.0	4.0	5.0
PC entrainment	25.0	0	25.0
Tertiary	58.0	60.0	50.0
Atomizing	0	139	0
Flue Gas Analysis			
O_2 (%)	7.9	7.7	7.9
CO (ppm)	168	165	186
CO_2 (%)	9.6	11.8	12.6[a]
SO_2 (ppm)	68	164	197
NO_x (ppm)	271	485	477
Char/Ash Analysis: - Combustibles in hopper char/ash	Not determined	64.0 wt.% (d.b.)[b]	48.3 wt.% (d.b.)
- Combustibles in baghouse char/ash	Not determined	31.8 wt.% (d.b.)	28.4 wt.% (d.b.)

[a]Analyzer was not stable
[b]Dry basis

formation of a substantial quantity of CO and a high baghouse temperature. The CO concentration in the baghouse outlet was higher than that at the economizer inlet. This, coupled with the rising baghouse temperature, was a cause for alarm and the test was terminated after 15 minutes of operation. The baghouse temperature was ~400°F and rising and was near the maximum operating temperature of the bags when the test was terminated.

Test #2

The procedure that was used when firing the mulled coal in slurried form was as follows:

1) The mulled coal was first mixed in a ribbon mixer with a dispersant (provided by EI) that transformed the mulled coal into a CWSF. This was performed by Penn State personnel under the direction of representatives from EI.
2) After the suspension test, the boiler was fired with natural gas at a rate of ~2 million Btu/h to maintain system temperatures until the CWSF test was conducted.
3) Atomizing air was introduced at a pressure of ~100 psig. The CWSF was then introduced and the flow rate was slowly increased to the desired rate while decreasing the natural gas flow to zero.

The flame appeared stable during the test but large particles were observed burning on the boiler hearth (floor). Char/ash samples were collected from the convective section hoppers and baghouse hopper and analyzed for their ash contents. The combustibles in the char/ash samples are reported in Table 3-1. The quantity of combustibles in the fly ash (~30%) is a typical value observed when firing pc or CWSF in Penn State's research boiler.

When evaluating a pulverized coal or CWSF, Penn State uses the ash content of the char/ash sample to determine the combustion efficiency. The ash content of the char/ash sample is related to the ash content of the feed material by the equation:

$$\Delta W = [1 - A_o(100-A')/A'(100-A_o)] \times 100 \qquad (3\text{-}1)$$

where ΔW = percent weight change (combustion efficiency), daf coal

A_o = proximate ash content of fuel, dry

A' = proximate ash content of char/ash sample, dry

Using this equation, the combustion efficiencies of the mulled coal based on the samples from the convective pass hoppers and the baghouse were 97 and 99%, respectively. However, the overall combustion efficiency was significantly lower than this since there was a significant amount of material deposited on the floor of the boiler. This material was not collected and analyzed but past experience firing pc and CWSF has shown that the material on the floor of the boiler is usually high in combustibles. With other pcs and CWSFs, however, the quantity deposited on the floor is usually not significant.

Figure 3-1, which shows the relationship between the ash content of a coal, the ash content of the char formed during combustion, and the resulting combustion efficiency, is in-

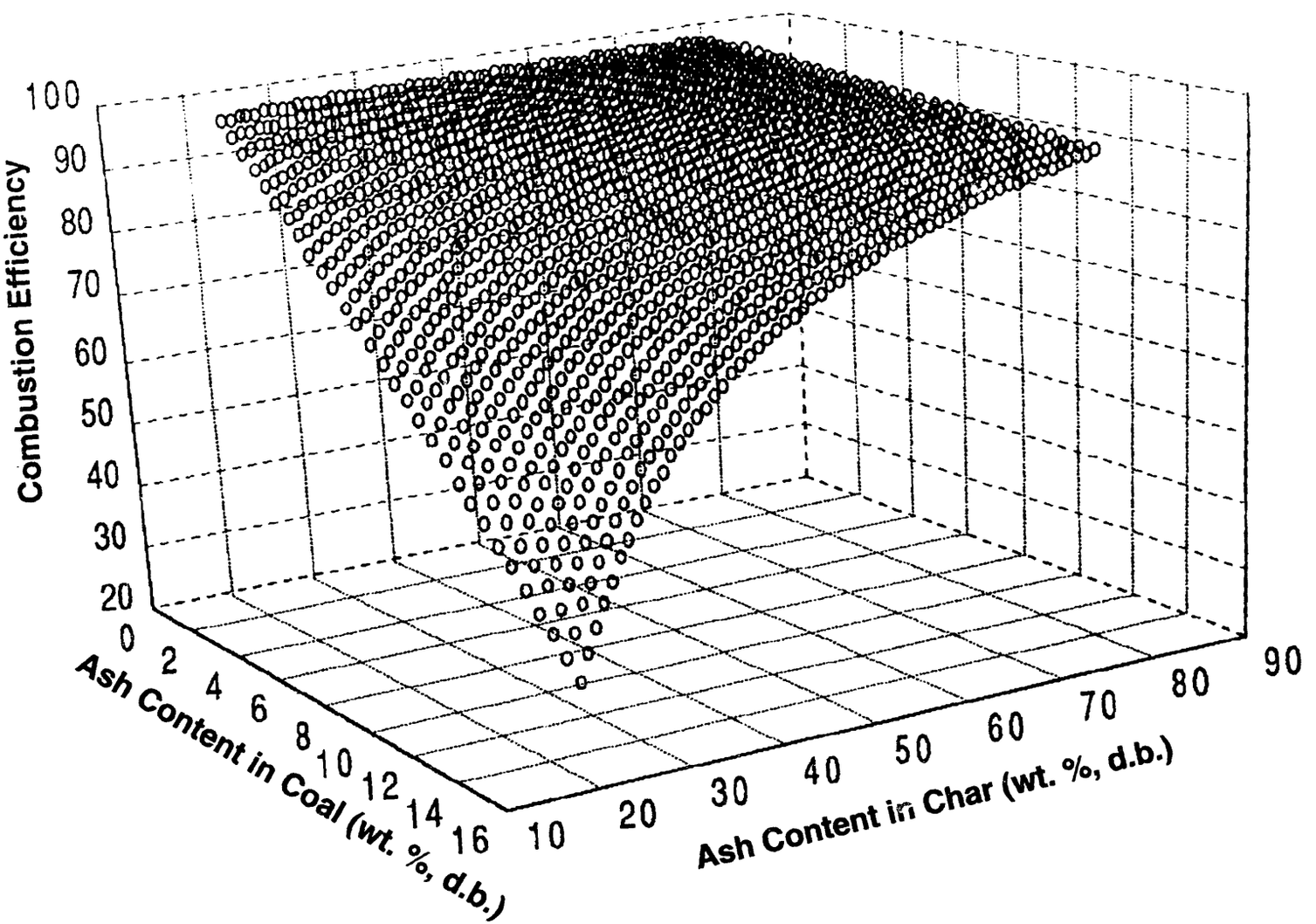

Figure 3-1. Relationship between the ash content in a coal, the ash content in the char formed during combustion, and the resulting combustion efficiency

cluded for reference. It shows that for a coal with a low ash content (*e.g.*, 2.0 wt.%), the coal combustion efficiency is likely to be high for char/ash samples with combustibles ranging from 20 to 80%.

Test #3

A second suspension firing test was conducted on April 7, 1993. The test procedure was identical to that listed above. Test 3 was a repeat of Test 1 except that the moisture content of the mulled coal was reduced from 44 to 17 wt.%. Less handling problems were experienced and the coal was burned without natural gas support. However, after 30 minutes of testing, the flame scanner did not sense the flame and the safety interlocks shut off the boiler. The reason for this is not clear. The results are summarized in Table 3-2.

Conclusions and Recommendations

The mulled coal that was produced into a CWSF was stored, pumped, atomized, and burned in a similar manner to other CWSFs tested at Penn State. The combustion performance of the slurried mulled coal was similar to that of the other CWSFs.

The mulled coal that was fired as received was more difficult to handle (feed from the hopper to the burner via the screw feeder and eductor) than other pulverized coals tested at Penn State. The mulled coal with the high moisture content could not be fired in the research boiler. The mulled coal with the lower moisture content was easier to handle than the case with the higher moisture content but was still more difficult to handle than other pulverized coals tested at Penn State.

The tests that were conducted were short in duration. It is recommended that longer tests be conducted in order to make a detailed evaluation. To be able to conduct pulverized mulled coal tests in the research boiler at Penn State, the coal feed system would have to be modified and the flame scanner relocated within the boiler.

MCWSF Testing

AMAX received four of the six candidate coals and will begin producing MCWSFs from them. Penn State will begin evaluating the MCWSFs as soon as they are received. The last MCWSF is expected in November 1993. For each fuel, Penn State will determine its composition (proximate and ultimate analysis), calorific value, particle size distribution, rheological characteristics, atomization characteristics, and combustion performance in the research boiler.

3.3 Subtask 2.3 Performance Evaluation of MCWSF and Dry, Micronized Coal in the Demonstration Boiler

Evaluate Erosion-Corrosion and Deposition Characteristics

Measurements of erosion by fly ash from coal-water fuel combustion were described in an earlier report (Miller et al., 1992). The measurements were interpreted using an erosion-corrosion model (Miller et al., 1993a). Recent work has been focused on improvement of the

metal oxidation component of the erosion-corrosion model. The changes in erosion rate with temperature and oxygen concentration were consistent with the model when the oxidation rate was assumed to be proportional to the oxygen partial pressure.

Experimental

Figure 3-2 shows the arrangement of the erosion probe in the convective section of the boiler. The flue gas oxygen concentration in this region was 3.7 vol% (Miller et al., 1992). A small orifice was supported on a sidearm attached to the probe and supplied with compressed gas from a cylinder outside the boiler. Details of the gas jet and metal sample are shown in Figure 3-3. The jet entrains surrounding flue gas and particles, and accelerates particles toward the surface of the sample.

Particle properties were determined by analysis of a sample from the baghouse. The apparent density of the particles was 870 ± 20 kg/m^3, determined from the mass and volume of a packed bed, assuming a voidage of 0.42 (Mitchell et al., 1992). The volume-based mean size of the baghouse catch varied over a range of roughly 65 ± 25 μm during the tests.

Motion of the particles in the turbulent jet was simulated by superimposing a randomly fluctuating component of gas velocity on the mean flow (Miller et al., 1993b). Some examples of particle trajectories are shown in Figure 3-3. A typical volume-based particle size distribution, shown in Figure 3-4, was used to calculate the total energy of impaction of particles at the surface of the specimen. The radial distributions for each size of particle are shown in Figure 3-5. The product of the kinetic energies with the probability density shows the comparison of the relative energies delivered to the surface by different sizes of particles.

The properties of particles colliding with the target were calculated at a distance of 2 mm from the jet axis where the peak of the integrated energy of impaction of particles occurred and was 10 times the initial energy of particles suspended in flue gas. The average impaction angle, weighted by the collision efficiency and size distribution, is 83°. The mean time interval between particle impacts is 1.1 ms, and the number flux of particles striking the surface is 32 x 106 s-1m-2, corresponding to a mean size of impacting particles of 78 μm, and an average impaction efficiency of 0.64.

Erosion was found to be greatest at distances from approximately 1.5 to 2 mm from the jet axis. The uncertainty in the erosion rate was estimated from the difference between the erosion craters on the right and left sides of the sample. Effects of metal temperature and jet gas oxygen content on the average maximum erosion rate are given in Table 3-3 and plotted as a function of temperature for each jet gas in Figure 3-6.

Observations of erosion in the presence of nitrogen, air, and oxygen provided data for determination of the oxygen concentration dependence of the erosion-corrosion rate. In the presence of the nitrogen jet, erosion steadily increased as temperature was increased from 450, to

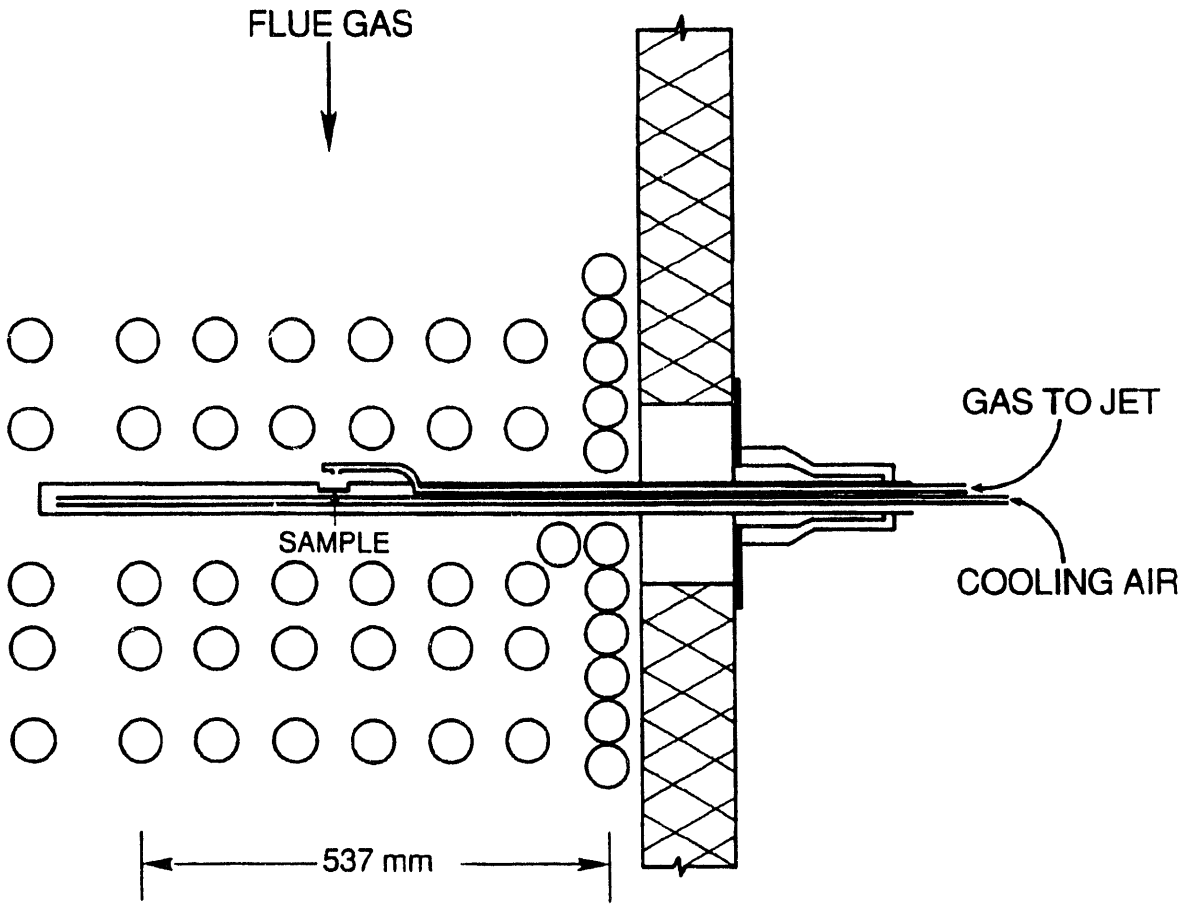

Figure 3-2. **Arrangement of the probe, carbon steel sample, and accelerating gas jet with respect to the flue gas flow and convective tubes. The probe is in a cavity intended for a superheater. 537 mm is one-half of the width of the convective section.**

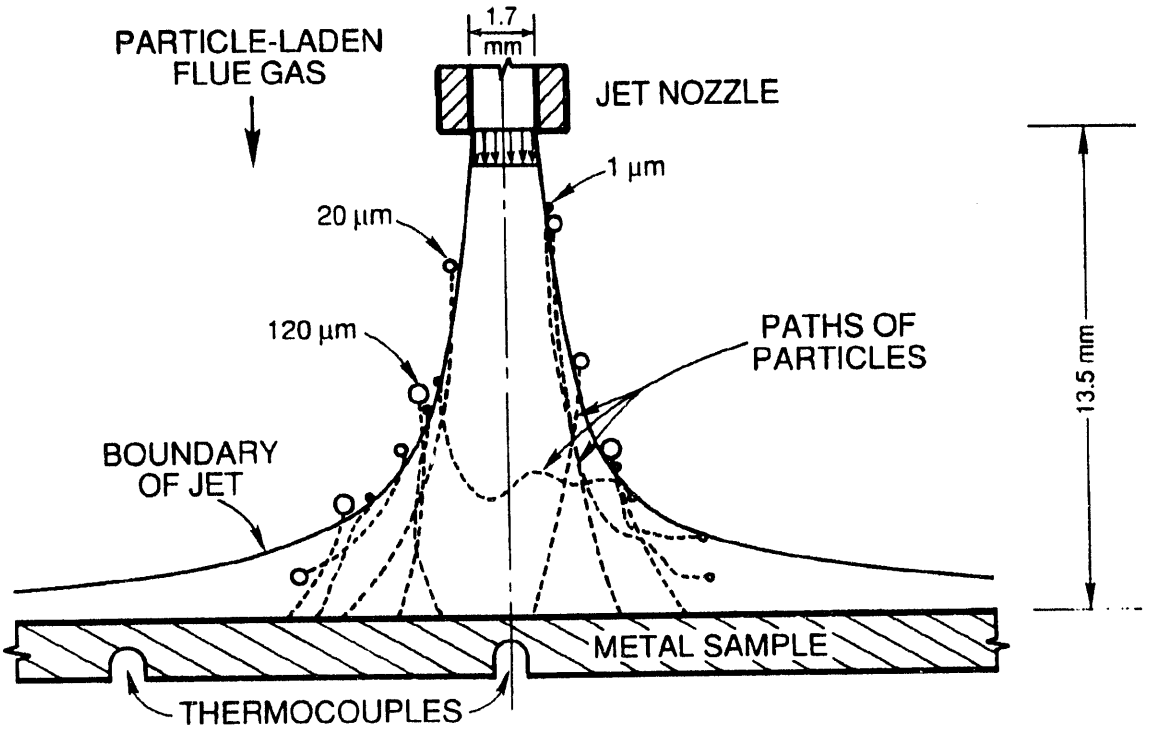

Figure 3-3. **Arrangement of the carbon steel sample, thermocouples, and gas jet used to accelerate particles toward the sample surface. Particles enter the clean jet from the surrounding flue gas. The partial pressure of oxygen at the sample surface was varied by using nitrogen, air, or oxygen as the jet gas.**

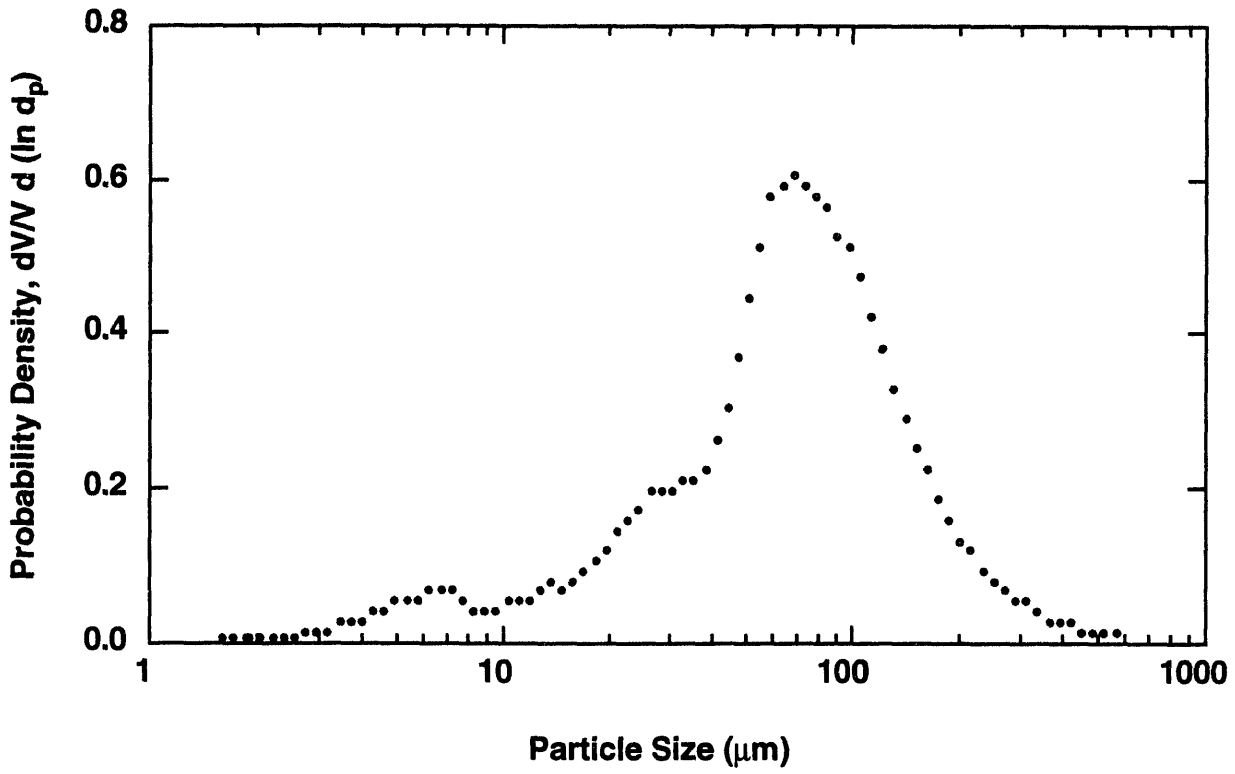

Figure 3-4. Volume-based size distribution of particles collected in the baghouse, determined using a Malvern Droplet and Particle Sizer.

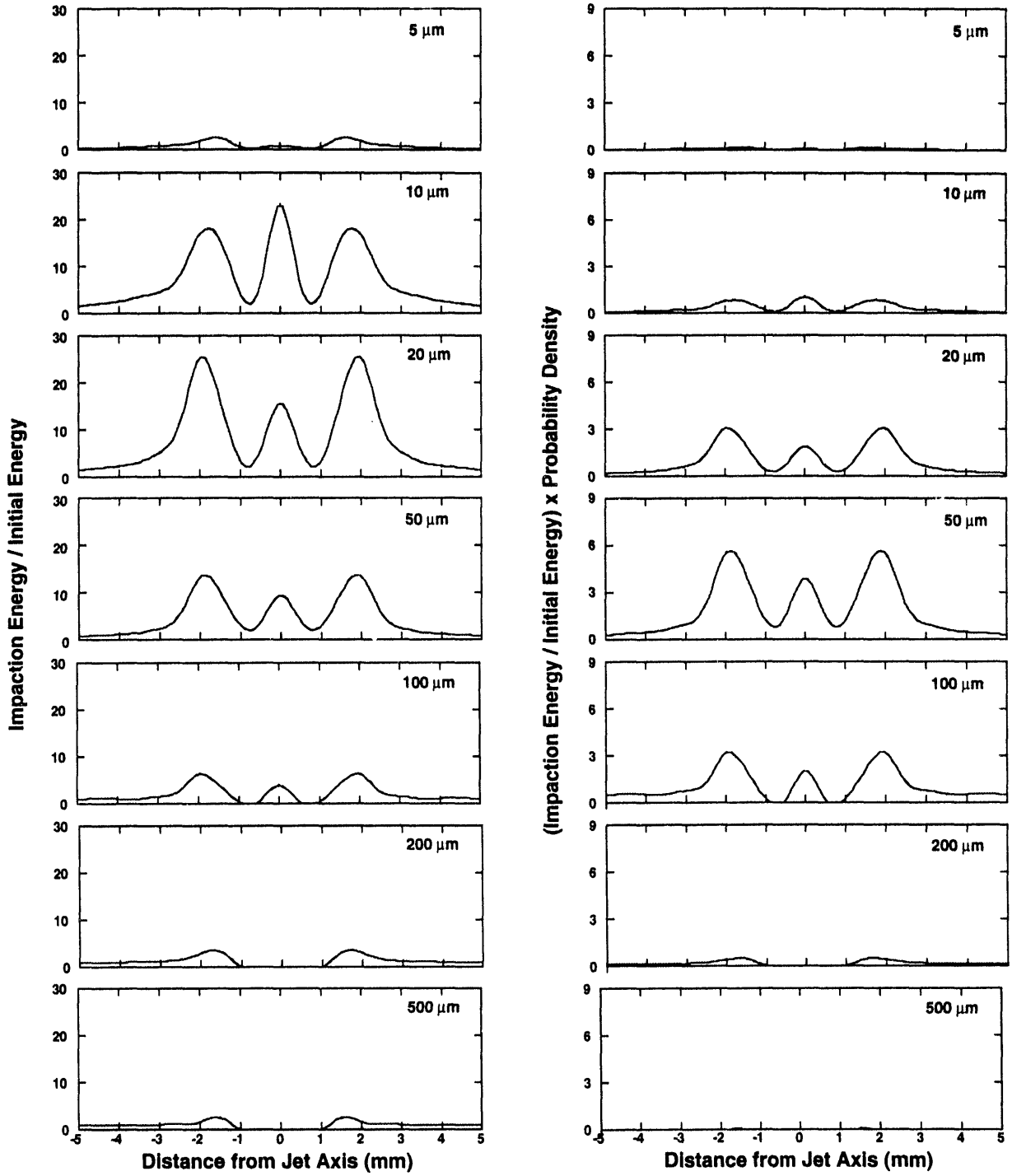

Figure 3-5. The radial distributions of the energy of impaction of particles at the target surface to their kinetic energies in the free stream. The right column shows the product of the radial distributions in the left column with the probability density for each size of particle, from Figure 3-4. Comparison of the peak heights provides relative energies delivered to the surface by different sizes of particles.

Table 3-3. Experimental Conditions[a] and Average Maximum Erosion Rates.

Average Erosion Rates[b] ± Uncertainty (μm/hour)	Metal Temperature K (°F) 450 (350)	550 (530)	650 (710)
Jet Gas, vol % O_2 in N_2			
< 0.1[c]	0.45 ± 0.15	1.25 ± 0.15	1.50 ± 0.20
21	0.50 ± 0.10	1.00 ± 0.20	0.60 ± 0.10
100	0.40 ± 0.10	0.60 ± 0.10	0.60 ± 0.10

[a]Initial jet velocity at the orifice was 200 m/s; exposure time was 2 hours (Miller et al., 1992).
[b]The rate was averaged over the 2 hour exposure period using the maximum depths of the erosion crater on the right and left sides of the jet axis.
[c]A typical value of 3 vol ppm O_2 as impurity was the supplier's specification, in agreement with our analyses of the O_2 contents of several cylinders, obtained later from the same manufacturer.

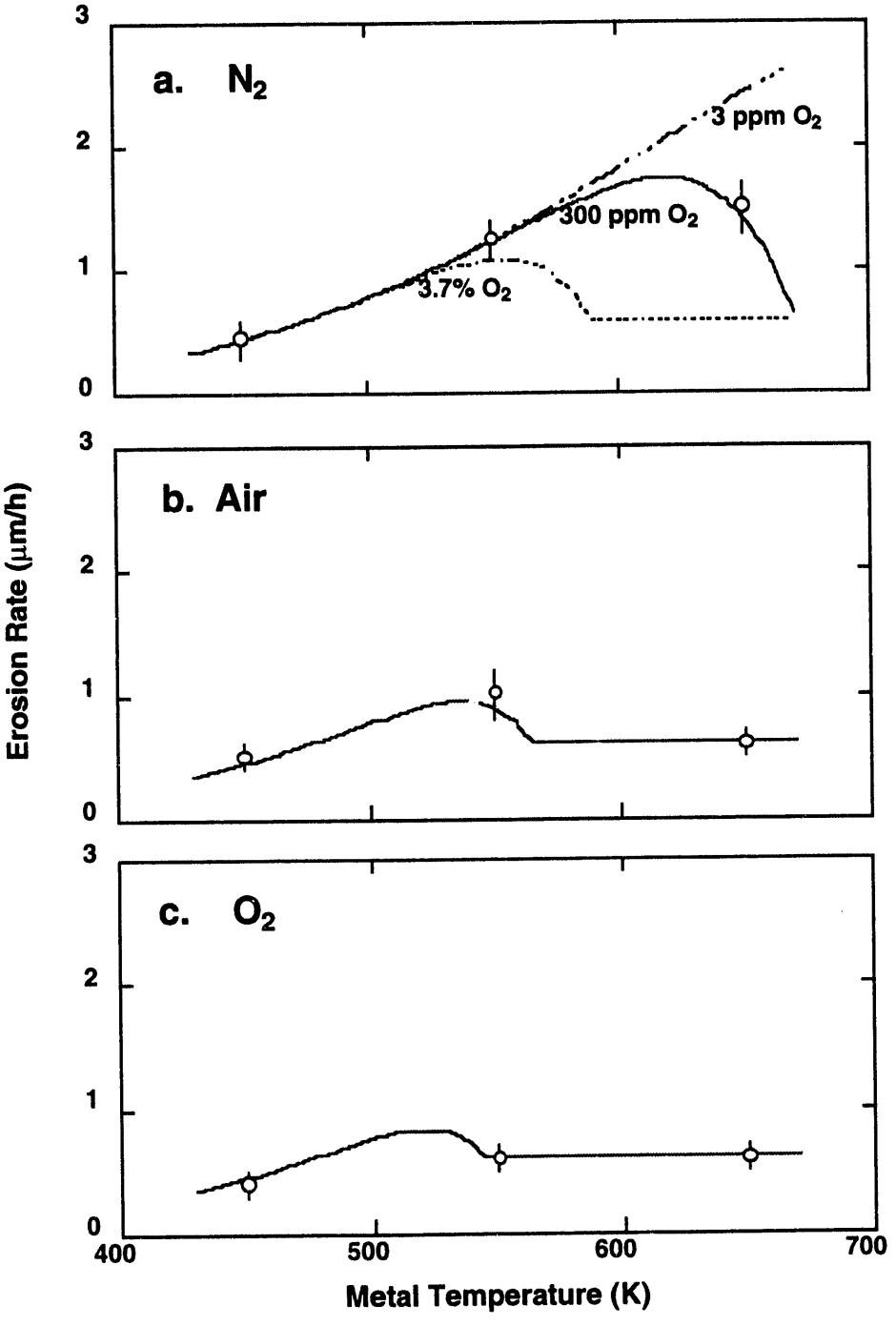

Figure 3-6. Measured and calculated erosion rates of carbon steel as functions of temperature and the jet gas oxygen content. The metal erosion rate coefficient was adjusted to fit the measurements in the nitrogen jet at the two lowest temperatures (450 and 550 K). The oxide erosion rate coefficient was adjusted to fit the measurements in the oxygen jet at the two highest temperatures (550 and 650 K). All curves for different volume fractions of oxygen, from 3 ppm to 100%, were calculated using the erosion rate coefficients determined from the nitrogen and oxygen jets.

550, to 650 K. In the air jet, erosion was greatest at the intermediate temperature. Under the oxygen jet erosion was slow, and similar rates were measured at all three of the temperatures.

Model

The system under consideration is a carbon steel surface undergoing simultaneous erosion and oxidation. The oxide scale is assumed to erode according to theoretical and empirical relations obtained for brittle materials, the metal substrate to behave according to equations describing ductile erosion, while the erosion of the composite is described by combination of the pure metal and pure oxide erosion behaviors (Miller et al., 1993a).

As shown in Figure 3-6a, the erosion of carbon steel by ash and char particles, in the presence of the nitrogen jet, increases with increasing metal temperature. The effective erosion rate coefficient was determined from the measurements at the two lowest temperatures (450 and 550 K). The rate coefficient which fit the measurements was:

$$C_d\varepsilon_p = 0.15 \exp(-21000 / RT) \qquad m^3/J \qquad (3\text{-}2)$$

Erosion was nearly independent of temperature in the presence of the oxygen jet, as shown in Figure 3-6c. The rate coefficient for brittle erosion of oxide was determined from the measurements at the two highest temperatures (550 and 650 K):

$$C_b\varepsilon_p = 400 \qquad m^2kg^{0.5}/J^{1.7} \qquad (3\text{-}3)$$

Once the ductile metal erosion and brittle oxide erosion have been determined from theoretical and empirical equations, the metal loss from simultaneous erosion and oxidation is obtained from the volume fractions of oxide and metal in the eroded composite by the inverse rule of mixtures (Miller et al., 1993b). At the temperatures under consideration here, magnetite is the major component of the oxide scale. According to the parabolic rate law, the rate coefficient for oxidation of FeO to Fe_3O_4 was obtained from the experimental measurements in the presence of 1 atm O_2 (Davies et al., 1951). The rate was further assumed to be proportional to the oxygen partial pressure:

$$k_o = 3.3 \times 10^{-4} P_{O_2} \exp(-195000/RT) \qquad m^2/s \qquad (3\text{-}4)$$

The characteristic dependence of erosion on temperature for each jet gas is shown by the calculations for different volume fractions of oxygen, from 3 ppm in Figure 3-6a to 100% in Figure 3-6c. At the low end of the temperature range the oxidation rate of carbon steel is slow, the oxide layer is very thin, the erosion behavior is that of bare metal, and the erosion rate in-

creases with increasing temperature. Increasing oxygen concentration from 3 ppm to 100% shifts the transition from the metal to oxide erosion regimes toward lower temperatures. Over most of the temperature range investigated (above approximately 475 K), the oxide is more resistant to erosion than metal, therefore, as the contribution of oxide to eroded volume increases, with increasing temperature and/or oxygen partial pressure, the erosion rate declines.

Three oxygen fractions as shown in Figure 3-6a reflect uncertainty in the oxygen content of the gas from the nitrogen jet adjacent to the sample surface. The supplier's specification is that the oxygen present as impurity should be no more than 0.1 vol%, with a typical value of 3 vol ppm. Analyses of the contents of three cylinders, obtained later from the same manufacturer, agreed with the oxygen content of 3 vol ppm. This oxygen level of nitrogen from the cylinder is thus determined as the lower limit. The upper limit, 3.7 vol%, is the excess oxygen in the combustion products, which would apply if the nitrogen jet were mixed with an excess of flue gas. The observed erosion rate at 650 K in Figure 3-6a suggests a level of oxygen between these two extremes. A volume fraction of 300 ppm O_2 would be obtained by mixing roughly 1 part flue gas with 125 parts pure nitrogen.

As oxygen concentration and/or temperature is increased, the oxidation rate increases, with a corresponding increase in the thickness of oxide scale and contribution of oxide to eroded volume, until the erosion rate becomes that characteristic of pure oxide, which is independent of temperature. This is the situation under the most oxidizing conditions, on the right hand sides of Figures 3-6b and 3-6c, and the curve for 3.7 vol% O_2 in Figure 3-6a. The maximum erosion rate in the presence of flue gas is expected at 550 K metal temperature.

Application

The upgraded model was used to relate the accelerated measurements to erosion expected in a boiler over longer periods of time, under normal operating conditions. The erosion rate was calculated for typical conditions in the convective section of the boiler: gas temperature 850 K, excess oxygen 3.7 vol%, particle concentration 2.7 g/m^3, 30° impaction angle, 550 K metal temperature, and 51 mm tube diameter. The impaction efficiency was obtained using the correlation of Israel and Rosner (1983). The erosion rate is shown as a function of convective section gas velocity in Figure 3-7. At low velocity the erosion rate is low, and erosion occurs only from the oxide layer. Under the conditions investigated, erosion is expected to be less than 0.05 μm/hour at flue gas velocities below approximately 12 m/s. Increasing the gas velocity increases the rate of oxide removal and decreases the thickness of the scale. At a velocity near 18 m/s, the oxide layer becomes thin enough that erosion removes both oxide and metal, and the rate begins to increase markedly. If velocities higher than this value are expected in the convective sections of certain boilers designed for oil firing, some modification for improvement of the heat exchanger tubes' life could be necessary in accomplishment of the retrofitting to burn coal-water fuel.

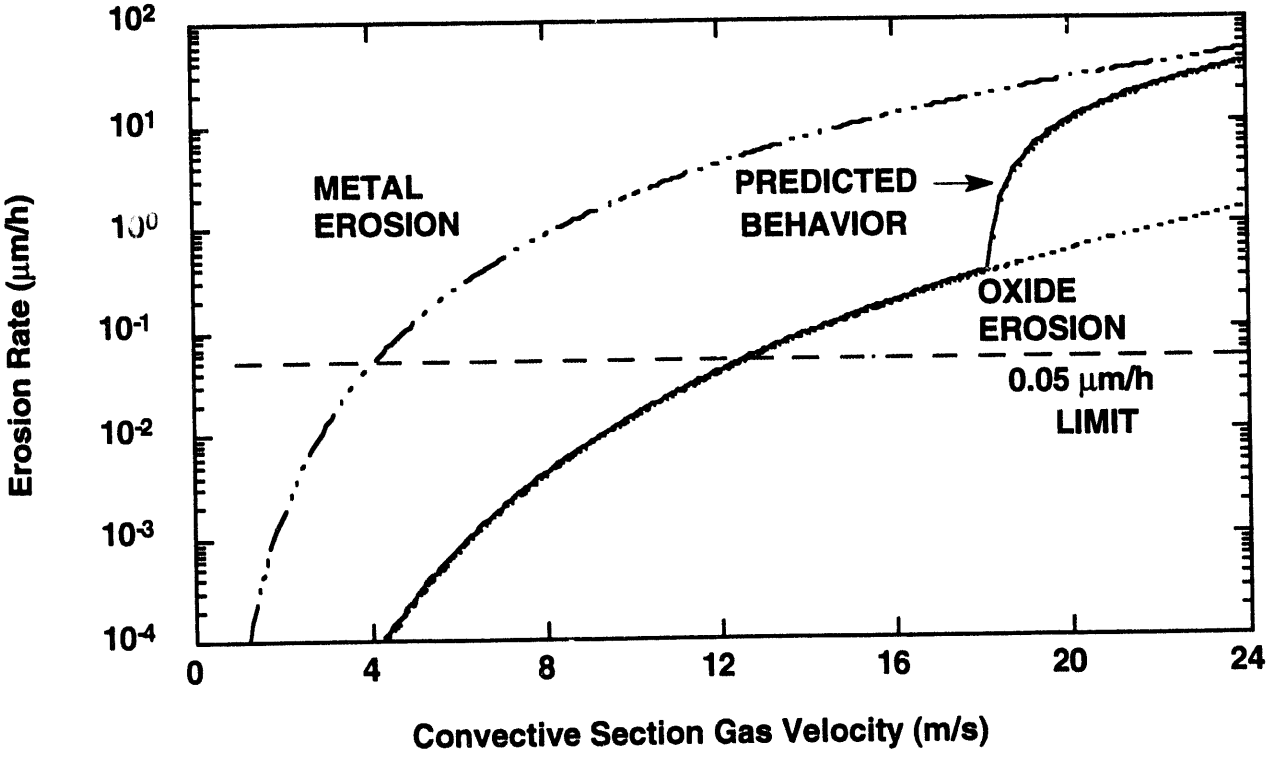

Figure 3-7. Estimate of the erosion rate of carbon steel by fly ash and unburned char from coal-water fuel combustion under the following conditions: gas temperature 850 K, excess oxygen 3.7 vol%, particle concentration 2.7 g/m^3, 30° impaction angle, 550 K metal temperature, and 51 mm tube diameter. The impaction efficiency was obtained using the correlation of Isreal and Rosner (1983).

Determine Erosion Characteristics of Materials Subjected to Atomized Coal-Water Slurry Fuel

Background/Introduction

The internally-mixed atomizer tips used in demonstration boiler during a recently completed 500-hour test program firing coal-water slurry fuel (CWSF) containing ~60 wt. % solids and 3.5 wt. % ash in the coal (Miller et al., 1993b), experienced excessive erosive wear under normal operating conditions. Droplet outlet passages became elliptical resulting in poor atomization and hence, inefficient combustion. Lifetimes of the nozzles ranged from 8 to 125 hours. The short atomizer life results in high operating costs and excessive boiler downtime. In an attempt to obtain more information on atomizer operation and materials of construction, a study has been started to evaluate the erosive behavior of different materials when subjected to an atomized CWSF spray.

When doing erosion studies, the most important parameters to monitor are impact angle and velocity. In order to conduct a study of candidate materials, an experiment was designed in which both angle of impact and droplet velocity are known and can be varied. The goal is to create diverse erosive environments covering a range of atomizer designs.

Experimental Design

The experiments will be conducted in a small test facility (Figure 3-8) that has been designed for investigating the effects of impact angle and atomization air pressure on erosion characteristics. Design considerations included atomizer selection and sizing, CWSF transport and containment, mist elimination, material sample mounting, and sample orientation.

The test facility, 2' x 2' x 2', is sufficiently large to allow the droplets to disperse before exiting the chamber and to provide room for housing additional instrumentation or plumbing. The body of the chamber consists of 1/2" thick aluminum plate and the sample stage is constructed from 1/4" aluminum plate.

Atomized CWSF will be collected in the bottom of the chamber and it will be removed after a test run is completed. CWSF that is not collected at the bottom of the container will be ventilated during operation through an 1/2" eductor mounted on the side of the chamber. Ventilated mist leaves the chamber and moves through flexible polypropylene tubing to the bottom of a water tank. Ventilated air bubbles to the surface and CWSF droplets disperse throughout the liquid.

The atomizer that will be used to produce droplets for the experiment is an internally mixed oil nozzle manufactured by Delevan, model 33769-9 (Figure 3-9). The nozzles have been modified to accommodate CWSF by drilling the outlet port to a larger dimension, (approximately 0.19 cm.) in order to prevent coal particles from blocking the orifice. The CWSF feed rate will be ~3.95 gph.

The materials to be analyzed for erosion will be situated on a stage fixed with a rotating axis. The center of the material sample can be varied to any length.

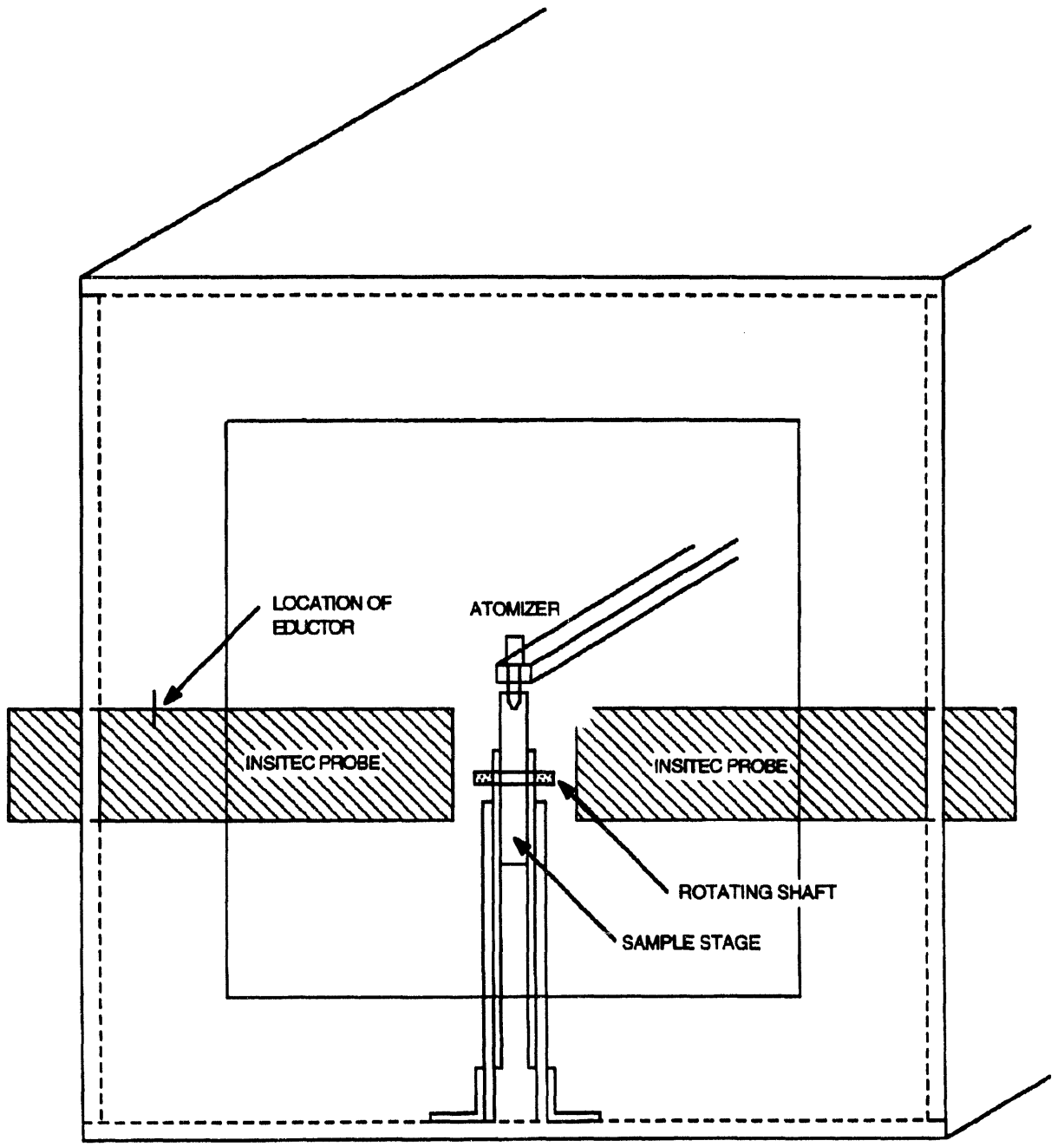

Figure 3-8. Atomization / Erosion test facility

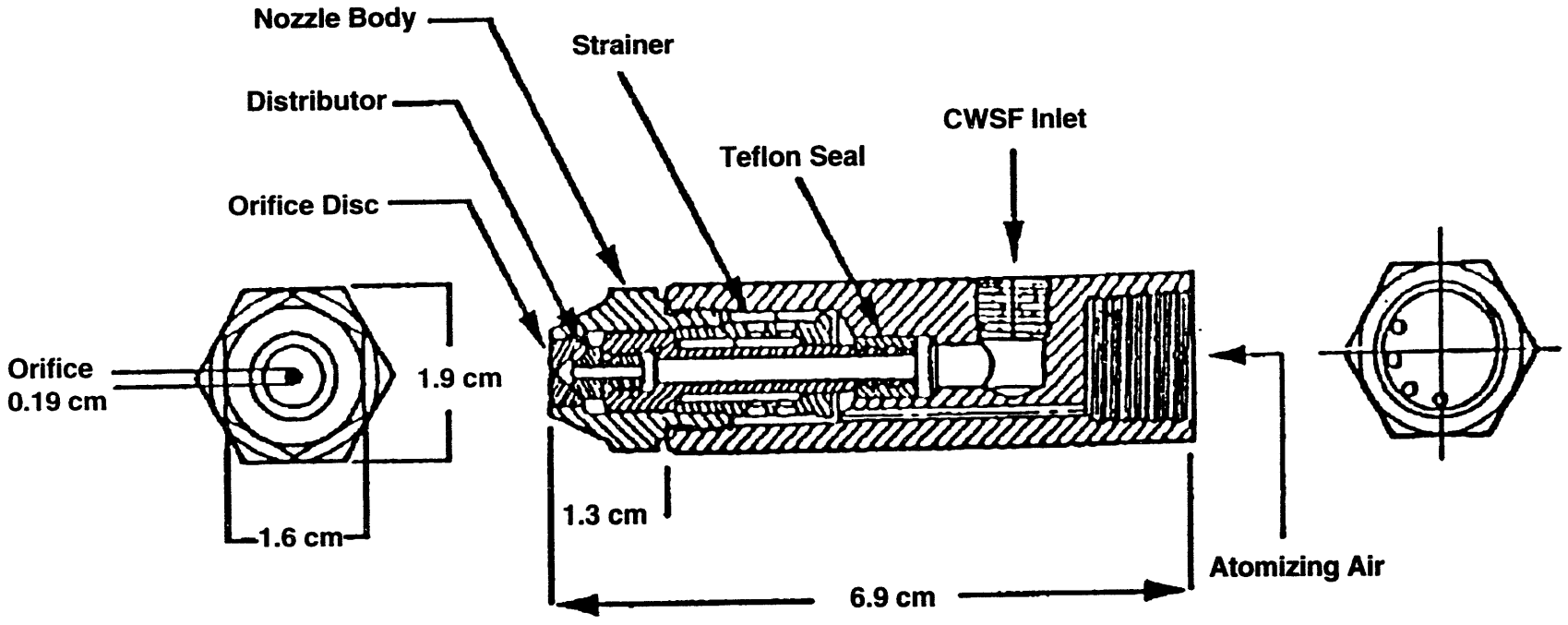

Figure 3-9. Schematic diagram of the Delavan Nozzle

Spray characterization will be done using an in-situ particle sizing probe. The probe works using laser light scattering principles and is capable of measuring droplet concentrations, size distributions, and velocities, all in real time.

CWSF Selection

Due to differences in the abrasiveness of different coals, the erosion data obtained for one CWSF may not be applicable to materials subjected to wear by another. The CWSF used therefore, will be the one used in the 1,000-hour demonstration. In addition to typical fuel analyses (proximate, ultimate, heating value, solids loading, viscosity, etc.), the mineral matter will be analyzed and the average particle size of the quartz and pyrite particles measured.

Material Selection

Many materials are reported to be wear resistant but often this means resistant to abrasion (sliding contact) not erosion (particle impact). In fact, many times wear resistant materials erode more quickly than soft materials due to the erosion mechanisms involved. The materials to be used will possess different mechanical properties. Five or six materials will be tested. The group will likely consist of metals, ceramics, and composites.

Analysis

The material sample will be removed from the testing chamber every two hours for analysis. Analysis will consist of surface profilometry, weight loss measurements, and scanning electron microscopy. From the data collected, erosion rates will be calculated, erosive mechanisms identified, and the material best suited for atomizer construction identified.

Theoretical and Experimental Studies of Particle Behavior in the Demonstration Boiler

The application of coal or coal based fuels to an industrial boiler presents several technical challenges which include:

- satisfactory combustion efficiency
- handling coal and ash
- controlling emissions

In order to overcome these challenges, the combustion process in the boiler needs to be analyzed, well understood, and characterized. The burning of volatile matter and char in a turbulent diffusion flame is a complex process. Despite a good deal of fundamental data available on this topic from single particle studies, there is a shortage of data available for industrial type combustors. While recognizing the importance of the role of the small-scale experiments, they do not simulate all of the many processes which occur in practical combustors. To increase understanding of pulverized coal and CWSF turbulent jet flames in an industrial boiler, theoretical and experimental work has been initiated.

Theoretical Background

Fragmentation During Devolatilization

Fragmentation of CWSF agglomerates during devolatilization has been observed in a number of bench scale experiments. It has been suggested that as jets of volatiles are issued from the CWSF agglomerate, they impart rotation to the agglomerate. This rotation (or more specifically angular velocity) produces an angular momentum, which in turn generates a centrifugal force. It is conceivable that this centrifugal force can promote the separation of weakly adhering coal particles from the CWSF agglomerate during devolatilization.

Char Fragmentation

Under combustion conditions typical of an industrial boiler, CWSF agglomerates and pulverized coal particles burn in a regime where O_2 penetrates partially into the pores of the particles. As the carbon is consumed in the outer regions of the particle and the porosity increases, the structural strength of this region is lowered. It has been suggested that beyond the critical porosity of 0.7-0.8, the integrity of the solid matrix is lost and the particle sheds off fragments. These fragments escape and burn separately. It is important to determine the conditions under which char fragmentation is favored, since this phenomenon is useful both from the point of view of burnout and obtaining a finer fly ash.

To investigate the phenomenon of fragmentation through an analysis of the behavior of the particles in the demonstration boiler, *in situ* particle counting, sizing and velocimetry technology will be used (using an Insitec PCSV-P) to gather data on the temporal and spatial variations of the particle size distribution and number densities of the pulverized coal particles and the CWSF agglomerates. To further analyze the behavior of the particles in the boiler, it is necessary to characterize the environment inside the boiler in terms of the operational parameters. This involves the correlation of the boiler's operational parameters to the aerodynamic properties of the jet flame. These operational parameters for a pulverized coal jet flame include:

-Amount of combustion air

-Amount of fuel

-Inlet temperature of the combustion air

-Swirl number

-Amount of tertiary air and hence level of excess air

The objectives of the project recently started are focused on the phenomena taking place during the combustion of CWSF, however, the experimental techniques will be applied to the combustion of dry, micronized coal so that the process of combustion in the boiler will be further characterized and understood.

The operational parameters for a CWSF jet flame include all of the aforementioned parameters for a DMC jet flame, plus the following:

- Different atomizer guns, resulting in different spray (or jet) angles, velocities, and droplet size distributions

- Inlet temperature of the CWSF

- Pressure and temperature of the atomizing air

- Length of penetration of the atomizer gun, axially into the boiler, which will affect the boiler residence time

To fully characterize the boiler, temperature and gas velocity profiles will be obtained for different operating conditions. Hence, in addition to the measurements carried out with the PCSV-P, suction pyrometry and pitot-tube measurements will also be performed.

The main aerodynamic properties of turbulent jet flames are: velocity, temperature and concentration. To correlate these three properties to the operational parameters of the jet, the conservation equations of mass continuity, energy and momentum (Navier-Stokes equations) will be applied to the jet flame, to obtain expressions for velocity, temperature and concentration of the jet.

Computational Modeling of Natural Gas Combustion in the Demonstration Boiler

To further enhance the theoretical understanding of the furnace environment in the demonstration boiler, the fundamental equations governing the fluid flow (the mass continuity equation, the energy equation and the Navier-Stokes equations) are solved employing a computational code (FLUENT, developed by Creare Inc.) which uses a finite difference numerical procedure. The numerical technique involves the subdivision of the domain of interest into a finite number of control volumes or cells. The partial differential equations are discretized over these cells to obtain sets of simultaneous algebraic relations. Because of the non-linearity and interdependence of the differential equations, an iterative solution has to be adopted.

The fluid is regarded as a continuum and is solved in an Eulerian frame of reference in the manner described above. Where a second, disperse phase is present a Lagrangian approach is preferred. Particles or droplets are followed by means of a particle tracking technique in which the equations of motion along with any auxiliary relations which may be in effect, are integrated with respect to time.

In order to fire pulverized coal or CWSF, the furnace environment in the boiler is initially heated by firing natural gas. Consequently, a two-dimensional model for the combustion of natural gas in the boiler has been set up employing FLUENT. In order to save considerable CPU time and to facilitate quick iterations, only a horizontal slice of the furnace environment is modeled with the assumption that the values of gas velocity, temperature, turbulence intensity, etc. in this slice are characteristic of the entire volume of the furnace. The validity of this assumption will be tested by repeating the calculations for different slices and finally by setting up a three-dimensional model for the combustion of natural gas in the boiler.

The details of the calculated flow field in the boiler are shown by means of graphical plots (Figures 3-10 to-3-19). The solution domain, including the grid locations, is displayed graphically in Figure 3-10. In Figure 3-11, the vector plot indicating the magnitude of the resultant velocity at each point in the flow field is shown. The vectors are scaled in length according to the magnitude of the velocity. In Figures 3-16 to 3-19, the profiles of the u-velocity (*i.e.*, the x-component of the velocity), and concentration profiles of natural gas, air and the combustion products are illustrated. The profiles are interpreted by noting that the dashed line refers to the datum location. The distance between the dashed line and the solid line indicates the magnitude of the variable being plotted. In the case of the profiles of u velocity, where the solid line is to the right of the datum line, the u-velocity is positive and when it is to the left the u-velocity is negative. Figures 3-10 to 3-14 show that the contours of the u-velocity, and species concentrations are drawn at equal intervals distributed between the minimum and maximum values of the variable throughout the flow field.

Having characterized the combustion of natural gas in the boiler, the next stage of this modeling work entails the injection of DMC particles and CWSF droplets into the furnace and following their combustion histories.

Experimental

Local particle behavior has received significant attention from a modeling perspective, however, it is only beginning to be addressed experimentally due primarily to the lack of instrumentation to carry out such studies. The objectives of the experimental section of this study is twofold.

Firstly, to obtain information on velocity, size distribution and number density of pulverized coal particles in the boiler. These measurements will provide validation data for the three-dimensional codes being developed to model pulverized coal combustion.

The second objective of this research is to look at the phenomenon of fragmentation during the devolatilization of CWSF and examine the hypothesis used to explain this phenomenon. In the event that this proves difficult to accomplish, the process of fragmentation during char burnout will be investigated. In fact due to the time scales involved (ms-s), it seems logical to investigate fragmentation during devolatilization and char burnout concurrently.

The phenomenon of fragmentation has never been investigated in an industrial-sized boiler and the above hypothesis has been developed out of the work done on numerous bench-scale experiments. Consequently, in the event that fragmentation does occur during devolatilization of CWSF in a the demonstration boiler, factors other than the angular velocity of the agglomerates may be responsible for the break up of the agglomerates. These factors may include the degree of swirl and the turbulence intensity of the jet flame.

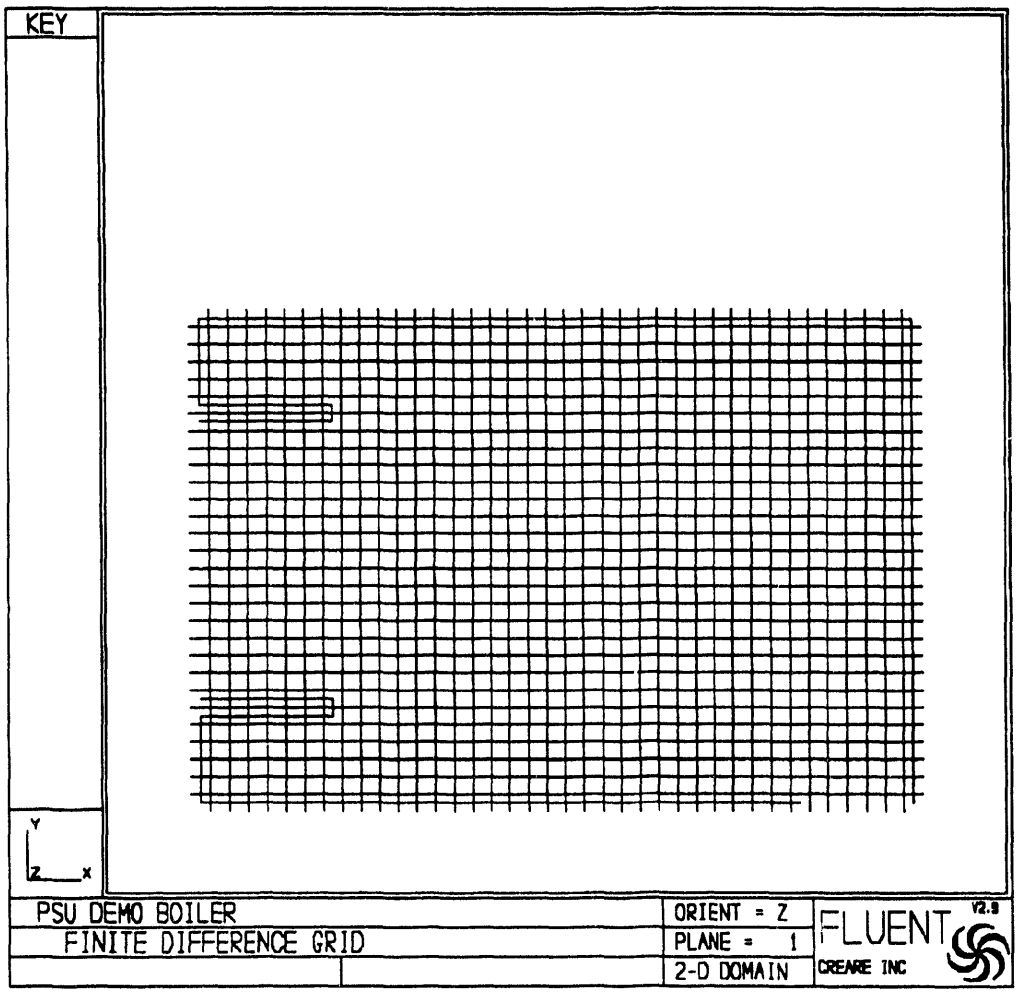

Figure 3-10. The finite difference grid for the 2 dimensional solution domain

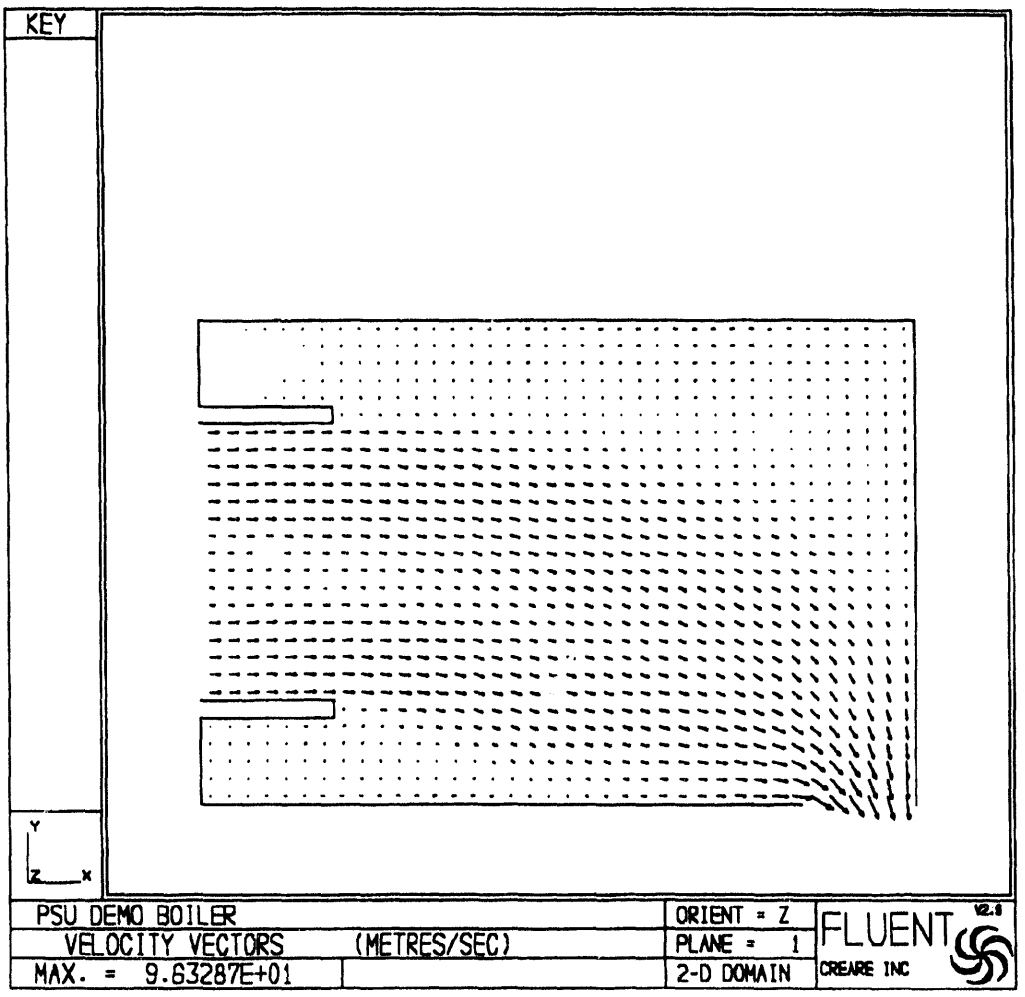

Figure 3-11. The velocity vectors in the demonstration boiler during the combustion of natural gas

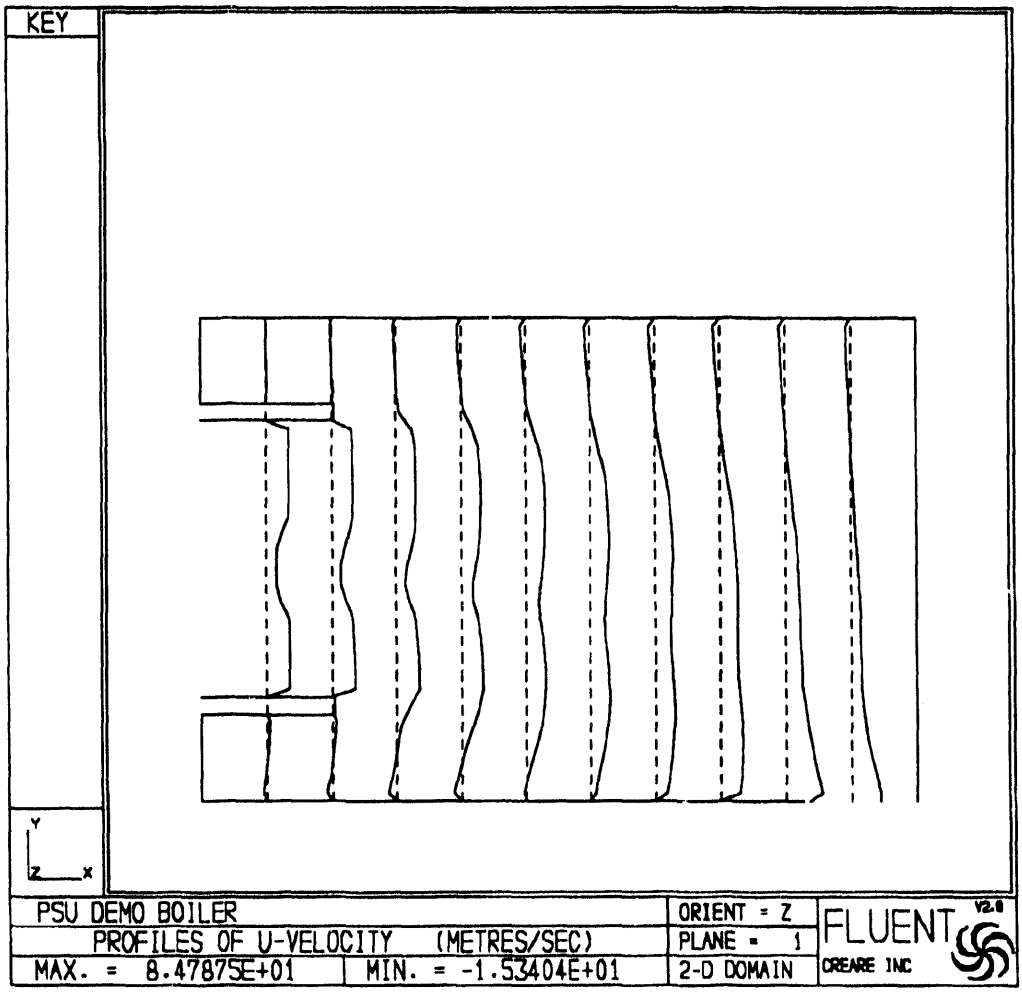

Figure 3-12. Profiles of u-velocity

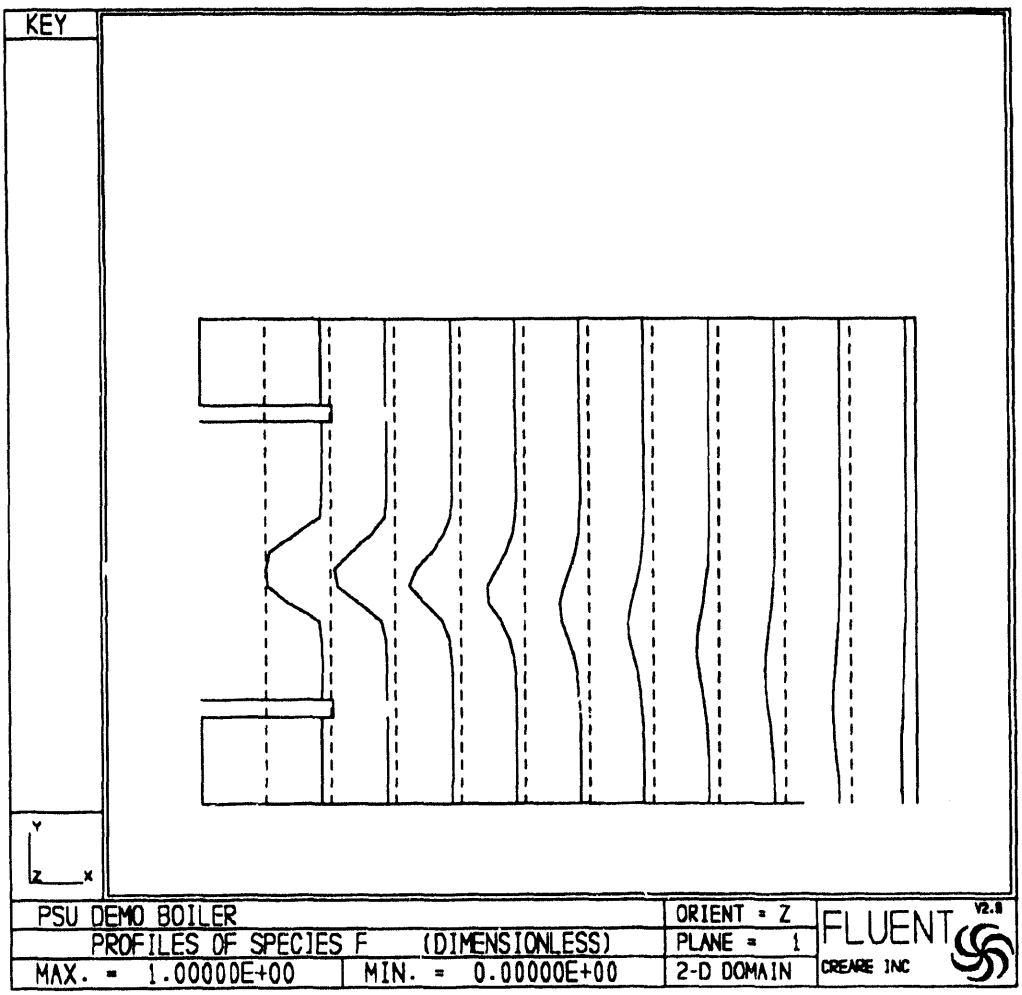

Figure 3-13. Concentration of profiles of fuel species (on a mass basis)

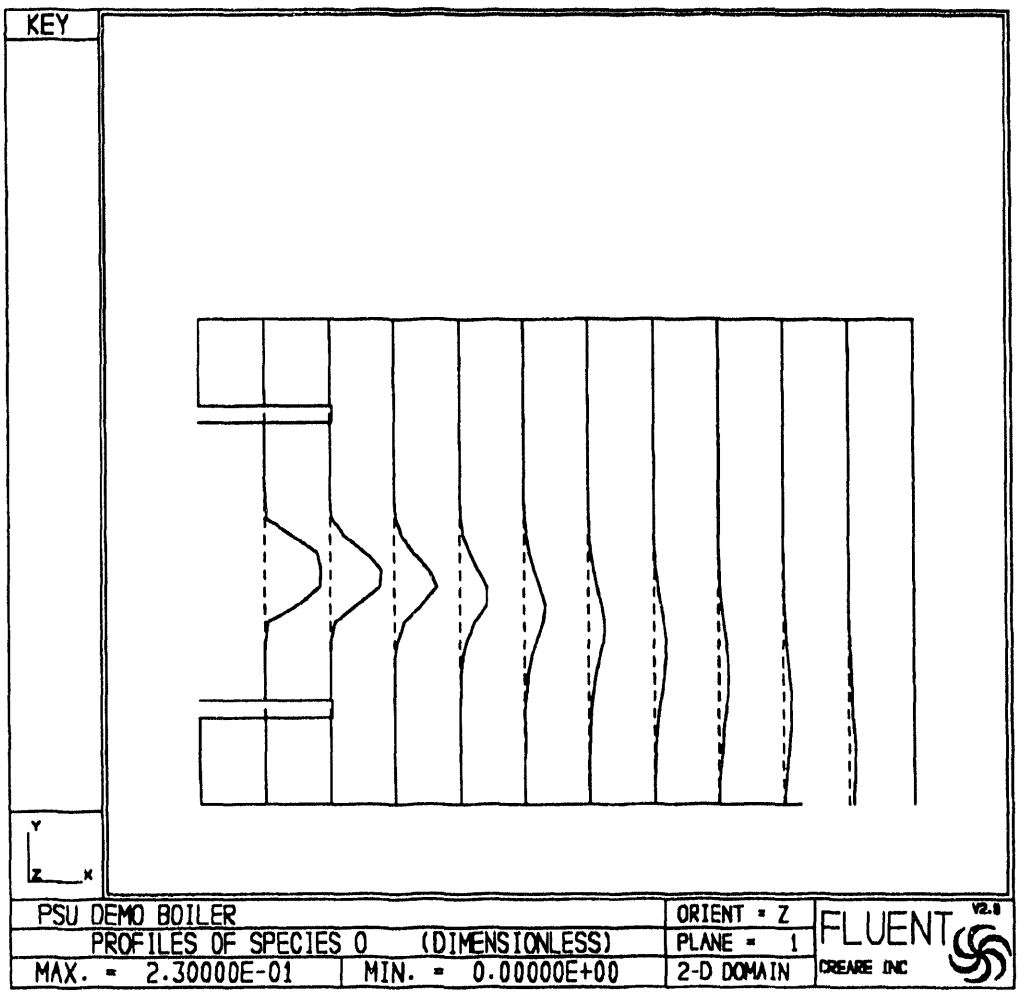

Figure 3-14. Concentration profiles of oxidant species (on a mass basis)

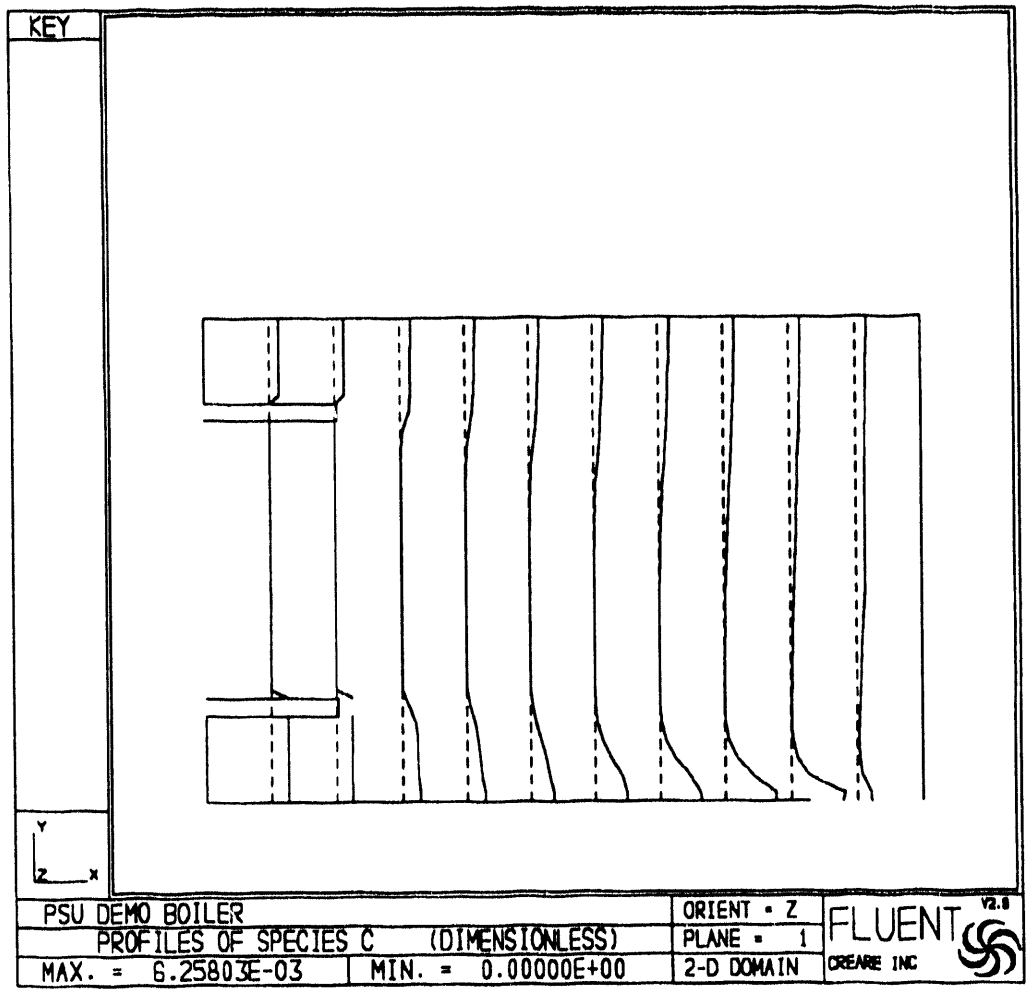

Figure 3-15. Concentration profiles of combustion products (on a mass basis)

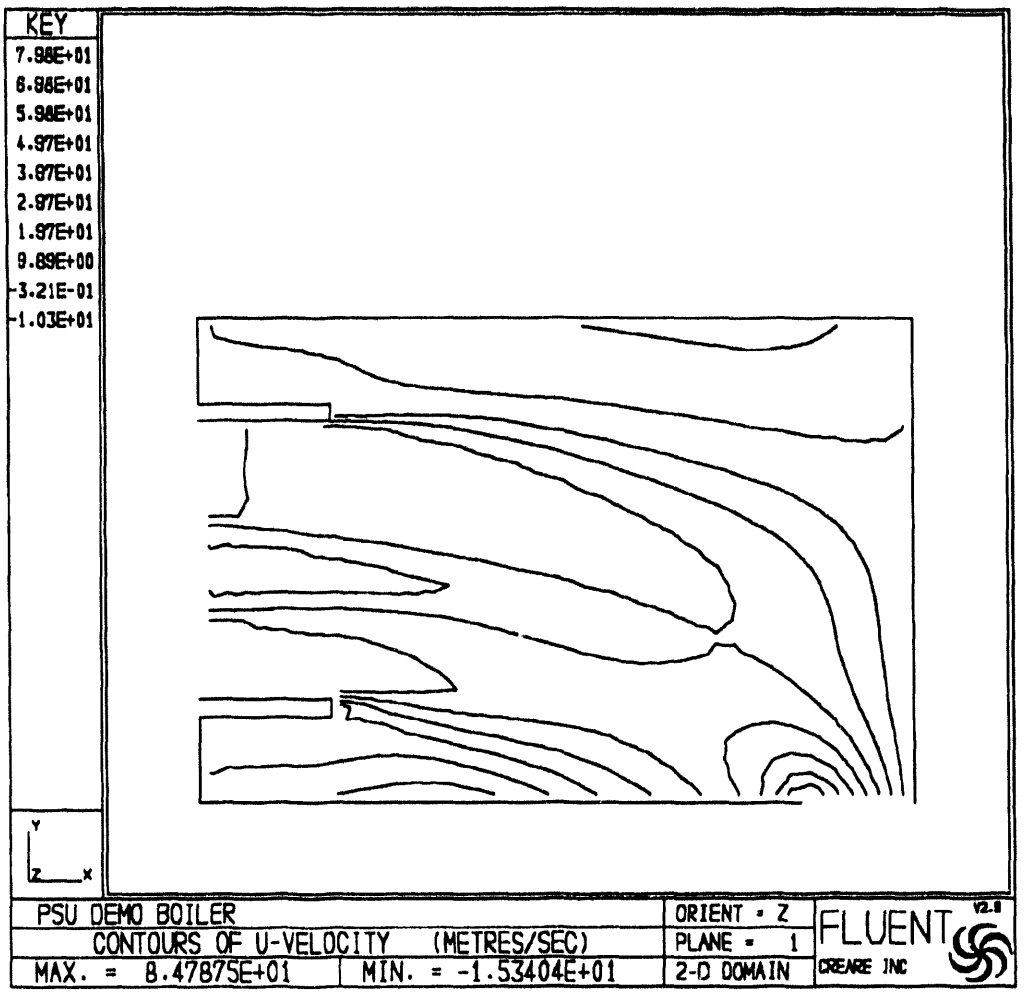

Figure 3-16. Contours of u-velocity

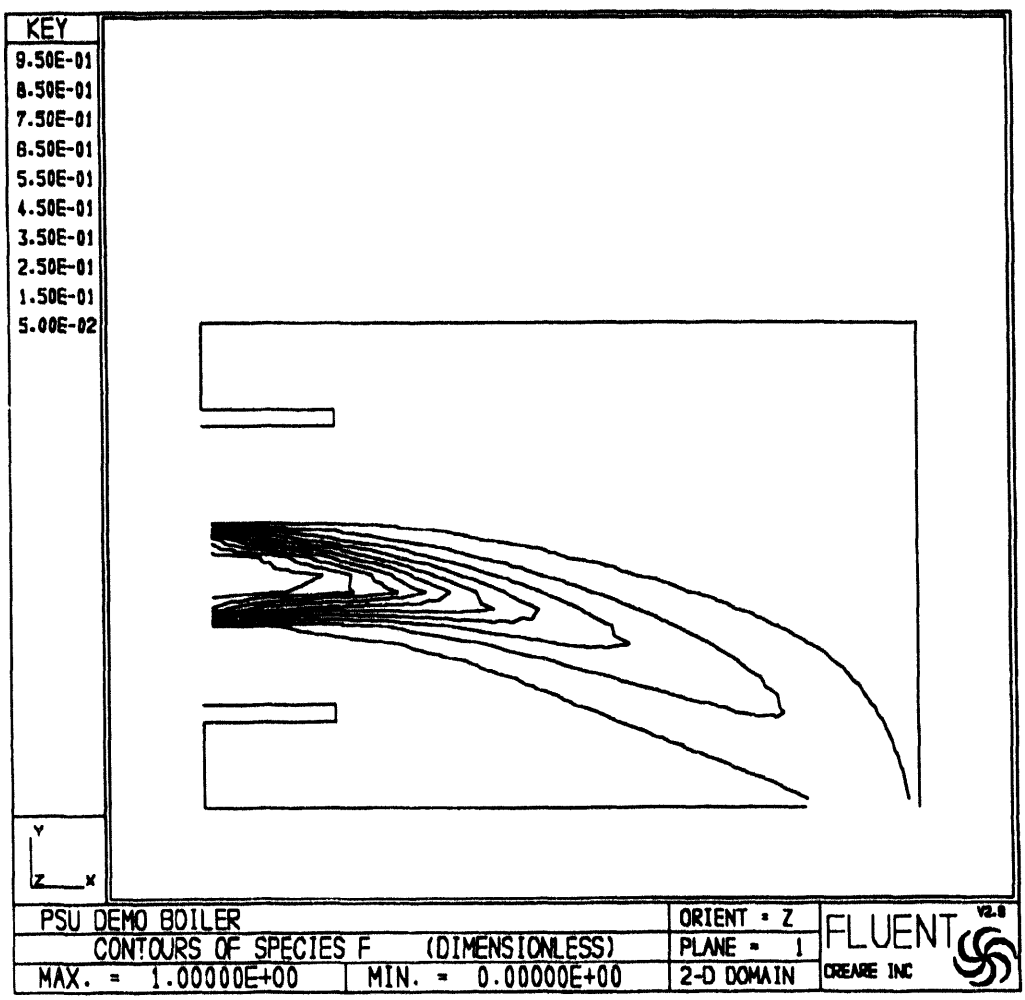

Figure 3-17. Concentration contours of fuel species (on a mass basis)

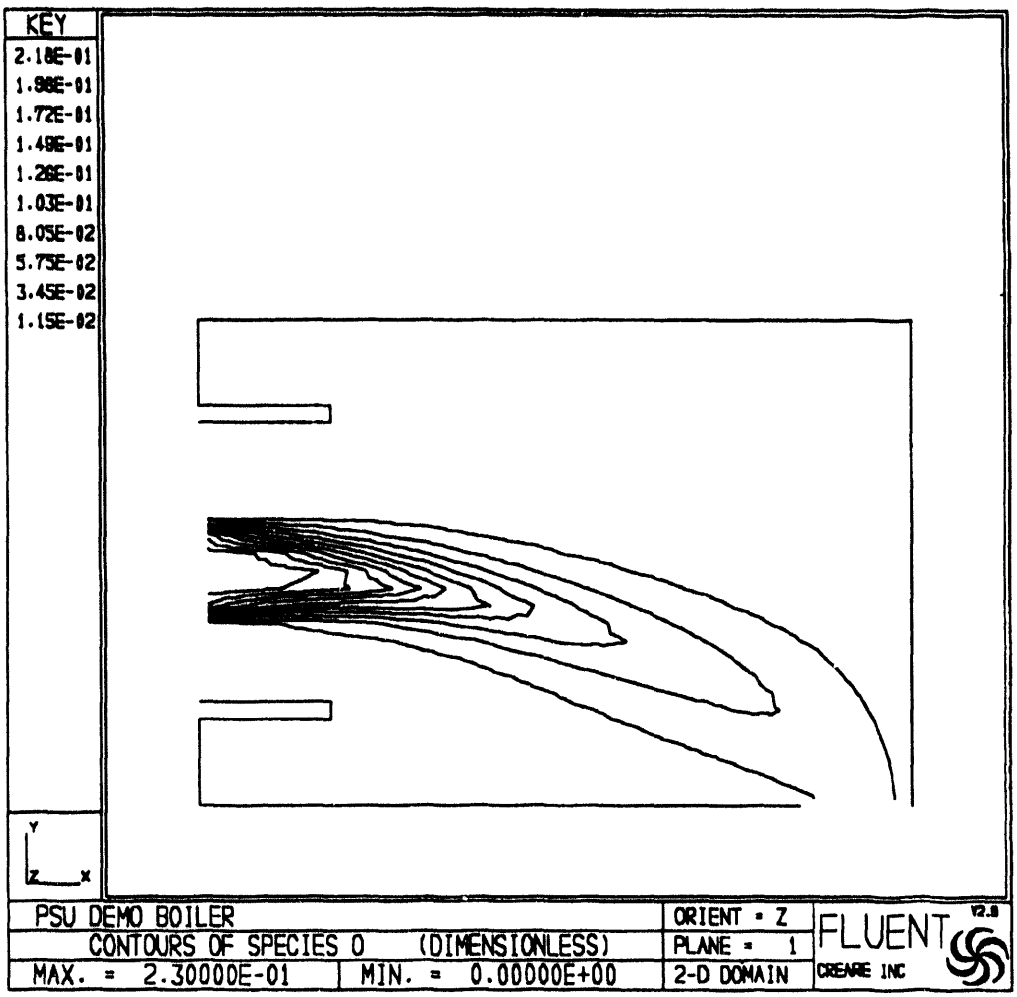

Figure 3-18. Concentration contours of oxidant species (on a mass basis)

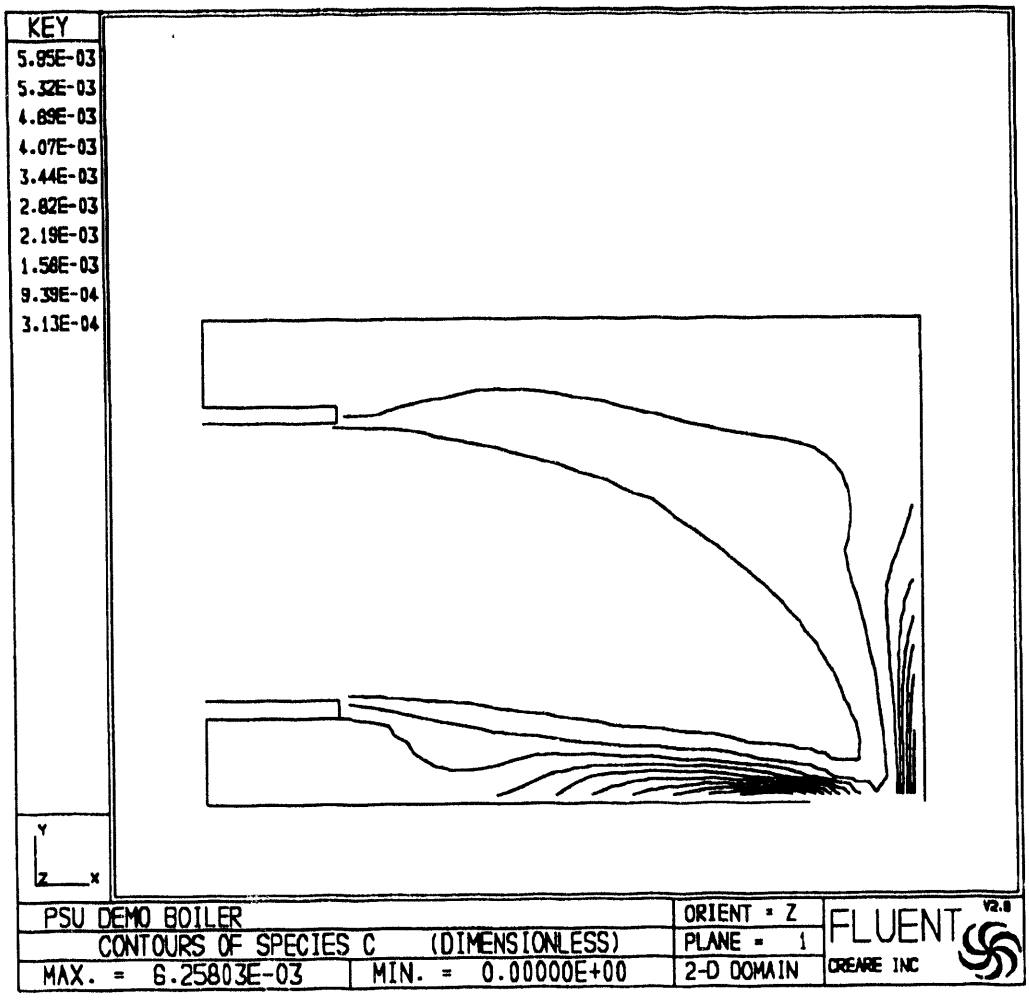

Figure 3-19. Concentration contours of combustion products (on a mass basis)

PCSV Technology

The PCSV (developed by Insitec, Inc.) is an *in situ* instrument capable of measuring the concentration number density, size distribution, and velocity of disperse particles (see Figure 3-20).

Particle sizes are inferred from the amplitude of the near-forward scattered He-Ne laser beam. For this application two laser beams will be used separately, one with a 25 μm beam waist used to size particles in the range 0.4-2 μm and the second with a 250 μm beam waist used to size particles in the range 2-140 μm.

Light scattered from the particles passing through the sample volume of the beam waist is collected over a solid angle and monitored with a photomultiplier tube. The size and the trajectory of the particles affect the maximum amplitude of the detected pulses in known ways. As long as the particles are small compared with the beam waist, Mie theory predicts their size dependence. Trajectory dependencies are calculated by a statistical technique based on the following assumptions: 1) the average flux of particles of a given diameter does not vary spatially over the width of the beam and 2) a large number of particles of each size are detected. Using this statistical technique, particle size distributions are calculated from the measured frequency of pulses of each amplitude.

Individual pulse duration is related to the known width of the beam waist and is used to calculate the particle speed. A distribution of the particle speeds is measured and the median of this distribution is used to calculate the particle number densities.

The PCSV system specifications are:

	Specification
Size range	General capability from 0.20 to 200μm
Concentration	Absolute particle concentrations up to 10 g^7/cm^3 for submicron range or up to 10 g/m^3 for supermicron range
Speed	0.1-400 m/s
Particle type	Solid, liquid, composite, volatile or nonvolatile
Particle environment	No sample conditioning required, capability to make in-line measurements of particles in gas or liquid carriers over a wide range of pressure and temperatures
Accuracy	Typically ±10% of indicated size
Calibration	Calibrated with monodispersed polystyrene latex spheres, standard polydispersed aerosols, and Insitec Reference Reticle
Particle pulse rate	Up to 500 kHz

3.4 Evaluate Emissions Reductions Strategies

No work was scheduled or conducted this reporting period.

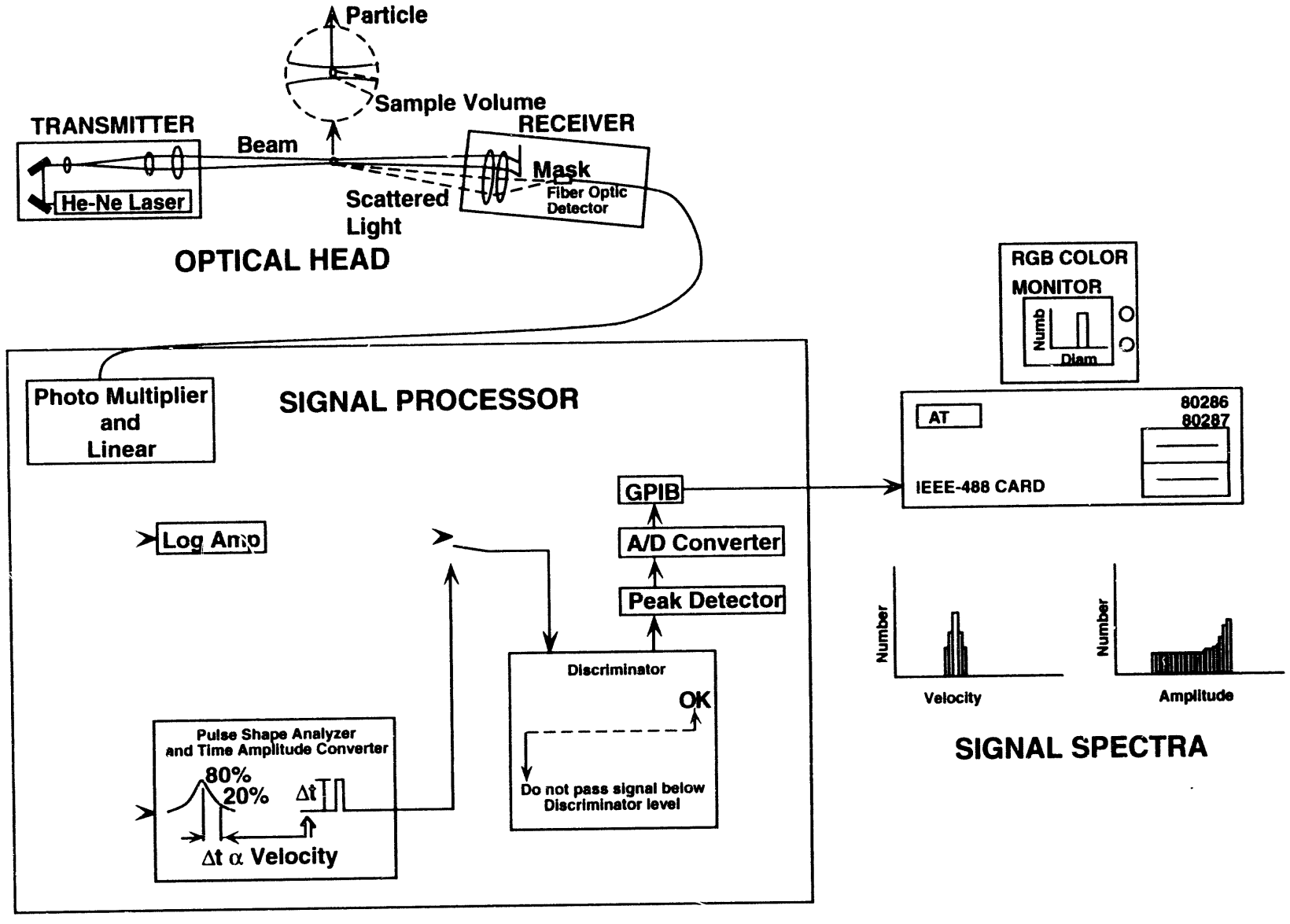

Figure 3-20. The components of PCSV

4.0 TASK 3: ENGINEERING DESIGN

EER visited Penn State to inspect Penn State's demonstration boiler site and fuel preparation facility, discuss various aspects of the designs (MCWSF and dry, micronized coal) to be completed, and receive guidance for the design efforts. The designs were started after receiving official approval from DOE — see Subtask 4.1. Discussions centered around MCWSF storage, handling, and combustion, and dry, micronized coal preparation. Penn State provided EER with recommendations for the designs.

EER visited the Crane facility and surveyed the site in preparation for site layout work. Discussions were also held with Crane personnel regarding various scenarios for locating equipment.

The following information was requested from Crane by EER:

- Boiler setting drawings;
- Boiler steel drawings;
- Plant property plot plan;
- Building structural steel drawings;
- Gas and oil analyses;
- Gas and oil header pressures;
- Topography map;
- Weather conditions;
- Local emissions codes for air and water; and
- Soil conditions (core samples if available).

4.1 Subtask 3.1 MCWSF/DMC Preparation Facilities

No work was conducted on the MCWSF preparation facility. The DMC preparation facility is incorporated into Subtask 3.2 (see below).

4.2 Subtask 3.2 Fuel Handling

A preliminary concept has been developed for the layout, sizing and orientation of the major equipment, and structural enclosure.

The air heater has been temporarily located on top of the building housing the boiler. However, the adequacy of the building to support the air heater must be verified prior to finalizing this location.

4.3 Subtask 3.3 Burner System

Information was obtained regarding the existing ignitor and flame scanner and the gas and oil delivery systems. The location for the combustion air metering was determined.

4.4 Subtask 3.4 Ash Removal, Handling, and Disposal

The preliminary baghouse location, size, and orientation were determined. Work started on the floor air blast nozzle(s) location. The sootblower manufacturer was contacted regarding the conversion of the sootblower to automatic. They stated that the conversion to automatic can be accomplished with a modification to the sootblower and the addition of an automatic valve on

the steam supply line.

4.5 Subtask 3.5 Air Pollution Control

Preliminary locations for the sorbent silo and injectors were determined. No further work will be performed on this subtask until it is determined that sorbent injection is required or will be used.

4.6 Subtask 3.6 Integrate Engineering Design

No work was scheduled on Subtask 3.6 during this reporting period.

5.0 TASK 4: ENGINEERING AND COST ANALYSIS

5.1 Subtask 4.1 Survey Boiler Population/Identify Boilers for Conversion

Boiler Selection

Penn State visited several military installations and has had discussions with both civilian and military personnel regarding the use of coal in the military (Miller et al., 1993a). Figure 5-1 shows the final candidates along with the coals to be tested in the program. As a consequence of this activity, Penn State recommended to DOE the Naval Surface Warfare Center at Crane, Indiana as the site for the retrofit designs in Phase I of the program. DOE and DOD (U.S. Army Corps of Engineers Construction Engineering Research Laboratory) concurred with Penn State's selection. Consequently, EER has started the engineering design (Section 4.0) and the Mineral Economics Department has focused the engineering and cost analysis on the Crane facility (see below).

The Crane facility has several boilerhouses, one of which contains three boilers that are good candidates for conversion. There are three Cleaver Brooks D-type watertube boilers firing natural gas with No. 6 fuel oil backup. Two of the boilers were installed in 1989 and have a firing rate of 25.2 million Btu/h. The third boiler was installed in 1972 and has a firing rate of 18 million Btu/h. The boilers are good candidates for a retrofit design. The two larger boilers have been installed such that they are raised off of the floor by ~1.5', which would facilitate ash removal from the convective pass. There is space outside the building to accommodate coal (or coal-water slurry fuel) and ash storage and handling. In addition, there is a rail spur that services the building. Only two of the three boilers are operated simultaneously. Steam demand is based upon the number of orders for filling bombs.

The Crane facility was selected for the retrofit for the following reasons:

- The boilers are of a size which is representative of many military boilers.
- The boilers are good candidates from a technical veiwpoint as discussed above.
- The installation is located in the coal fields of a coal-producing state.

5.2 Subtask 4.2 Identify Appropriate Cost Estimating Methodologies

Subtask 4.2 was completed. A report, coauthored by Juan Benavides, Adam Rose, and Richard L. Gordon, is contained in Appendix A and presents an introduction to the basic economic principles of cost estimation, a brief discussion of all major cost-estimation methodolo-

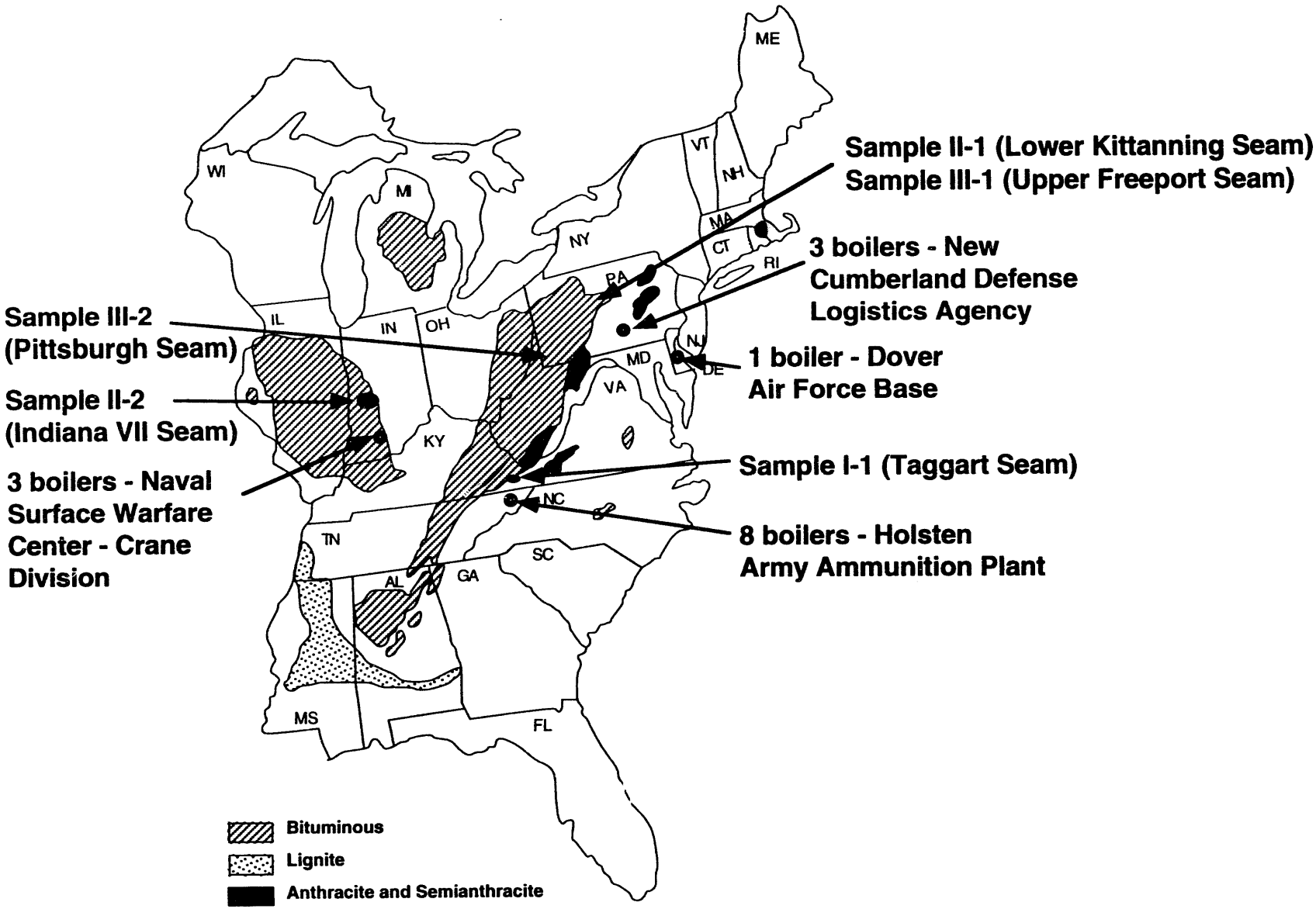

Figure 5-1. Candidate boilers and test coals

gies, a justification of several evaluative criteria, and a detailed assessment of the alternative methods. The major conclusion was that no one cost-estimation method dominates all others, but that some methods, such as process analysis/linear programming, have very distinct advantages in the context of this project.

5.3 Subtask 4.3 Estimate Basic Costs of New Technologies

A baseline linear programming model was developed to evaluate the costs of supplying fuels of acceptable quality to an oil-designed industrial boiler which has been retrofitted to fire MCWSF. The intended first use of the model will be to evaluate the costs of supplying MCWSF to the Crane, Indiana site from different coal suppliers. The model will also serve as a basis to evaluate fuel supply options for other potential retrofit sites. A summary of the model is contained in Appendix B.

5.4 Subtask 4.4 Process Analysis of MCWSF and Dry, Micronized Coal

This section focuses on the models developed and the use of the models and results as decision aids in the retrofitting of existing oil fired industrial boilers to fire MCWSF. The objective in developing a cost minimizing (or net benefit maximizing) model of retrofitting an existing oil-fired boiler to fire MCWSF is based on the flexibility that the facility has to be retrofitted. The decision to convert to MCWSF should be based on the useful life of the plant, the degree (or extent) of retrofitting required, and the nature of financing. Two types of models have been developed: 1) Spreadsheet models using Microsoft Excel 4.0, and 2) Algebraic programming models using the general algebraic modeling system (GAMS). Stochastic analysis was performed using Crystal Ball, a forecasting and risk management program for the Macintosh, developed by Comtech Services, Inc. The models are based on Carpenter & Berg (1984), Combustion Engineering (1989), and the cost analysis for firing coal-water slurry fuel, oil, and natural gas at Penn State (Miller, et al., 1993b). The models are structured along the lines of the first two references and utilize cost data from the third. The cost data are for a 15,000 lb steam/hr boiler at Penn State. The Penn State data were used because it is more current than that contained in the other two references, and the boiler size (in terms of lb steam/hr) is more representative of the DOD boilers under consideration than in the case in the two other references.

The total capital requirement (TCR) has been modeled as a function of boiler derated capacity (BDC) since the capital requirement is based to a significant degree on the extent of retrofitting desired. Figure 5-2 shows the three ways in which TCR has been considered in this study. TCR has been considered: (1) as an increasing linear cost curve with increasing BDC, (2) as a convex cost curve, and (3) as a linear constant cost curve. Below is a discussion of the models and their results and uses.

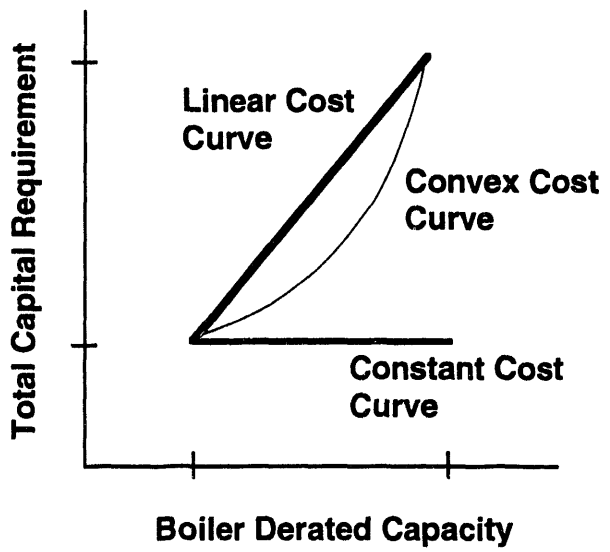

Figure 5-2. Total capital requirement as a function of boiler derated capacity

Spreadsheet Models

The spreadsheet models perform a straight forward engineering economic analysis. They require certain technical and economic data exogenous to the model. Input to the models are shown in Table 5-1. The models then output the operating and maintenance cost savings (OMCS), TCR, specific capital requirements (SCR), and the payback period (PP), which also shown in Table 5-1. In calculating the OMCS, TCR, SCR, and PP, the models yield some intermediate outputs such as capacity factor, annual steam generated (MM lb), MCWSF consumption, oil consumption, and fuel savings. The TCR must be provided if known, otherwise the models use the cost-capacity method with a factor of 0.75. Although the model uses the cost-capacity method to generate the TCR given plant size, the TCR can be entered if it is known prior to the analysis. There is one spreadsheet model for each consideration of the TCR (i.e. whether constant, convex, or linear). The three separate considerations will be combined into one which will yield the same output but for all three. This combined spreadsheet is currently under development. They can be used to determine if the payback period for retrofitting a particular site is acceptable or not. They can also be used for sensitivity studies and can be modified to find conditions under which retrofitting is attractive or beneficial.

GAMS Models

The GAMS (General Algebraic Modeling System) models are representations of the spreadsheet models including a consideration of retrofit capital requirement variation with boiler derating. Expected boiler life is another variable considered in the GAMS model which is absent from the spreadsheet models. The results are present values of retrofit costs, retrofit cost savings (i.e., costs of firing oil), and net benefits of retrofitting. Boiler plant sizes of 10,000 to 70,000 lb steam/hour were considered over a range of boiler derated capacities, 65-100%. Different expected boiler plant lives, from 5-25 years, are considered. The Penn State 15,000 lb steam/hr boiler was used as basis, and the ten to seventy thousand range was considered because the cost-capacity factor method was used (with a factor of 0.75) to estimate TCR for the plants. This method is not recommended for capacities 10 or more (or less) times the capacity of the basis.

These models take the same inputs as the spreadsheet models and are representations of those same models. However, they are different from the spreadsheet models in that they yield maximum benefits of retrofitting. The differential fuel cost (DFC) and boiler derated capacity (BDC), are endogenous. In this way the models can yield the optimal DFC and BDC that maximize the net benefit of retrofitting. The results reported are for present values of costs of retrofitting , benefits to be gained from retrofitting, and net benefits. Table 5-2 shows examples of the net benefit output from the convex TCR case for two discount rates. These figures are in thousands of dollars. The models generate the results given the inputs and the economic variables of interest. The table shows the net present value of retrofitting for different boiler plant sizes,

Table 5-1. Input to, and Output from the Models

Input

Plant size (1000 lb./hr)
MCWSF price ($/MM Btu)
Base oil price ($/MM Btu)
Differential fuel cost ($/MM Btu)
MCWSF heat rate (Btu/lb. steam)
Base oil heat rate (Btu/lb. steam)
Boiler derated capacity (%)
Boiler efficiency (fraction)
Capacity factor (fraction)
Ash content (tons/MM Btu)
Ash disposal costs ($/dry ton ash)
Incremental fixed O&M costs (% of project)
Variable O&M costs ($/thousand lb. steam)
Discount rate (%)
Inflation rate (%)

Output

Annual steam generated (MM lb.)
Annual MCWSF consumption (MM Btu)
Annual oil consumption (MM Btu)
Annual fuel savings
Incremental fixed O&M costs
Variable O&M costs
Variable O&M savings

TOTAL (OMCS)

TOTAL CAPITAL REQUIREMENT
Specific capital requirement ($/lb steam /hr-derated)

PAYBACK PERIOD (YEARS)

Table 5-2. Output from GAMS Model

DIFFERENTIAL FUEL COST (DOLLARS) D1 = 1.0

BOILER PLANT CAPACITY (THOUSANDS LB STEAM PER HOUR) B3 = 30

BOILER DERATED CAPACITY (%)
S1 = 65 ; S2 = 70 ; S3 = 75 ; S4 = 80 ; S5 = 85 ; S6 = 90 ; S7 = 95 ; S8 =100

EXPECTED BOILER PLANT LIFE (YEARS)
N1 = 5 ; N2 = 10 ; N3 = 15 ; N4 = 20 ; N5 = 25

Convex TCR @ 7% financing

INDEX 1 = D1 INDEX 2 = B3

	N1	N2	N3	N4	N5
S1	-559	-109	211	440	603
S2	-680	-201	41	384	558
S3	-826	-319	43	301	485
S4	-999	-466	-85	186	379
S5	-1204	-646	-249	35	237
S6	-1445	-865	-452	-157	53
S7	-1726	-1127	-700	-396	-179
S8	-2054	-1439	-1000	-687	-464

Convex TCR @ 4% financing

INDEX 1 = D1 INDEX 2 = B3

	N1	N2	N3	N4	N5
S1	-505	58	520	900	213
S2	-623	-23	470	875	1208
S3	-765	-130	392	821	1173
S4	-935	-267	282	733	1103
S5	-1137	-439	135	606	994
S6	-1375	-650	-53	437	840
S7	-1654	-905	-288	218	634
S8	-1980	-1210	-577	-57	371

given the boiler derated capacity (BDC), differential fuel costs (DFC) and expected boiler plant life. The table therefore gives the expected net benefits of retrofitting given the plant size, discount rate, expected plant life, boiler derated capacity and DFC.

The GAMS models do not provide the ease of dealing with TCR as do the spreadsheet models. For better decision making using the GAMS results, the decision maker should know a priori the TCR for the project. The models have been refined to output TCR too. This makes for easy comparison with the results. If the TCR is higher than that calculated by the model, then the net benefit would be lower. The decision maker should determine which is the appropriate model by comparing the known TCR with the linear, convex, or constant TCR values, and use the corresponding tables.

The GAMS models analyses are more general and should be selected over the spreadsheet analyses for centralized decision making. However, the spreadsheet models are powerful tools for specific site decision making. This is because the GAMS models assume that all boiler plants face uniform conditions, which may not necessarily be true.

Discussion and Conclusions

It must be noted that there are certain strong assumptions implicit in the models. These are that the variables and inputs stay constant over the life of the plant. Also the modeling of TCR as a function of BDC may not be fixed. The experience of the Penn State facility showed improved performance in terms of increased BDC with time. Such improvements can be characterized as areas under the convex cost curve. That region represents conditions under which the expected net benefits from retrofitting are greater than those calculated and presented in the tables. Similarly, the region above the convex cost curve represents lower expected benefits than presented. From the Penn State experience, it seems that the real modeling of TCR as a function of derating should incorporate a learning curve to account for such improvements. What this suggests is a real TCR curve much lower than shown in Figure 5-1, but definitely lying above the constant cost curve.

The variables which most strongly influence the economic feasibility of retrofitting to fire MCWSF are the differential fuel cost, the expected life of the boiler plant, its size (or capacity), total or specific capital requirement, boiler derated capacity, and the discount rate. There are economies of scale in retrofitting. The models show that some boilers will realize a net benefit from retrofitting while others will not. This is dependent on the economic factors of interest but in general, the larger the boiler (in terms of capacity) the more economically feasible is the retrofit consideration (i.e. economies of scale are present). Also, the longer the useful life, the greater the benefits from retrofitting.

The differences in net benefits with size suggest that DOD can consider gains from a retrofitting distribution scheme in which the gains from retrofitting large (and more economic) boilers are given to boiler plants that will realize some operational gains by retrofitting but

cannot afford the capital costs. With increasing DFC, increasing expected boiler plant life, and increasing boiler plant size, it appears that it would make both engineering and economic sense to install or build new MCWSF boilers only if the TCR of retrofitting is higher than that calculated in the model. As discussed previously, if the real TCR curve is below the model cost curve then retrofitting is recommended. A stochastic analysis of retrofitting gave an average payback period of 7.5 years for a 50,000 lb steam/hr boiler plant at 63% BDC and $1.50/ MM Btu DFC.

A sensitivity analysis showed that the MCWSF cost had the most influence on the analysis. This means that the DFC has the most influence since the fuel oil cost was kept constant. A DFC of at least $1.50/ MM Btu is preferred. With current oil prices at about $3.00/ MM Btu, this requires a delivered MCWSF cost of at most $1.50/ MM Btu.

The desired payback period is reduced with increases in the differential fuel cost. Given the uncertainties in a study of this kind, the desirable payback period should be considerably or significantly less than the useful plant life. Depending on the sizes of DOD boiler plants, it may well be the case that DOD will have to set a desirable payback period close to the useful plant life. Technological improvements that lead to reduction in boiler capacity losses would reduce the capital requirement for retrofitting and encourage retrofitting. It may be the case that beyond a certain BDC level it may not be economical to continue to invest in research into boiler capacity losses due to retrofitting.

The cost model developed in this work can be applied to other coal-based fuels with some modifications. It takes as input, technical and economic data and outputs the variables required for an economic analysis of retrofitting to fire the alternate fuel. Such studies will demonstrate the competitive advantage (if any) of alternate fuels. The models are under refinement to make them better decision aids for retrofitting.

5.5 Subtask 4.5 Analyze/Identify Transportation Cost of Commercial Sources of MCWSF and Cleaned Coal for Dry, Micronized Coal Production

No work was conducted in Subtask 4.5 during this reporting period.

5.6 Subtask 4.6 Determine Community Spillovers

No work was conducted in Subtask 4.6 during this reporting period.

5.7 Subtask 4.7 Regional Market Considerations and Impacts

An input-output model for an 8-county region surrounding the Crane Naval Weapons Center has been constructed using the IMPLAN Modeling System. A regional I-O table for 1990 and a set of multipliers are presented in Tables 5-3 and 5-4, respectively. Table 5-3 separates Military Expenditures in the region from Non-Military Government Expenditures and other elements of Final Demand (Consumption, Government, Investment, and Exports).

Table 5-3. Input-Output Table for the Crane, Indiana Region, 1990
(MM $1990)

INDUSTRY	1	2	3	4	5	6	7	8	9	10	11	12	13	14	TOTAL INT. DEM.	FINAL DEMAND Military	FINAL DEMAND Other
1. Agriculture	66.3	*	*	2.3	104.7	0.6	0.2	*	*	0.1	14.0	1.8	0.5	*	190.5	*	
2. Coal Mining	0.1	1.0	*	*	*	0.2	*	2.2	*	*	*	*	0.3	*	3.9	*	
3. Other Mining	0.2	*	25.2	2.2	0.6	8.6	0.1	0.1	*	*	*	*	0.1	*	37.1	*	
4. Construction	6.8	1.0	1.8	1.1	2.6	22.4	14.7	14.4	0.9	1.8	40.1	15.0	39.4	*	161.8	28.7	
5. Non-durable Manufacutring	4.4	0.5	0.9	5.5	43.4	39.5	0.9	0.4	0.1	4.0	11.7	6.8	1.3	*	119.4	*	
6. Durable Manufacturing	1.9	0.4	1.3	36.0	3.4	334.2	1.8	0.2	0.1	0.8	21.1	10.3	0.6	*	412.0	2.2	2837.7
7. Transport/Communication	9.0	0.5	4.1	16.0	17.0	54.1	25.0	2.3	0.1	5.0	17.1	7.6	2.3	*	160.0	*	
8. Electric Services	5.2	1.3	5.0	1.7	7.2	26.9	1.5	*	*	3.2	5.9	4.6	7.6	*	70.2	*	
9. Other Utilities	0.6	*	1.8	0.4	2.1	8.9	0.1	8.0	0.8	0.4	1.0	1.5	11.1	*	36.7	*	
10. Trade	7.1	0.7	1.1	32.9	12.4	80.3	2.1	0.4	0.1	0.5	10.2	3.5	1.3	*	152.6	*	
11. Services	22.7	2.4	5.0	52.4	15.0	89.3	17.5	2.8	0.3	15.6	107.9	41.1	4.3	*	376.3	*	2133.4
12. Health, Social Services	0.8	*	0.1	*	1.0	3.4	0.3	0.1	*	0.2	2.1	2.2	0.1	*	10.4	*	
13. Government Enterprises	4.4	0.5	2.2	2.1	6.5	22.6	2.4	2.5	0.2	3.3	14.3	9.5	5.5	*	76.0	14.0	
14. Adjustment & Other	*	*	*	*	*	*	*	*	*	*	*	*	*	*	0.0	*	
Total Imports	224.4	20.8	150.8	319.5	456.2	1411.6	92.0	35.2	55.2	50.2	333.4	173.8	49.3	*	3372.5[22]		[3179.1]
Total Value Added	152.5	92.1	193.8	285.2	295.9	1140.9	266.3	97.5	19.3	500.8	1927.6	335.5	134.6	13.1	5455.0		
Errors & Omissions	4.1	0.3	0.8	7.6	1.8	8.3	0.6	0.2	0.1	0.5	3.4	1.1	0.2	-6.0	22.7		
Total Industry Outlays	510.3	121.5	393.9	764.8	969.8	3251.9	425.6	166.3	77.2	586.4	2509.6	614.2	258.4	7.1	10657.0	10657.0	

*Less than $0.05 million
[ ] Not part of column total

Table 5-4. Employment Multipliers

Indiana $MM 1990 Employment Multipliers — Invert Report #606 7/8/93

	Sector		Direct	Indirect	Induced	Total	Type I	Type III
1	Agg 1	Agriculture	15.6891	5.5983	8.7867	30.0741	1.3568	1.9169
37	Agg 2	Coal Mining	9.3913	1.3757	4.4442	15.2112	1.1465	1.6197
38	Agg 3	Other Mining	2.2313	1.2799	4.3566	4.8679	1.5736	2.1816
48	Agg 4	Construction	14.8449	4.7897	8.1045	27.7390	1.3226	1.8686
58	Agg 5	Non-Durable Mfg.	7.7411	4.3859	5.0056	17.1326	1.5666	2.2132
133	Agg 6	Durable Mfg.	9.5663	3.8940	5.5560	19.0163	1.4071	1.9878
433	Agg 7	Transport/Commun.	13.9290	3.3480	7.1314	24.4084	1.2404	1.7523
443	Agg 8	Electric Services	3.9147	3.2226	2.9460	10.0833	1.8232	2.5757
444	Agg 9	Other Utilities	2.6431	.5425	1.2308	4.4165	1.2053	1.6709
447	Agg 10	Trade	33.7340	1.2997	14.7360	49.7697	1.0385	1.4754
454	Agg 11	Services	27.2261	2.2970	12.4181	41.9413	1.0844	1.5405
490	Agg 12	Health, Soc. Serv.	28.2149	3.7919	13.4628	45.4696	1.1344	1.6115
510	Agg 13	Government	16.6697	4.7773	9.0211	30.4681	1.2866	1.8278
524	Rest of the World Industry		.0000	.0000	.0000	.0000	1.2866	1.8278
525	Household Industry-low Income		230.9353	.0000	97.6771	328.6124	1.0000	1.4230
528	Inventory Valuation Adjustment		.0000	.0000	.0000	.0000	1.0000	1.4230

Note: The induced and total components are based upon the Type III multipliers.

The research team is in the process of verifying the Military expenditures and other economic transactions in the Crane I-O table. The table was based on a data reduction (non-survey) method inherent in the IMPLAN Modeling System. This essentially means combining data on national average technological relationships (production functions), with survey-based data on regional income and product accounts, and a set of simplifying assumptions regarding interregional trade. Local and state data bases are being examined first. Local military and non-military officials will be contacted and the Crane Area will be visited.

To complete Phase I, regional I-O tables will be used to determine the economic impacts of using MCWM and MPC at Crane and two or three other sites. The impacts of adoption of these combustion technologies on all DOD boilers within the state of Pennsylvania will also be analyzed. Simulations will be performed with both an I-O model and a computable general equilibrium model. The results will be compared to assess the relative strengths of these two modeling approaches.

The empirical specification of a computable general equilibrium model for Pennsylvania has been completed. The construction of this model is nearly completed. It will prove especially useful in performing economic impact assessments of widespread adoption of new coal utilizing technologies.

5.8 Subtask 4.8 Integrate the Analysis

No work was scheduled or conducted this reporting period.

6.0 TASK 5: FINAL REPORT/SUBMISSION OF DESIGN PACKAGE

No work was conducted on Task 5.

7.0 MISCELLANEOUS ACTIVITIES

A DOD/DOE Information Transfer Session was held at Penn State July 9, 1993 to review the Phase I work being conducted at Penn State. Penn State personnel gave thirteen presentations covering Tasks 1, 2, and 4. Attendees from DOD and DOE were Mike Lin (U.S. Corps of Engineers Construction Engineering Research Laboratory) and John Winslow (U.S. DOE, Pittsburgh Energy Technology Center).

A poster was prepared for the Ninth Annual Coal Preparation, Utilization, and Environmental Control Contractors Review Meeting at Pittsburgh, Pennsylvania, July 19-22, 1993.

A continuation application was prepared and submitted to DOE in July to begin the Phase II research and development activities.

8.0 NEXT SEMIANNUAL ACTIVITIES

During the next reporting period, the following will be done:

- Prescribe specific cleaning strategies for Types I, II, and III coal samples;
- Complete the dense-medium separation testing using the "batch" centrifuge;

- Initiate testing of continuous dense-medium centrifugation using the high-speed, solid-bowl centrifuge;
- Investigate magnetic fluid-based centrifugal separations for fine coal cleaning;
- Complete evaluation of flotation kinetics results for Type III coal;
- Complete flotation tests for Type II coal and evaluate the results;
- Measure contact angles on a selected coal in the presence of several block co-polymers;
- Install 0.076 m diameter flotation column on a test rig;
- Determine operational characteristics of the static an Cominco bubble generators as a function of frother concentration, gas velocity, etc.;
- Conduct column flotation of Type II and III coals;
- Investigate the use of bimodal size distributions for high-solids CWSF formulation;
- Investigate stirred-media and attrition milling for fine grinding of coal;
- Set up apparatus for measurement of charge on particles;
- Complete the characterization of the Triboelectrostatic separator for various operating conditions;
- Complete the preliminary study on the effects of charging mechanisms on Triboelectrostatic separation;
- The conversion design will continue;
- MCWSF will be produced from the candidate coals and characterized, including testing in the research boiler;
- A burner will be procured and installed on the demonstration boiler;
- The 1,000-hour demonstration firing DMC will be conducted;
- The 1,000-hour demonstration firing MCWSF will begin;
- Boilers will be identified for conversion, cost data secured, and the cost-estimation model designed;
- The report discussing the identification of appropriate cost-estimation methodologies will be finalized;
- The development of the fuel supply model will be continued;
- The cost of coal cleaning and delivery to the Crane site will be determined;
- Process analysis focusing on retrofitting to fire DMC utilizing standard NPV techniques to evaluate the retrofit, and stochastic analysis to incorporate uncertainty into the analysis will be conducted;
- Sensitivity analyses will be conducted on both MCWSF and DMC retrofitting to determine areas to focus on to facilitate retrofitting;
- Transportation cost for delivery of coal to a preparation plant and then to the Crane

site will be determined;

- Estimates will be made of air emissions and other residual products of coal preparation and coal combustion from MCWSF and DMC technologies; and
- The accuracy of the input-output table constructed with the use of the IMPLAN System for Crane, Indiana will be verified.

9.0 REFERENCES

Austin, L.G., C.H. Lee, F. Concha, and P.T. Luckie, "Hindered Settling and Classification Partition Curves," accepted for publication in **Minerals and Metallurgical Processing.**

Capes, C.E., J.D. Hazlett, and B.L. Ignasisk, "Novel Application of Oil Agglomeration Technology for Coal Preparation, Upgrading of Low Quality Fuels and Environmental Clean-up", in **Eleventh International Coal Preparation Congress**, Tokyo, Japan, October 22-25, (1990).

Carpenter, R.G., and R.D. Berg, "The Conversion of Industrial Oil-Fired Boilers to Coal-Water Slurry," **Sixth Int. Symp. on Coal Slurry Comb. and Tech.**, pp. 51-66 (1984).

Clayfield, E.J., E.C. Lumb and P.H. Mackey, **J. Coll. Interf. Sci.**, 37, 382 (1971).

Combustion Engineering, Inc., "Combustion and Fuel Characterization of Coal-Water Fuels" Volumes 2-6, Final Report," U.S. Department of Energy, Pittsburgh Energy Technology Center, DE-AC22-82PC50271 (February 1989).

Cross, M., "Prediction of the Voidage of Packed Beds", in **Agglomeration '85 Proceedings of the 4th International Symposium on Agglomeration.** (C.E.Capes, ed), Toronto, Canada, (1985).

Davies, M.H., M.T. Simnad, and C.E. Birchenall, **Journal of Metals, Transactions, AIME**, p. 889, 1951.

Fowkes, F.M., **Ind. Eng. Chem.**, 54, 40 (1964).

Gregory, J., **J. Coll. Interf. Sci.**, 138 (1981).

Hamaker, H.C., "The London-van der Waals Attraction between Spherical Particles," **Physica**, 4, 1058 (1937).

Hogg, R., Healy, T.W., and D.W. Fuerstenau, "Mutual Coagulation of Colloidal Dispersions", **Trans. Faraday Soc.**, 62 1638-1651 (1966)..

Hunter, R.J., **Zeta Potential in Colloid Science**, Academic Press, London.

Israelachvili, J.N., **Intermolecular and Surface Forces**, Academic Press, New York, (1985).

Israel, R. and D.E. Rosner, "Use of a Generalized Stokes Number to Determine the Aerodynamic Capture Efficiency of Non-Stokesian Particles from a Compressible Gas Flow," **Aerosol Science and Technology**, Vol. 2, pp. 45-51, (1983).;

Ityokumbul, M.T., "A New Modelling Approach to Flotation Column Design," **Minerals Engineering**, 5, 585-593 (1992).

Ityokumbul, M.T., "Maximum Gas Velocity in Column Flotation," **Minerals Engineering**, in press (1993).

Klima, M.S., and P.T. Luckie, "Using Model Discrimination to Select a Mathematical Function for Generating Separation Curves," **Coal Prep.**, 3, pp. 33-47 (1986).

Klima, M.S., and P.T. Luckie, "Application of an Unsteady-State Pulp-Partition Model to Dense-Medium Separations," **Coal Prep.**, 6, pp. 227-240 (1989).

Klima, M.S., and P.T. Luckie, "Use of an Unsteady-State Pulp-Partition Model to Investigate Multiple Variable Interactions," **Coal Prep.**, 8, pp. 185-193 (1990).

Lee, C.H., "Modeling of Batch Hindered Settling," PhD Thesis, The Pennsylvania State University (1989).

Link, T., R.P. Killmeyer, R. Elstrodt, and N. Haden, "Initial Study of Dry Ultrafine Coal Beneficiation Utilizing Triboelectrostatic Charging with Subsequent Electrostatic Separation," **DOE/PETC/TR-90/11**, 19 pp. (1990).

Melhotra V.P., K.V.S. Sastry and B.W. Morey, "Review of Oil Agglomeration Techniques for Processing of Fine Coals", **International Journal of Mineral Processing**, 11 (3), 175-201 (1983).

Meloy, T.P., "Analysis and Optimization of Mineral Processing and Coal-Cleaning Circuits — Circuit Analysis," **International Journal of Mineral Processing**, 11 (3), pp. 175-201 (1983).

Miller, B.G., and A.W. Scaroni, "The Pennsylvania State University's Superclean Coal-Water Slurry Demonstration Program," **Proceedings of the Fifteenth Int. Conf. on Coal and Slurry Tech.**, Coal & Slurry Technology Association, Washington, D.C., p. 77 (1990a).

Miller, B.G., and A.W. Scaroni, "Superclean Coal-Water Slurry Combustion Testing in an Oil-Fired Boiler," **6th Annual Coal Prep., Util., and Environ. Control Contractors Conf.**, U.S. Department of Energy, Pittsburgh Energy Technology Center, Pittsburgh, Pennsylvania, p. 81 (1990b).

Miller, B.G., S.V. Pisupati, R.L. Poe, J.L. Morrison, J. Xie, P.M. Walsh, S. Shamanna, H.H. Schobert, and A.W. Scaroni, "Superclean Coal-Water Slurry Combustion Testing in an Oil-Fired Boiler, Semiannual Technical Progress Report for the Period 02/15/1992 to 08/15/1992," U.S. Department of Energy, Pittsburgh Energy Technology Center, DE-FC22-89PC88697, (October 13, 1992).

Miller, B.G., A.W. Scaroni, R. Hogg, S. Chander, M.T. Ityokumbul, M.S. Klima, P.T. Luckie, A. Rose, T.J. Considine, R.L. Gordon, K. McClain, P.M. Walsh, P.C. Painter, M.J. Rini, M. Jha, D. Morrison, R. Melick, and T. Sommer, "The Development of Coal-Based Technologies

for Department of Defense Facilities," U.S. Department of Energy, Pittsburgh Energy Technology Center, DE-FC22-92PC92162, (May 13, 1993a).

Miller, B.G., A.W. Scaroni, S.A. Britton, D.A. Clark, J.L. Morrison, S.V. Pisupati, R.L. Poe, P.M. Walsh, R.T. Wincek, and J. Xie "Superclean Coal-Water Slurry Combustion Testing in an Oil-Fired Boiler, Technical Report for Phases I-III," U.S. Department of Energy, Pittsburgh Energy Technology Center, DE-FC22-89PC88697, (July 21, 1993b).

Mitchell, R.E., R.H. Hurt, L.L. Baxter, and D.R. Hardesty, "Compilation on Sandia Coal Char Combustion Data and Kinetic Analyses: Milestone Report," SAND92-8208.UC-361, Sandia National Laboratories, Livermore, California, pp. 28-31, (1992).

Napier-Munn, T.J., "Modelling and Simulating Dense Medium Separation Processes — A Progress Report," **Minerals Engineering**, 4, pp. 329-346 (1991).

Napper, D.A., **Polymeric Stabilization of Colloidal Dispersions**, Academic Press, New York, (1983).

Overbeek, J.Th.G., in **Colloid Science, I.** (H.R. Kruyt, ed.) Elsevier, Amsterdam, (1952).

Overbeek, J.Th.G, **J. Chem. Soc. Faraday Trans. 1**, 84, 3079 (1988).

Pawlak, W., K. Szymocha, Y. Briker and B. Ignasiak, "High-sulphur Coal Upgrading by Improved Oil Agglomeration", in **Third International Conference on Processing and Utilization of High-sulfur Coals**, Ames, IA, (1989).

Scheffler, P., and P. Zahr, "Wet Classification at Cut Points Below 10 Microns," **World Mining**, 50-53 (March 1980).

Schenkel, J.H., and J.A. Kitchener, **Trans Faraday Soc.** 56, 161 (1960).

Simmons, F.J., and D.V. Keller, "Two Ton-per-day Production of Otisca T-process Ultraclean Coal/water Slurry", **Tenth International Coal Preparation Congress**, Edmunton, Alberta, Canada (1986).

Smellie, R.H., and V.K. LaMer, "Flocculation, Subsidence and Filtration of Phosphate Slimes, VI, A Quantitative Theory of Filtration of Flocculated Suspensions," **J. Colloid Sci.**, 23, 589 (1958).

Visser, J., **Adv. Coll. Interf. Sci.**, 3, 331 (1972).

Walker, M.S., A.L. Devernoe, and W.S. Urbanski, "Separation of Non-Magnetic Minerals Using Magnetic Fluids in a Flow-Through MHS Rotor," **Minerals and Metallurgical Processing**, 209-214 (November 1990).

Ynchausti, J.A., J.D. McKay, and D.G. Foot, Jr., "Column Flotation Parameters - Their Effects," in **Column Flotation** '88 (K.V.S. Sastry, ed.), SME Littleton, CO, Chap. 18, 157-172 (1988).

10.0 ACKNOWLEDGMENTS

Funding for the work was provided by the U.S. Department of Defense (via an inter-agency agreement with the U.S. Department of Energy) and the Commonwealth of Pennsylvania under Cooperative Agreement No. DE-FC22-92PC92162. The project is being managed by the U.S. Department of Energy, Pittsburgh Energy Technology Center (PETC). John Winslow of PETC is the project manager.

The following Penn State staff were actively involved in the program: David A. Bartley, Scott A. Britton, David A. Clark, Robert C. Gilbert, Howard R. Glunt, Samuel P. Gross, Ruth Krebs, Michael A. Hill, Sarma V. Pisupati, and Roger L. Poe.

The following Penn State graduate students were actively involved in the program: Ronghua Zhou, Hurriyet Polat, Mehmet Polat, Mohamed Fofana, Daode Xu, Mitra Ahmadi, Robert Weiland, Girish Ahuja, Timothy Wilkinson, and John Kovalchick.

DATE
FILMED
4/14/94
END